Heme Protein Assemblies

Charles J. Reedy and Brian R. Gibney*

Department of Chemistry, Columbia University, 3000 Broadway, MC 3121, New York, New York 10027

Received June 20, 2003

Contents

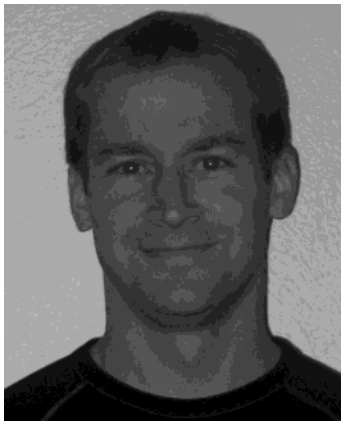

Charles Reedy was born in Lombard, IL, in 1975. He earned his B.A. in chemistry at Northwestern University in 1997, after conducting research in the laboratory of Professor Tobin Marks. After college he worked at UOP in Des Plaines, IL, for three years, developing catalysts for fuel cell applications. Since 2000, he has been a graduate student at Columbia University in Professor Gibney's laboratory. His research focuses on the de novo design of heme proteins.

Brian R. Gibney was born in Orange Park, FL, but grew up in Tallahassee, FL. He earned his B.S. in chemistry from Florida State University and Ph.D. in inorganic chemistry from the University of Michigan (with Vincent L. Pecoraro). After a postdoctoral fellowship in the Johnson Research Foundation and the Department of Biochemistry and Biophysics at the University of Pennsylvania (with P. Leslie Dutton), he accepted a faculty position in the Department of Chemistry at Columbia University in 2000. His research interests lie in the fields of bioinorganic and biophysical chemistry with an emphasis on the development of peptide-based synthetic analogues, or *maquettes*, for redox enzymes containing heme and iron–sulfur cofactors.

1. Introduction

1.1. Approaches to the Study of Heme Proteins

Hemes remain one of the most visible and versatile classes of cofactors utilized in biology.[1] Since their discovery, the structural and functional aspects of heme proteins have fascinated biochemists and synthetic chemists alike.[2,3] Nature has evolved heme binding sites within a variety of protein scaffolds[4] to carry out such diverse tasks as electron transfer,[5,6] substrate oxidation,[7,8] metal ion storage,[9] ligand sensing,[10−12] and transport.[13] As such, heme proteins are integral components in numerous vital biological processes including steroid biosynthesis,[14,15] aerobic respiration,[16] and even programmed cell death.[17] Found from the archaea to higher organisms, the ubiquity of hemoproteins further emphasizes their operational importance within biological systems.

Heme proteins have played important roles in establishing our understanding of the chemical underpinnings of protein structure and function. From a structural biology viewpoint, the first protein X-ray crystal structure determined was that of the dioxygen carrier myoglobin,[18] shown in Figure 1E.[19] From a bioenergetics perspective, studies on the heme proteins in the mitochondrial respiratory chain, specifically the lack of high-potential cytochromes, led to

* To whom correspondence should be addressed. Phone: (212) 854-6346. Fax: (212) 932-1289. E-mail: brg@chem.columbia.edu.

10.1021/cr0206115 CCC: $48.50
Published on Web 01/24/2004

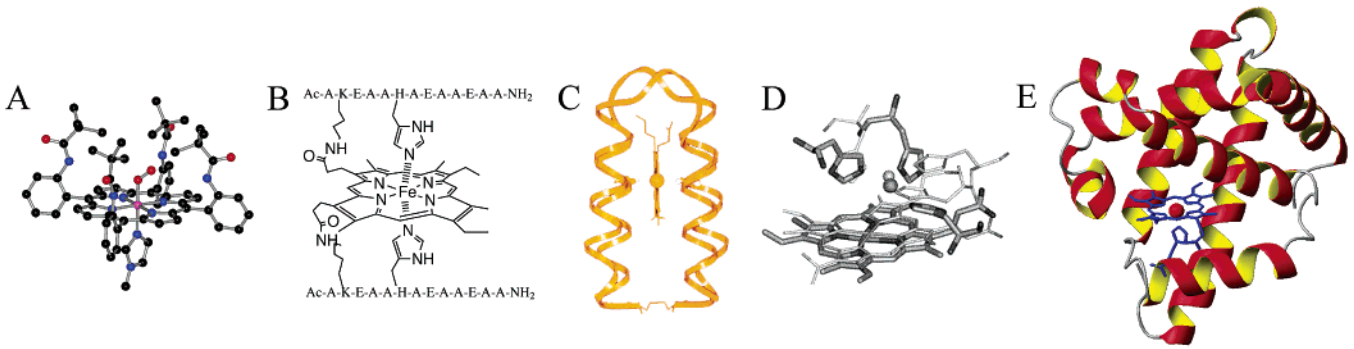

Figure 1. Conceptual progression of heme protein models from synthetic analogues to natural heme proteins: (A) a picket-fence porphyrin, (B) a peptide-sandwiched mesoheme (Reprinted with permission from ref 37. Copyright 1995 American Chemical Society.), (C) a de novo-designed heme protein (Reprinted with permission from ref 56. Copyright 1994 American Chemical Society.), (D) an engineered heme−copper myoglobin (thick line) (Reprinted with permission from ref 48. Copyright 2003 National Academy of Sciences.), and (E) the natural heme protein myoglobin[19] (all protein X-ray structure figures prepared using the program MOLMOL[386]).

the acceptance of Mitchell's chemiosmotic theory.[20] From a biophysics point of view, cytochrome *c*, an electron-transfer heme protein, has played an indispensable role as a laboratory in which to study the pathways of protein folding via equilibrium[21] and kinetic methods.[22] From a medical standpoint, evidence that sickle cell anemia was caused by heme protein dysfunction demonstrated the molecular basis of this human disease.[23]

The recognition that heme proteins as a class of metallobiomolecules are, fundamentally, highly elaborated coordination compounds continues to guide bioinorganic approaches to the study of heme proteins.[24] The time-honored synthetic analogue approach to bioinorganic chemistry continuously provides novel coordination chemistry and further insight into heme protein active sites.[25] Early small-molecule models based on natural and synthetic metalloporphyrins with exogenous axial ligands focused on elucidating the effects of metal ion coordination on the spectroscopy, electrochemistry, magnetism, and chemical reactivity in the absence of the influence of the protein matrix.[26−34] The robust literature on structural and spectroscopic models of heme proteins is peppered with successful functional models including the picket-fence porphyrin (X-ray structure shown in Figure 1A) that binds O_2 reversibly.[35,36] The traditional small-molecule bioinorganic approach has further evolved to include more biologically relevant ligands, as represented by the peptide-sandwiched mesoheme[37] shown as a model in Figure 1B, and to provide more elaborate constructs as model complexes for heme proteins including a functional analogue of cytochrome *c* oxidase.[38,39]

The advent of site-directed mutagenesis,[40] and later the development of the polymerase chain reaction,[41,42] provided a parallel biochemical approach to the bioinorganic chemistry of heme proteins. The use of genetically engineered proteins offered the ability to probe the chemistry of heme proteins within natural protein scaffolds. Aside from primary coordination sphere effects, site-directed mutagenesis also supplied a mechanism to study the influence of the protein matrix on the inherent chemical properties of the heme moiety. This approach has demonstrated the role of various factors in heme protein function, including heme burial[43] and electrostatics.[44] Coupled with advances in structural biology, these mutational studies have provided a wealth of detailed information on natural heme protein structure−function relationships. These methods have now progressed to the rational redesign of heme proteins[45−47] to alter chemical reactivity, such as the design of a cytochrome *c* oxidase active site into the myoglobin scaffold shown in Figure 1D.[48] Additionally, directed evolution provides another mechanism to genetically screen heme protein mutants for enhanced chemical reactivity or altered substrate specificity.[49,50] These biochemical methods provide mechanisms for generating new functional enzymes from natural starting points in sequence space.[51]

An emerging approach to bioinorganic chemistry has progressed out of the creation of novel proteins from first principles, i.e., de novo design.[52] This approach provides rigorous, constructive tests of our understanding of biochemical structure and function.[53] De novo protein design has progressed to the point where the design of simple folded protein motifs is feasible,[54,55] as represented by the model of the designed heme protein in Figure 1C.[56] Designed proteins have provided keen insight into the fundamental governors of protein secondary and tertiary structural specificity[53,57−68] as well as the principles of protein folding.[69] The use of proteins with greater biological homology has facilitated the incorporation of metal cofactors, e.g. iron−sulfur clusters,[70−72] hemes,[56,73] zinc,[74] copper,[75−77] nickel,[78] mercury,[79] arsenic,[80] and lanthanides,[81] as well as the synthesis of a number of proteins containing a combination of metal cofactors as models of complex metalloenzyme active sites.[82−89] These model systems have demonstrated their utility in elucidating the molecular basis of biological phenomena such as metal-induced protein assembly[90] and folding[37] as well as proton-coupled electron transfer.[91] Furthermore, the emergence of atomic-level structural definition and chemical reactivity in de novo-designed proteins promises to expand our fundamental understanding of biochemical structure and function.[92−94]

Metalloprotein design represents the integration of the small-molecule and biochemical approaches to bioinorganic chemistry.[95−97] On one hand, this ap-

proach represents a natural stage in the evolution in the use of synthetic analogues. As a constructive methodology, de novo design gleans insight from small-molecule synthetic analogues as well as natural proteins in an effort to fabricate novel metalloproteins from first principles. These simplified model systems have proven useful in delineating the engineering specifications and tolerances of metalloproteins. From an inorganic coordination chemistry perspective, coordination compounds with chiral peptide and protein ligands can be designed to access the well-recognized and unique properties of protein ligands.[98] The use of biological ligands and the study of these designed systems in aqueous buffers facilitate comparison via the touchstone of the robust biochemical literature on natural proteins. On the other hand, de novo metalloprotein design represents an extension of the biochemical approach to bioinorganic chemistry. Protein design affords rigorous testing of our fundamental concepts of protein structure−function relationships in simpler protein systems. Furthermore, protein design allows the delineation of the minimal structures requisite to achieve biological function.[99−102] Therefore, many of these designed metalloproteins are simplified relative to their more elaborate natural counterparts.

Herein, we review the literature on heme protein design from a coordination chemistry perspective (previous reviews are also available[103,104]). We start with a survey of natural heme protein structure and function to glean insight from natural systems. The design of novel peptide- and protein-based synthetic analogues of heme proteins is catalogued on the basis of structural complexity starting with simple metalloporphyrin−amino acid complexes and progressing to the design of multi-cofactor proteins. The insight gained from designed heme proteins in terms of heme protein structure−function relationships is discussed prior to a perspective view of the field.

1.2. Overview of Natural Heme Proteins

Nature utilizes heme proteins to carry out a myriad of diverse biological functions. Early reports of heme proteins described the O_2 transport properties of hemoglobin in the blood of numerous animals and the process by which the pigment could be removed by acid and crystallized as hemin, i.e., Teichmann's crystals.[105] The heme proteins involved in electron transfer were initially described in 1884 by MacMunn as respiratory pigments (myohematin or histohematin).[106] In the 1920s, Keilin rediscovered these respiratory pigments and named them the cytochromes, or "cellular pigments",[107] and classified these heme proteins, on the basis of the position of their lowest energy absorption band in the reduced state, as cytochromes *a* (605 nm), *b* (∼565 nm), and *c* (550 nm). The UV−visible spectroscopic signatures of hemes are still used to identify heme type from the reduced bis-pyridine-ligated state, i.e., the pyridine hemochrome method.[108] Within each class, cytochrome *a*, *b*, or *c*, early cytochromes are numbered consecutively, e.g. cyt *c*, cyt c_1, and cyt c_2, with more recent examples designated by their reduced state α-band maximum, e.g. cyt c_{559}. The critical involvement of heme proteins in O_2 transport and the conversion of O_2 to H_2O in aerobic respiration only hint at the rich dioxygen chemistry of heme proteins.[109] Hemes are essential components of peroxidases, catalases, and oxidases as well as mono- and dioxygenases.[7,110] Most recently, heme proteins have been shown to be involved in controlling gene expression as biological sensors for O_2 and CO.[11]

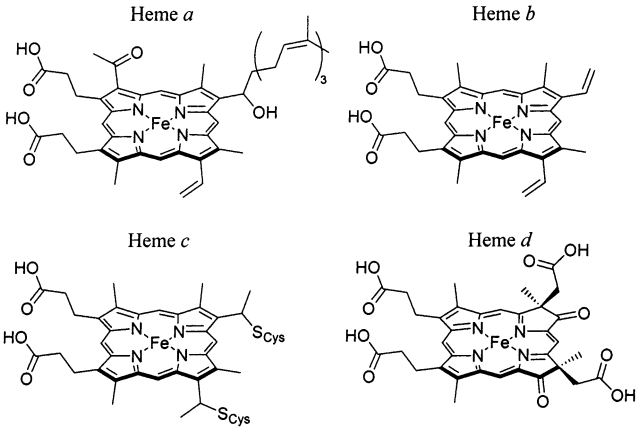

Figure 2. Chemical structures of commonly occurring natural hemes *a*, *b*, *c*, and *d*.

Regardless of their individual function, the chromophore in each type of natural heme protein is a tetrapyrrole macrocycle whose identity is distinguished by its peripheral β-pyrrolic substituents, as shown in Figure 2. The most common heme tetrapyrrole macrocycle is heme *b* or iron(II) protoporphyrin IX, whose structure was synthetically demonstrated by Hans Fischer.[111] The term "heme" specifically refers to the ferrous complex of protoporphyrin IX, with the ferric−hydroxy and ferric−chloride complexes referred to as hematin and hemin, respectively. Heme *b*, also called protoheme, has methyl groups at positions 1, 3, 5, and 8, vinyl groups at positions 2 and 4, and propionates at positions 6 and 7 on the macrocycle. All the porphyrins are synthesized in vivo as the free base forms before incorporation of the iron(II) by the enzyme ferrocheletase.[112,113] Additionally, heme *b* serves as the structure from which hemes *a* and *c* are biosynthetically derived.[114−116] Aside from *b*-type cytochromes, heme *b* is also found in globins, cytochromes P-450, and hemesensor proteins. Protein scaffolds bind hemes via the combination of the axial coordination positions available on iron, hydrophobic interactions with the heme macrocycle, and polar interactions with the propionic acids.[117−121]

Heme *c* is structurally similar to heme *b* except that thioether bonds to cysteine residues replace one or both of the vinyl groups and covalently link the heme macrocycle directly to the protein scaffold.[122] The covalent attachment of heme to the protein is effected by the enzyme heme lyase,[123] but in vitro chemical synthesis has also been used to form the thioether bonds in *b*-type cytochrome and *c*-type cytochrome scaffolds.[124−127] Cytochromes *c* typically contain a CXXCH sequence motif from which the two cysteines link to the porphyrin macrocycle and the histidine binds to the encapsulated iron. The pres-

ence of the covalently linked heme designates it a *c*-type heme that includes all cytochromes *c* as well as cytochrome *f*.[128]

Heme *a* is biosynthesized from heme *b* by conversion of the vinyl group at position 2 into a hydroxyethylfarnesyl side chain, yielding heme *o*, followed by subsequent oxidation of the methyl at position 8 to a formyl group.[115] These alterations render heme *a* both more hydrophobic and more electron-withdrawing as an equatorial ligand to iron than heme *b*. Heme *a* is found only in terminal oxidases such as mammalian cytochrome *c* oxidase. Other less common heme architectures include heme *d*,[129] heme,[130] heme P-460,[131] siroheme,[132] and chlorocruoroheme.[133]

While heme proteins containing a single copy of the cofactor, the simple heme proteins, are well recognized, protein ligands are adept at organizing multicomponent metalloproteins that contain different cofactors performing distinct biological functions. Many multi-heme proteins are designed for efficient electron transfer to provide electrons/holes to a catalytic active site. In physiological electron-transfer chains, 14 Å appears to be the upper engineering limit for the cofactor edge-to-cofactor edge distance.[134] The observed heme−heme distances are highly variable in natural heme proteins and range from 4 Å, close to van der Waals contact, in the di-heme split-Soret cytochrome[135−137] to 16 and 26 Å between the four hemes of hemoglobin.[138] An example of a multiheme protein containing two different types of heme is nitrite reductase (or cytochrome cd_1) that contains both heme d_1 and a covalently linked *c*-type heme.[139]

Complex heme proteins are those that contain both a heme and a non-heme cofactor. The photosynthetic and respiratory complexes, which perform multielectron catalysis, provide numerous examples of complex heme proteins. Hemes are found combined with cofactors such as amino acid radicals,[140] chlorophylls,[141] flavins,[142] iron−suflur clusters,[143,144] molybdenum,[145,146] copper,[147] and zinc.[148] In cytochrome *c* oxidase, which performs the four-electron reduction of dioxygen to water with the pumping of four protons across the inner mitochondrial membrane, hemes *a* and a_3 are combined with a structural $Zn(II)(Cys)_4$ site as well as the binuclear Cu_A site involved in electron transfer.[148] The six-coordinate bis-histidine-ligated heme *a* is involved in an electron-transfer chain, delivering electrons to the mono-histidine-ligated heme a_3 which, along with Cu_B, binds and reduces O_2 at the binuclear heme a_3−Cu_B active site. In addition to their catalytic role in dioxygen reduction, hemes *a* and a_3 are also implicated in the proton pumping mechanism.[149−154] Since the structure of the heme protein and the identity of the amino acids juxtaposed to the heme are critical to binding the iron and controlling the heme chemistry, the next section outlines the findings from structurally characterized heme proteins.

2. Natural Heme Protein Engineering

2.1. Structural Engineering

The ever-expanding Protein Data Bank (PDB) currently contains more than 20 000 protein structures, of which >1000 (~5%) contain at least one heme moiety.[155] This collection of diverse structures provides significant insight into the engineering of natural heme proteins within biological constraints. From the coordination chemist's perspective, the PDB provides the identity and geometry of the primary coordination sphere of the iron and the array of amino acids in the secondary coordination sphere. Furthermore, the PDB provides the protein secondary structure elements local to the heme macrocycle and the global protein fold that provides the scaffold holding the constellation of amino acids that control heme protein function. Here, we explore the range of observed heme protein structures in the PDB as a guide to the engineering constraints for rational heme protein design, cognizant of the fact that new heme protein structures continue to expand these limits.

The primary coordination sphere of the iron in heme proteins of known structure is dominated by histidine. In particular, the most frequently observed coordination number and ligation motif is five-coordinate mono-histidine, as found in myoglobin and hemoglobin. The second most common coordination motif, six-coordinate bis-histidine, is found one-third as often as mono-histidine. Typically, histidine ligates heme iron via the N^{ϵ}, but there is a single extant example of N^{δ}-bound histidine, His102 of *Nitrosomonas europea* cyt c_{554}.[156] It is worth noting that the propensity of histidine N^{ϵ} or N^{δ} coordination is variable between metalloprotein active site types due to steric constraints, with diiron proteins preferring N^{δ}-bound histidine.[157,158] Depending on side-chain packing, the histidine planes in bis-His-ligated heme proteins range from nearly parallel (cyt b_5[159]) to perpendicular (heme IV of cyt c_3[160]). In six-coordinate heme proteins, histidine is also found in combination with other axial ligands. The second most common ligation motif for six-coordinate heme proteins is histidine with methionine, as exemplified by cyt *c*.[161] The combination of histidine with other amino acid ligands is relatively rare and includes the neutral N-terminal amine donor (Tyr1 of cyt *f* [128] and Pro2 of ferric CooA[162]), the side-chain amine of lysine (cyt *c* nitrite reductase[163]), and the asparagine amide donor (ferric SHP[164]) as well as the charged donors tyrosine phenoxide (HasA[165]) and glutamate carboxylate (hemoglobin Milwaukee[166]). Finally, two other coordination motifs are observed for six-coordinate heme proteins: bis-methionine (bacterioferritin[167]) and the aquo-sulfido (sulfite reductase[132]). In five-coordinate heme proteins, histidine coordination remains prevalent, with cysteine thiolate ligation observed in cytochromes P-450[168] and nitric oxide synthase[169] and tyrosine phenoxide utilized in heme catalase.[129] In all the observed structures, few potential amino acid ligands are absent, including Ser, Thr, and Asp. Thus, Nature employs a majority of the available set of amino acid side-chain ligands to affect heme binding with an observed preference for histidine N^{ϵ} ligation.

The coordination environment of iron in heme proteins need not be static. Obviously, five-coordinate heme irons provide an open site for the binding of

substrate, as observed in the oxygen transport/activation/sensor proteins. Substrate binding may also compete off weakly bound ligands, e.g. H_2O, in six-coordinate heme proteins, as observed in cyt P-450cam.[110] Additionally, several six-coordinate heme proteins are known to swap ligands upon oxidation/reduction. The d_1 heme of cyt cd_1 is bound by His-Tyr in the ferric state and shifts to five-coordinate mono-His upon reduction, while the adjacent *c* heme is bis-His in the ferric state and converts to His-Met upon reduction. These ligand changes gate the catalytic electron-transfer event and lead to marked hysteresis in electrochemical measurements.[130]

While the axial ligands to heme iron establish the basic coordination chemistry, the interaction of amino acids beyond the primary coordination sphere is critical to modulating the chemical properties of the heme, allowing it to perform a variety of biochemical functions. Hydrophobic amino acids predominate at the heme−protein interface. Heme binding sites are mostly comprised of aliphatic hydrophobes (Leu, Ile, Met, Val, Ala), as expected from their placement within hydrophobic cores. Additionally, the majority of heme protein structures contain at least one aromatic residue (Phe, Tyr, Trp, or His) that interacts with the heme macrocycle.[170] This leads to a higher probability of observing an aromatic amino acid at a heme binding site than elsewhere in a protein. These aromatic amino acids stabilize the heme macrocycle through π-stacking or edge-to-face interactions.[171] In fact, the four-helix bundle heme proteins *E. coli* cyt b_{562}[172] and *R. molischianum* cyt c'[173] share three practically superimposable aromatic residues near their heme groups.[174] The observed hydrophobic interactions of the protein with the heme macrocycle are substantial enough to allow myoglobin to bind free base protoporphyrin IX without the contribution from metal−ligand interactions.[120,121,175]

Polar amino acids also contribute to heme protein binding site specificity by providing critical hydrogen bond donors/acceptors and modulating the polarity of heme binding sites. The presence of hydrogen bonding to the N^{δ} proton of histidine tunes the donor ability of the N^{ϵ} ligand. In horseradish peroxidase (HRP[176]), the hydrogen-bonding Asp247 side chain provides for greater imidazolate character at the axial His170 ligand and the push of the Push−Pull mechanism[177] of peroxide O−O bond cleavage, while the distal polar residues His42 and Arg38 provide the pull on the peroxide substrate. The dioxygen transport protein myoglobin[18] has a nonpolar distal pocket and lacks the hydrogen bond acceptor at the proximal His residue, and thus provides a counter example to HRP with the same primary coordination sphere, five-coordinate mono-histidine, with a polar distal pocket. Electrostatic interactions are also observed at the heme propionate groups that are often salt-bridged to arginine residues. Additionally, local protein side chains establish the polarity of the heme microenvironment. The polarity of the protein environment local to the heme ranges from nonpolar (cyt P-450) to relatively polar (peroxidases), which helps control the chemistry of the heme moiety. While these polar interactions are critical to modulating the chemical properties of the heme, hydrophobic interactions are more important in terms of binding energies than the electrostatic interactions of the propionates.[175]

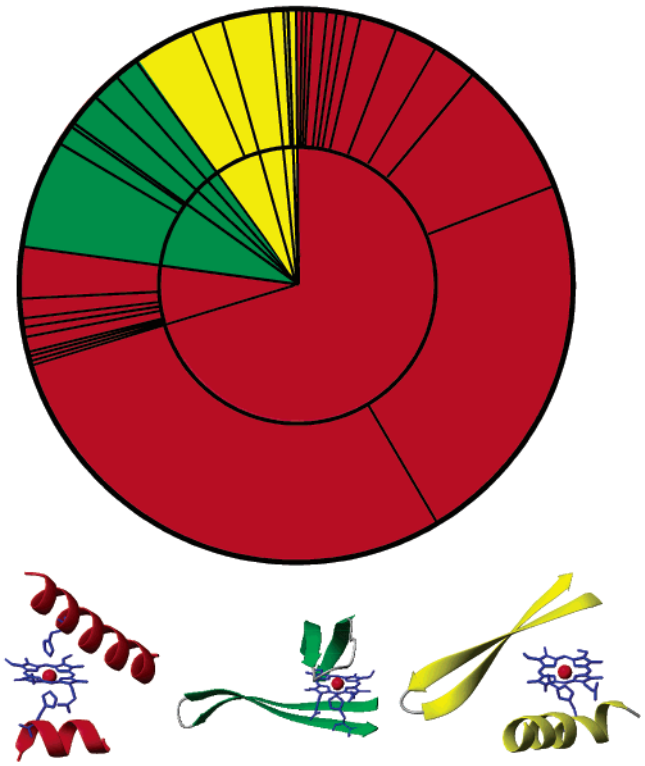

Figure 3. Structural classification of natural heme proteins. (Top) A CATH wheel representation of natural heme protein structures inspired by ref 4. (Bottom) Illustration of mainly α-helical (myoglobin in red),[19] mainly β-sheet (nitrophorin in green),[387] and mixed α/β (FixL in yellow)[388] secondary structure binding sites for heme.

All the amino acids that interact with the heme are fixed in space by the global fold of the protein scaffold. Several algorithms have been developed for the purposes of classifying the compendium of known protein structures. For the purposes of this review, we have analyzed the known heme protein structures using the CATH database (release 2.4, January 2002), which hierarchically categorizes protein structure by **C**lass, **A**rchitecture, **T**opology and **H**omologous superfamily.[178] Figure 3 presents a graphical representation, known as a CATH wheel,[4] of the nonredundant heme protein structure set color coded by Class. Additionally, an example of a heme binding site from each Class is shown. While heme proteins composed of mainly β sheets (green, 13%) or mixed α/β (yellow, 10%) structure are not uncommon, the graph clearly shows the current dominance of the mainly α-helical (red, 77%) secondary structures in heme proteins of known structure.

The inner circle of the CATH wheel represents the architectural classification. The mainly α-helical protein class shown in red subdivides into two architectures, the orthogonal bundle proteins (91% of mainly α proteins) and the up−down bundles (9%). Representative examples of the orthogonal bundle architecture are hemoglobin,[138] myoglobin,[18] and cyt *c*,[180] whereas the up−down bundle architecture includes cyt b_{562}[172] and cyt c'.[173] The outer circle of the

CATH wheel further classifies the heme proteins by protein topology. Thus, the classification of heme protein structures demonstrates a dominance of α-helical proteins (77% of all heme proteins), especially those with orthogonal bundle architectures.

It is important to catalog the known heme protein structures as done above to begin to understand the synthetic targets for a biomimetic[181,182] approach to heme protein design. This analysis demonstrates that the initial choice of heme protein designers to utilize histidine ligands within an α-helical protein scaffold to bind heme is reasonable. It also suggests that other coordination spheres, e.g. Met-Met, and other folds, e.g. β sheet and mixed α/β structures, are conceivable. While instructive, this analysis may misleadingly suggest that heme protein chemistry is narrowly defined. The following section demonstrates the breadth and versatility of natural heme protein function that designers seek to access and expand.

2.2. Functional Engineering

As with all classes of metalloproteins, heme proteins perform a multitude of functions in biology. Hemes are integral structural components of hemoproteins; indeed, cyt *c* does not fold without the bound heme.[183] Hemoproteins are also involved in metal ion storage, as exemplified by the four-α-helix bundles of bacterioferritin that assemble an 8-nm-diameter cavity containing ~4500 irons as $Fe_2O_3 \cdot H_2O$.[184,185] There are numerous examples of heme proteins involved in electron transfer from the soluble electron carriers such as cyt *c* and cyt b_5 to the integral membrane protein complexes involved in photosynthesis and respiration, e.g. succinate dehydrogenase.[186] Aside from transporting electrons, heme proteins are also well recognized for their ligand transport functions.[13] While hemoglobin and myoglobin serve to carry O_2 and nitrophorins transport NO, other heme proteins that regulate gene transcription are critical biosensors of O_2 (FixL) and CO (CooA).[11] Finally, heme enzymes are a fascinating class of enzymes vital to life processes including aerobic respiration (cytochrome *c* oxidase[16]), drug detoxification (cyt P-450[109]), and protection from reactive oxygen species (catalase, peroxidase[7]). The diversity of function that biochemistry derived from the iron porphyrins may appear to distinguish hemes from other cofactors. However, other biochemical cofactors, e.g. the iron−sulfur clusters,[187] demonstrate a similar breadth of function in biochemical systems.

One fundamental functional consequence of the observed differences in structure at natural heme sites in proteins is changes in the resultant electrochemistry of the encapsulated iron. Within the set of structurally characterized heme proteins, the Fe(III)/Fe(II) electrochemical couple spans values from −550 (HasA[188]) to +362 mV (cyt *f* [189]) vs SHE, as shown in Figure 4. These midpoint reduction potentials, E_m values, are critical to cytochrome function since they control both the thermodynamic driving force and the kinetic rate of electron flow between cofactors in electron-transfer chains. As with all coordination compounds, the range of E_m values for heme proteins is a direct result of changes to the relative stability of metal−ligand bonding in the two metal oxidation states,[30] as shown below:

$$-nF\Delta E_m = \Delta G = -RT \ln [K_a^{Fe(III)}/K_a^{Fe(II)}] = -RT \ln [K_d^{Fe(II)}/K_d^{Fe(III)}] \quad (1)$$

As such, changes in the equilibrium midpoint potential may be due to stabilization or destabilization of either one or both of the heme iron oxidation states. The majority of heme affinity studies are performed using the air-stable oxidized ferric heme, so the absolute stabilization/destabilization of the ferric and ferrous oxidation states by various environmental effects in proteins is not well delineated.

The observed 862 mV (20.5 kcal/mol) range in E_m values represents a 10^{15} shift in the ratio of the ferric and ferrous heme association constants, $K_a^{Fe(III)}/K_a^{Fe(II)}$. This shift manifests itself in several ways relevant to biochemistry. First, the reduction potential of a metalloprotein is intimately coupled to the stability of the protein fold in the two oxidation states. The global fold of the protein in high-potential heme proteins, like many *c*-type cytochromes, is more stable in the reduced state.[190] Second, differences in axial ligand affinity for the ferric and ferrous heme may result in dissociation of the cofactor. The biological function of the extracellular heme acquisition system A (HasA) protein is to extract and deliver heme from hemoglobin to the HasR receptor. A consequence of the low reduction potential of HasA, −550 mV vs SHE, is an $\sim 10^6$ difference between the $K_a^{Fe(III)}$ and $K_a^{Fe(II)}$ values. The tight ferric heme affinity ($K_d \approx 10$ pm[188]) coupled with the reduction potential indicates that the ferrous heme affinity is weak ($K_d \approx 10\ \mu$m). Thus, reduction of the iron may facilitate heme release from the transport ligand.

The primary coordination sphere provides the base midpoint reduction potential of the encapsulated iron, which can be dramatically modulated by the surrounding protein matrix.[191−193] The relative effect of the porphyrin peripheral architecture on iron redox activity has been measured by comparing the electrochemistry of the bis-imidazole-ligated forms, the hemochromes, in aqueous solution at pH 8. The reduction potential of bis-imidazole-ligated heme *b*, Fe(protoporphyrin IX)$(Im)_2$, is −235 mV vs SHE and slightly more positive than the −285 mV value measured for Fe(mesoporphyrin IX)$(Im)_2$, a model for a *c*-type heme.[91] Both of these values are significantly more negative than the reduction potential of the hemochrome of heme *a*, −120 mV vs SHE.[194,195] As observed for these natural iron porphyrins, the midpoint potentials of synthetic iron porphyrins with electron-withdrawing substituents are more positive. This is due to the decrease in donor power of the equatorial ligands as observed by the increase in the acidity of the tetrapyrrole nitrogen donors. This not only affects the donation of the equatorial ligands but via a cis-effect it also modulates the affinity for axial ligands.[196,197]

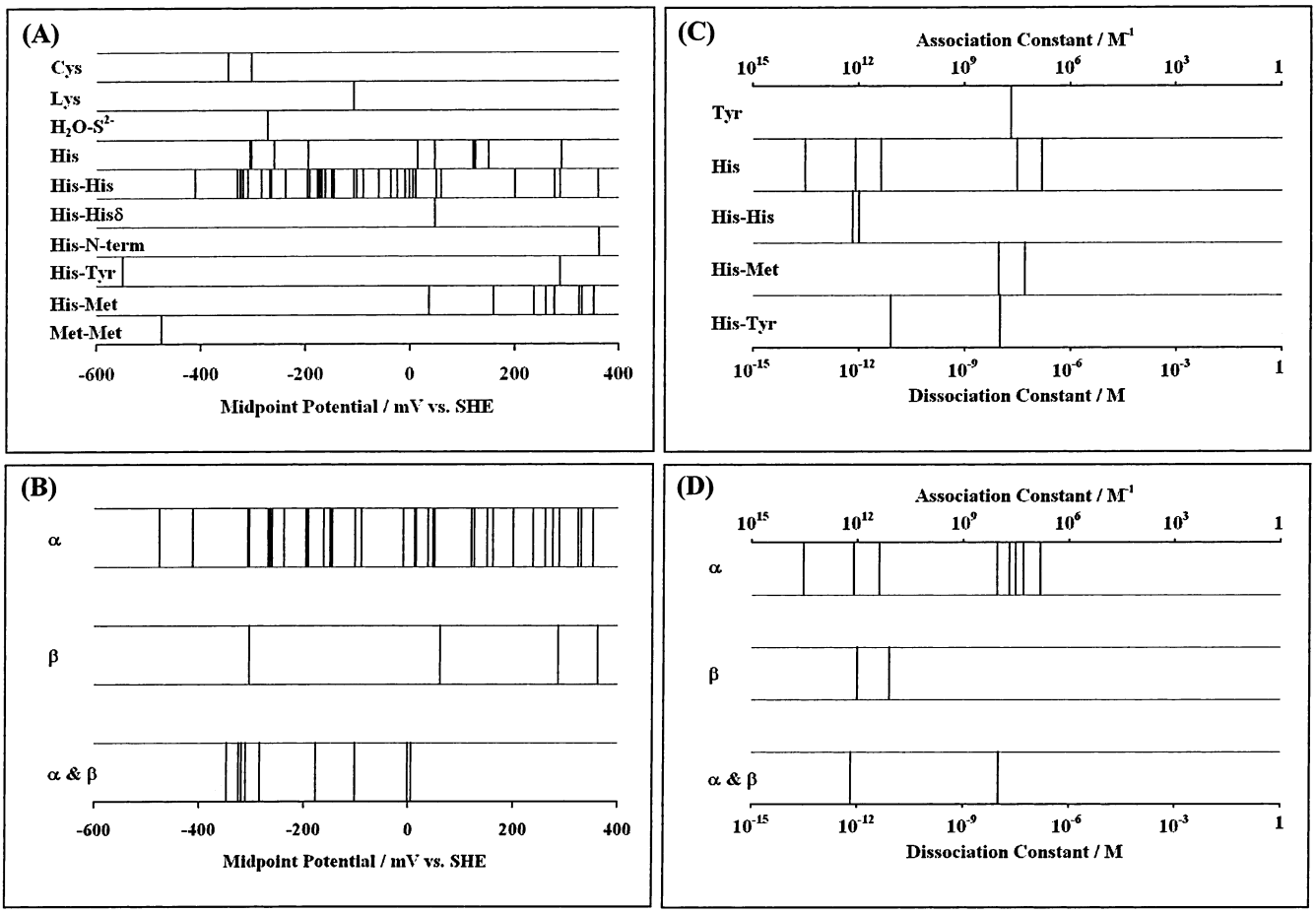

Figure 4. Compilation of heme affinity and redox activity in natural proteins. Midpoint reduction potentials as a function of (A) ligation motif and (B) CATH domain fold. Ferric heme equilibrium association constants of natural heme proteins as a function of (C) coordination motif and (D) CATH domain fold.

The influence of several coordination motifs can be gleaned from studies of exogenous ligand binding to microperoxidases. In general, the observed trends follow expectations based on the hard−soft acid−base (HSAB) principle.[198] In comparative terms, Fe(II) is softer than Fe(III) and binds with higher affinity to softer ligands, e.g. methionine sulfur.[199] Conversely, the harder histidine imidazole binds more tightly to Fe(III) than to Fe(II). Consistent with this analysis, the reduction potential of bis-His-ligated microperoxidase-8 (MP-8) is −200 mV vs SHE, a value 170 mV lower than that for the His-Met complex. The five-coordinate mono-His-ligated form of MP-8 has a reduction potential of −160 mV, relatively close to that of the bis-His form.[200−202]

While the type of porphyrin and the primary coordination sphere serve to determine the fundamental reduction potential of a heme, the surrounding protein matrix significantly modulates this value. As shown in Figure 4A, the midpoint reduction potentials of mono-histidine-ligated hemes range from −306 (HRP[203]) to +290 mV (heme a_3[204]). Restriction to the same porphyrin architecture, hemes *b*, results in an only slightly smaller range of −306 (HRP[203]) to +150 mV (human hemoglobin[205]). Within bis-His-ligated heme proteins, E_m values range from −412 (HAO[206]) to +360 mV (cyt b_{559}[207]). Indeed, within the multi-heme enzyme hydroxylamine oxidoreductase (HAO), the bis-His-ligated heme midpoint potentials span 700 mV, a difference of 2×10^{12} in the ratio of the Fe(III) heme to Fe(II) heme affinity constants.[206] A similar range is also observed for His-Tyr-ligated heme proteins, −550 (HasA[188]) to +287 mV (heme d_1 of cyt cd_1[208]). In addition to differences in the heme type and environment at the binding sites in these two proteins, this wide range may indicate a difference in Tyr protonation state between these two proteins. His-Met-ligated heme proteins show less variability, +37 (cyt c_{553}[209]) to +352 mV (cyt c_6[210]). While His-Met heme proteins generally possess more positive midpoint reduction potentials than bis-His heme proteins, as expected on the basis of their coordination sphere, there are examples of bis-His proteins of higher potential than His-Met-ligated heme proteins. Thus, the influence of the protein microenvironment on E_m can outweigh the contribution from the primary coordination sphere. Last, bis-Met-ligated bacterioferritin, an iron storage protein, has a fairly negative reduction potential of −475 mV vs SHE (filled $Fe_2O_3 \cdot H_2O$ core, shifts to −225 mV with a vacant core).[211]

Considerable variation in heme reduction potentials is also observed within a protein fold, as shown in Figure 4B. In the mainly α-helical proteins, E_m values range from −475 (bacterioferritin[211]) to +352 mV (cyt c_6[210]). Despite the few examples of mainly β-sheet heme proteins, a similar range is observed, −303 (nitrophorin[212]) to +362 mV (cyt *f* [189]). In mixed

α/β scaffolds, the observed range is smaller, from −347 (inducible nitric oxide synthase[213]) to +5 mV (bovine liver cyt b_5[214]). Within monomeric four-α-helix bundles, the range of electrochemical function is quite limited from +14 (cyt c'[215]) to +160 mV (cyt b_{562}[216]), but the oligomerized four-α-helix bundle bacterioferritin has a potential of −475 mV.[211] Recent combinatorial mutagenesis of cyt b_{562}, the His-Met-ligated four-α-helix bundle heme protein, has been able to shift the heme reduction potential by 160 mV. Interestingly, all but one of the cyt b_{562} mutants studied demonstrated more negative reduction potentials, approaching the limit of −50 mV observed for His-Met MP-8. These authors suggest that the wild-type structure of cyt b_{562} as well as cyt *c* may have evolved to the highest possible reduction potential.[217]

The breadth of electrochemical function in proteins of known structure has provided a wealth of information on the various factors that set and modulate heme redox activity. Aside from the obvious influence of the primary coordination sphere, there is significant emphasis in the literature on the role that electrostatics play in modulating heme electrochemical function.[218−220] Since the oxidized [Fe(III)(porphyrin)]$^+$ is a formal cation and the reduced state [Fe(III)(porphyrin)]^0 is formally neutral, electrostatic interactions between the two states differ and provide a mechanism by which to alter the redox activity.[43] At a more fundamental level, these interactions should alter the Fe(III) heme affinity more than the corresponding Fe(II) heme affinities.

Electrostatic interactions come in many guises in metalloproteins.[221] First, burial of the heme in a protein interior lowers the dielectric local to the heme. Alternatively, the degree of solvent exposure of the heme, or accessible surface area, alters the electrostatic potential at the heme site. Indeed, in His-Met-ligated cytochromes *c*, the midpoint potential is observed to fall 50 mV per 4 Å^3 of exposed heme surface, which may result in up to 500 mV of heme reduction potential modulation.[199] Second, the exposure of heme to high dielectric solvent also rapidly diminishes the effect of local charges. These charged groups may include other oxidized hemes, amino acids residues, propionates, amide backbone dipoles, and water dipoles. Third, the dielectric response of the protein to heme reduction/oxidation may involve the protonation/deprotonation of an amino acid side chain to maintain charge neutrality, a redox Bohr effect.[122] Such proton-coupled electron-transfer events are becoming well recognized as fundamental functional units of the chemiosmotic proton pumps such as cytochrome *c* oxidase that are critical to ATP synthesis.[16,153,222,223] While the evaluation of all the electrostatic contributions in the inhomogeneous environment of a heme protein is not trivial, continuum electrostatic computational methods have shown success in modeling the observed reduction potentials.[192,224−226]

While progress in the modeling of electrostatic effects in heme and also iron−sulfur proteins[227,228] is impressive, there are numerous examples of mutations that result in counterintuitive alterations in heme redox activity. These complications arise from the multitude of structure−function relationships in heme proteins that cannot always be faithfully predicted. Additionally, since the E_m values are fundamentally derived from ferric and ferrous heme affinities, the lack of studies on the effect of mutations of heme binding constants is problematic. Indeed, the paucity of Fe(III) heme binding constants and the dearth of Fe(II) heme affinities illustrated in Figure 4C,D makes conclusions as to the absolute stabilization/destabilization of the heme iron oxidation states in heme proteins virtually impossible.

Chemical properties, such as the equilibrium midpoint reduction potentials discussed above, belie the ultimate biochemical functions of metalloproteins. The inherent reactivity of iron porphyrins is precisely controlled at heme protein active sites. While it is common to focus on the role of the protein in augmenting chemical reactivity for a particular biochemical function, it should be recognized that the role of protein ligands is also to minimize unproductive chemical reactivity. In protein design terminology, engineering toward a function is positive design while engineering against a function is considered negative design.[54,59] If one views natural heme protein engineering from a protein design vantage point rather than from an evolutionary perspective, the presence of the distal His residue in myoglobin that provides a hydrogen bond that stabilizes the bound O_2 as a ferric−superoxo complex can be seen as an example of positive design. An example of negative design in myoglobin is the encapsulation of a heme within a protein matrix, which prevents the nonspecific aggregation of the heme macrocycle as well as reactions between reduced hemes and O_2 that form the ferric−μ−oxo porphyrin dimer. Thus, one can choose to view heme protein engineering as a combination of both positive and negative design. The polarity differences at the distal side of the heme active sites in myoglobin and cytochrome P-450 design each toward their particular chemical reactivity with O_2 and at the same time effectively suppresses the alternative O_2 reactivity.

In the cytochromes, electron-transfer heme proteins, the protein ligand can be viewed to be positively designed to allow for efficient electron transfer and negatively designed away from other chemical reactivity. Placing the heme near the protein surface (interprotein electron transfer)[229,230] or within 14 Å of another cofactor (intraprotein electron transfer) provides for sub-millisecond electron-transfer rates.[134,231] Additionally, cytochromes typically demonstrate only slight structural changes between the ferric and ferrous oxidation states, which minimizes the inner-sphere contribution to the reorganization energy or λ. In terms of negative design, the presence of two endogenous axial ligands in six-coordinate cytochromes may be seen to suppress the affinity for exogenous ligands, H_2O, O_2, and CO, which would alter the redox activity.

For the five-coordinate heme proteins involved in O_2 transport/activation/sensing, the lack of a sixth endogenous ligand can be viewed as positive design, which facilitates their function. Aside from an open,

or readily displaced exogenous ligand, these proteins provide further engineering that differentiates their function. The burial of the heme deep in a globin can be seen as positive design since it protects the ferric−superoxo complex[232] from solvent and from physiologically relevant intraprotein electron transfer. While the globins can be analyzed to be negatively designed to prevent proton or solvent intrusion into the heme site, cytochrome *c* oxidase can be viewed as positively designed to include proton channels that facilitate O−O bond scission reactions. While much more subtle, the polarity of the heme active sites of catalases, peroxidases, and oxygenases may provide examples of positive design. Thus, the breadth of natural heme biochemical function illustrates the effectiveness of protein ligands in controlling the precise chemistry at heme protein active sites. These environmental factors may be viewed in the context of positive and negative design. Ultimately, the complete delineation of the fundamental engineering of heme proteins would provide a conceptual basis for the design of heme proteins tailored for a variety of industrial and biomedical applications.

3. Designed Heme Proteins

3.1. Metalloporphyrinyl–Peptides and Metalloporphyrin–Polypeptides

The inherent complexity of natural heme proteins continues to obscure the full description of their fundamental engineering specifications and tolerances. Simplification, long since an inspiration of both the synthetic analogue and biochemical approaches, provides a mechanism by which to separate the interrelated structure−function relationships in heme proteins. In an effort to isolate each factor for study, heme binding sites are being designed into simplified protein scaffolds. Some of the most simply designed heme protein systems are those with minimal peptides covalently attached to porphyrins (metalloporphyrinyl−peptides) and those composed of hemes self-assembled in homopolymers of amino acids (metalloporphyrin−polypeptides).

A well-studied class of metalloporphyrinyl−peptides derived from natural heme proteins are the microperoxidases.[200] The microperoxidases (MPs) are the heme-containing products from cyt *c* proteolysis that contain the consensus cyt *c* CXXCH sequence motif, as shown in Figure 5. Microperoxidase-11 (MP-11), isolated from pepsin digestion, and microperoxidase-8 (MP-8), isolated from trypsin digestion, contain 11 and 8 amino acids, respectively. While the number of residues contained in microperoxidases depends on the proteolysis conditions, all contain the covalently linked *c*-type heme with a histidine axial ligand. The removal of the remaining amino acids opens the sixth coordination site for exogenous ligands. In aqueous solution, ferric MP-8 is a six-coordinate His-aquo complex between pH 4 and 9. Above pH 9 it becomes six-coordinate His-hydroxo.[233] Ferrous MP-8 is a six-coordinate His-aquo complex from pH 7.5 to 12.0.[234] Because of their coordination properties, MPs have been exploited as one of the few mono-histidine-ligated synthetic heme proteins, as will be discussed in section 4.2.

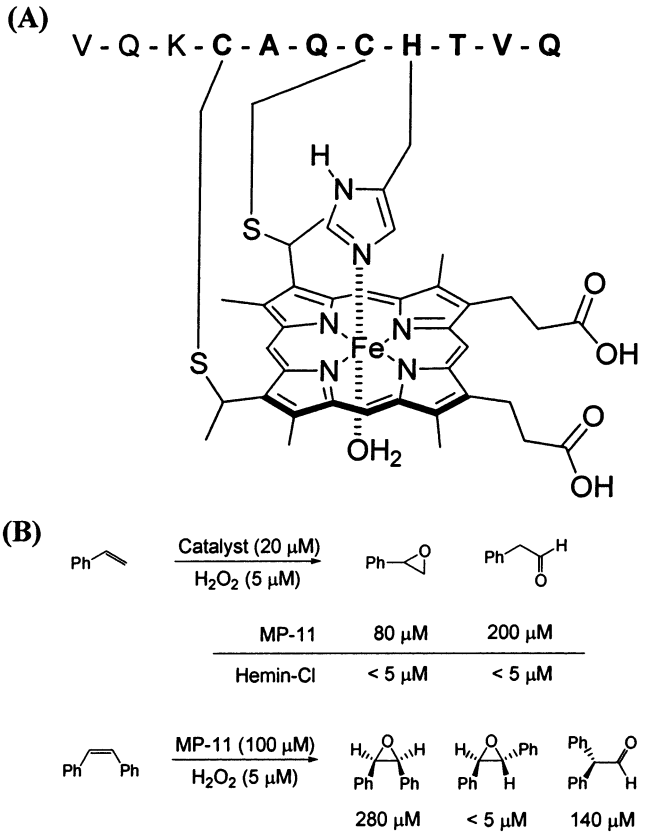

Figure 5. (A) Chemical structure of microperoxidase-11 (MP-11) indicating metal binding and heme attachment. The related microperoxidase-8 contains only the residues in bold. (B) MP-11-catalyzed oxidation of styrene (above) and epoxidation of *cis*-stilbene (below). Data from ref 389.

The solution speciation of the MPs in aqueous buffers complicates their analysis. Exposure of the distal heme face results both in a tendency of MPs to aggregate in aqueous solution and in their ability to form intermolecular coordination complexes. The tendency toward aggregation can be attenuated by addition of alcoholic co-solvents. The association constant, or K_a value, of MP-8 dimer formation decreases from $(1.17 \pm 0.02) \times 10^5$ M^{-1} to $(1.21 \pm 0.02) \times 10^4$ M^{-1} and $(2.16 \pm 0.21) \times 10^3$ M^{-1} in 20% and 50% (v/v) methanol:water mixtures, respectively.[233] Since the primary amines from the N-terminus and Lys-13 are potential ligands for intermolecular complexes, acetylation of these groups in MP-8[235] and MP-11[236] decreases their aggregation tendencies. However, the acetylated MP-8 and MP-11 still form π-stacked face-to-face dimers at high concentrations.

Other than acetylation of free amines, there are several other reports on the covalent modification of MPs. An N-terminal proline residue was added to MP-8 to introduce a general acid−base functionality that is lacking in MPs and present in natural peroxidases.[237] Additionally, MP-11 has been appended to an analogue of RNase A S-peptide through a disulfide bond. UV−vis and CD spectroscopy indicate that a His residue from the S-peptide binds to the iron and that the protein closes down on the distal face. Thus, this construct yields a monomeric

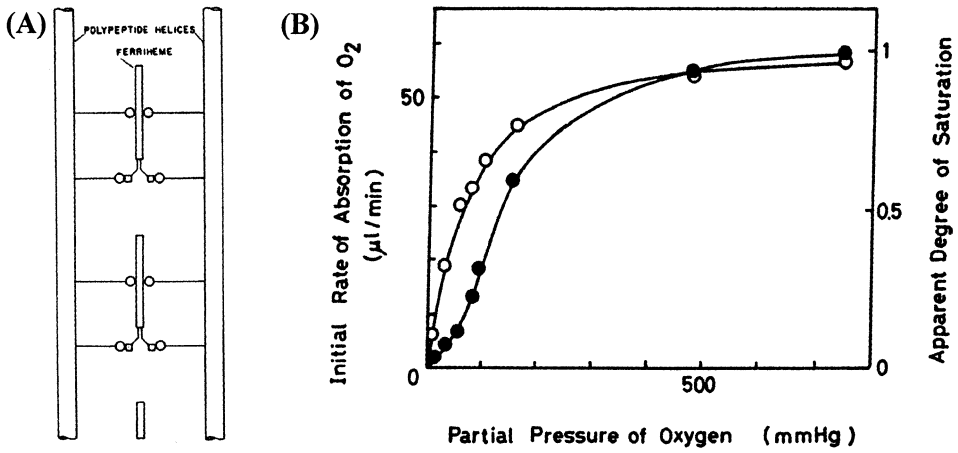

Figure 6. (A) Schematic diagram of the proposed structure of the heme−poly-L-lysine complex. Circles represent ϵ-amino groups of lysine; squares represent carboxylates of hemes (center rectangles). (Reprinted with permission from ref 253. Copyright 1964 Elsevier.) (B) Plot of initial rate of oxygen absorption by heme−poly-L-lysine with (●) and without (○) added poly(ethylene glycol) as a function of oxygen partial pressure. (Reprinted with permission from ref 361. Copyright 1976 Elsevier.)

bis-histidine compound that is slightly more helical than the parent fragment.[238] Another appended MP was constructed using trypsin-catalyzed reverse proteolysis.[239] To introduce an endogenous sixth axial ligand, three variants of MP-8 were made with C-terminal His, Tyr, and Met additions. The His- and Tyr-appended MP-9s formed low-spin, six-coordinate complexes based on UV−vis and resonance Raman spectroscopy. Interestingly, the Met-appended MP-9 did not form six-coordinate species in either iron oxidation state.

The flexibility and oligomeric propensity of MPs present challenges to definitive structural characterization. Paramagnetic NMR studies of the low-spin ferric cyanide-bound forms of MP-8[240] and MP-11[241] in water:alcohol mixtures find that the loop between the Cys residues are rigid and structurally similar to that of the parent cyt *c*. Additionally, the orientation of the histidine ligands relative to the porphyrin plane is conserved. As expected, the remaining residues form flexible C-termini.[240] These structures parallel the findings from the denaturation studies of cyt *c*, where the helix between the Cys residues and the axial His ligand is retained in the unfolded state.[242]

The synthesis of heme−peptide complexes by covalent attachment of amino acids or polyamino acids to porphyrin templates provides for greater sequence diversity in the construction of metalloporphyrinyl−peptide systems. Thus, it represents an elementary progression from small-molecule synthetic analogues toward total heme protein design. The propionic acid groups of mesoheme have been used to link amino acids via amide bonds to create mono- and bis-histidine, mono- and bis-methionine, and histidine−methionine mesoheme constructs.[243] Due to porphyrin aggregation, these compounds were poorly soluble in aqueous media and required dioxane as a cosolvent. The mono- and bis-histidine ligands form strong complexes with ferric and ferrous iron with spectroscopic features reminiscent of natural cytochromes consistent with their design. However, the bis-methionine construct formed a very weak complex with Fe(III), and six-coordinate bis-Met ligation was observed only in the reduced Fe(II) state.[243] Similar work with di-amino acid-modified iron protoporphyrin IX and deuterioporphyrin IX demonstrated that placing the ligand on a slightly longer tether from the propionate increased the strength of the interaction between the His and iron.[244]

Metalloporphyrinyl−peptides with increasing peptide content have been utilized to study the influence of peptide length on histidine coordination. Covalent attachment of a non-coordinating undecapeptide derived from a natural protein to one of the deuterioheme propionates provides both aqueous solubility and steric hindrance, preventing the binding of a second exogenous imidazole. The attachment of a histidine to the second propionate provides an endogenous axial ligand. In this construct, the presence of a Phe at the third position from the propionate group further weakened the affinity for an exogenous His ligand by blocking the distal face of the heme, presumably by forming ring-stacking interactions with the deuterioheme. Further research with metalloporphyrinyl−peptides has provided synthetic analogues of cytochrome *c* oxidase and cytochromes P-450.[245−250]

Aside from covalent architectures, self-assembly reactions have also been used to construct metalloporphyrin−peptide systems. One of the earliest reported attempts at the self-assembly of a synthetic heme protein employed the peptide homopolymers poly-L-lysine and poly-L-histidine to ligate heme.[251] As shown in Figure 6, Fe(III)(protoporphyrin IX) binds to poly-L-lysine (~5000 amu) as evidenced by the formation of a red compound (λ_{max} = 420 nm) at pH 11, where the peptide is helical, and a green compound (λ_{max} = 388 nm) at pH 9−10, where the peptide has less helical content. Control experiments demonstrated that monomeric L-lysine and low-molecular-weight poly-L-lysine (~600 amu) at equivalent concentrations did not bind to the heme. Additionally, racemic poly-DL-lysine formed only the yellow-green complex between pH 9 and 11. Both the red and green heme−polylysine complexes are six-

coordinate low-spin ferric hemes, with the red complex postulated to be bis-Lys ligated and the green complex hydroxyl-lysyl bound. The differences in primary coordination sphere are due to changes in the secondary structure of the poly-L-lysine scaffold and protonation state of the lysine residues as a function of pH. Aside from the iron coordination, heme−polylysine complex formation is further stabilized by Coulombic interactions between the heme propionates and other lysine residues. The authors indicate that one heme binds per 12 lysine residues.[251−254]

Poly-L-histidine has also been used to coordinate hemes as a homopolymer and as a copolymer with L-glutamic acid.[255] The heme−poly-L-histidine complex possesses absorption spectra (λ_{max} = 414 nm) consistent with low-spin six-coordinate bis-histidine ligation at pH 5.8. The authors estimate that 24 histidines were required per heme binding site. The heme−(His-Glu)copolymer complex possesses spectra at pH 6.2 (λ_{max} = 411 nm) consistent with monohistidine ligation, with the sixth coordination site occupied by water or glutamate. Increasing the solution pH to 7.1 results in a shift in the heme−copolymer complex spectra (λ_{max} = 413 nm) consistent with bis-histidine ligation that is possibly related to an increase in randomness of the polymer chain.[255]

The inherent uncertainties in polymer composition, polydispersity, and structure have limited the utility of polyamides as synthetic analogues of heme proteins. Despite these complications, two conclusions from these studies foreshadowed future protein-based biomimetics. First, peptides bound heme more tightly than the corresponding amino acid monomers. Second, the structure of the protein or peptide ligand influenced the coordination state of the heme iron. In other words, protein folding, as well as the amino acids in the secondary coordination sphere, affects the affinity of primary coordination-sphere ligands for the metal.

3.2. Metalloporphyrin-Directed Folding

Not only is the global fold of a heme protein scaffold essential to biochemical function, but the process by which the protein folds from an ensemble of unfolded structures into a discrete three-dimensional structure is also critical. The simple heme protein cytochrome *c* has played a significant role in deciphering the fundamental mechanisms of protein folding. Equilibrium H/D exchange experiments revealed the presence of cooperative folding units and discrete intermediates in the protein folding pathway of ferric cyt *c*, which suggested a linear protein folding pathway.[256] Kinetic experiments by photoinduced electron injection into denatured ferric cyt *c* demonstrate rapid folding of ferrous cyt *c*.[257] The kinetics suggest an initial collapse into a compact denatured structure, followed by reorganization into the native structure. The kinetics and thermodynamics of the cyt *c* protein folding pathway are influenced by metal ion coordination. A significant misfolding trap results from axial coordination of His26 or His33 to the heme iron that must be eventually dissociated to achieve the final fold. Since imidazoles bind Fe(III) hemes more tightly than Fe(II) hemes, it has been suggested that the depth of this kinetic trap may be deeper for ferric cyt *c*. Additionally, the final step of the cyt *c* folding pathway includes the ligation of the axial methionine residue, Met80. Aside from the interactions of the heme iron with axial ligands, hydrophobic contacts between the porphyrin macrocycle and the hydrophobic core are fundamental to heme protein folding.

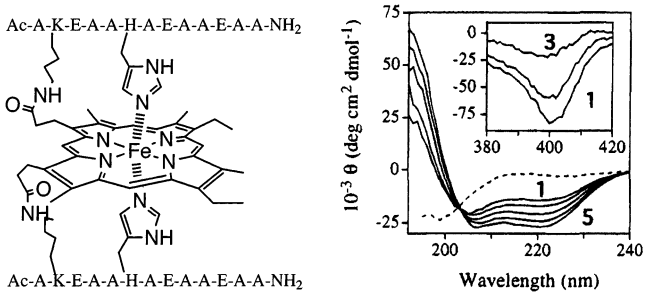

Figure 7. (A) Chemical structure of the prototype peptide-sandwiched mesoheme (PSM) and (B) evidence for heme induction of helical secondary structure. (Reprinted with permission from ref 37. Copyright 1995 American Chemical Society.)

As observed in cyt *c* and other metalloproteins,[258] metal ion coordination to protein ligands induces protein folding. Early metalloprotein designs demonstrated that complex formation at exchange-inert metal centers[259] could be used to overcome the entropic penalty of organizing unfolded monomeric peptides into folded oligomers. The NMR structure of a related three-helix bundle containing Ni(II) or Co(II) has been determined.[260] In the case of exchange-labile metals, the peptide-sandwiched mesohemes (PSMs) represent an excellent example of secondary structure induction mediated by metal coordination.[37] As a class of metalloporphyrinyl−polypeptides, the PSMs are constructed by covalent attachment of peptides to the propionic acids of mesoporphryins via lysine side chains, as shown in Figure 7. While the early PSMs based on mesoporphyrin IX resulted in the formation of diastereomers, more recent PSMs utilize the C_2-symmetric mesoporphyrin II to avoid this complication.[261] The two identical 13-amino acid peptides on the PSM were designed to axially coordinate the heme iron in an α-helical secondary structure. Random coil in the absence of heme−metal ion ligation nucleates helix formation, and the PSMs show 50% helical content in aqueous solution that improves to 97% upon addition of 25% v/v TFE, as evidenced by a negative Cotton effect at 222 nm.[37,262] The helix can be further stabilized by a structural disulfide bond (94% helix).[263] Furthermore, detailed NMR studies illustrate that the placement of a Phe or a Trp one helical turn away from the His residues increases helix content via aromatic−porphyrin interactions (65 and 75% helix, respectively).[95,263] However, a full NMR structure of a PSM has not yet been reported. Alternatively, the PSM helices can be destabilized by introducing springboard strain into the design by altering the distance between the two connection points, the His residue and the Lys linked to the heme propionate.[264] The mono-PSMs,[264] which have only a single peptide linked to the heme

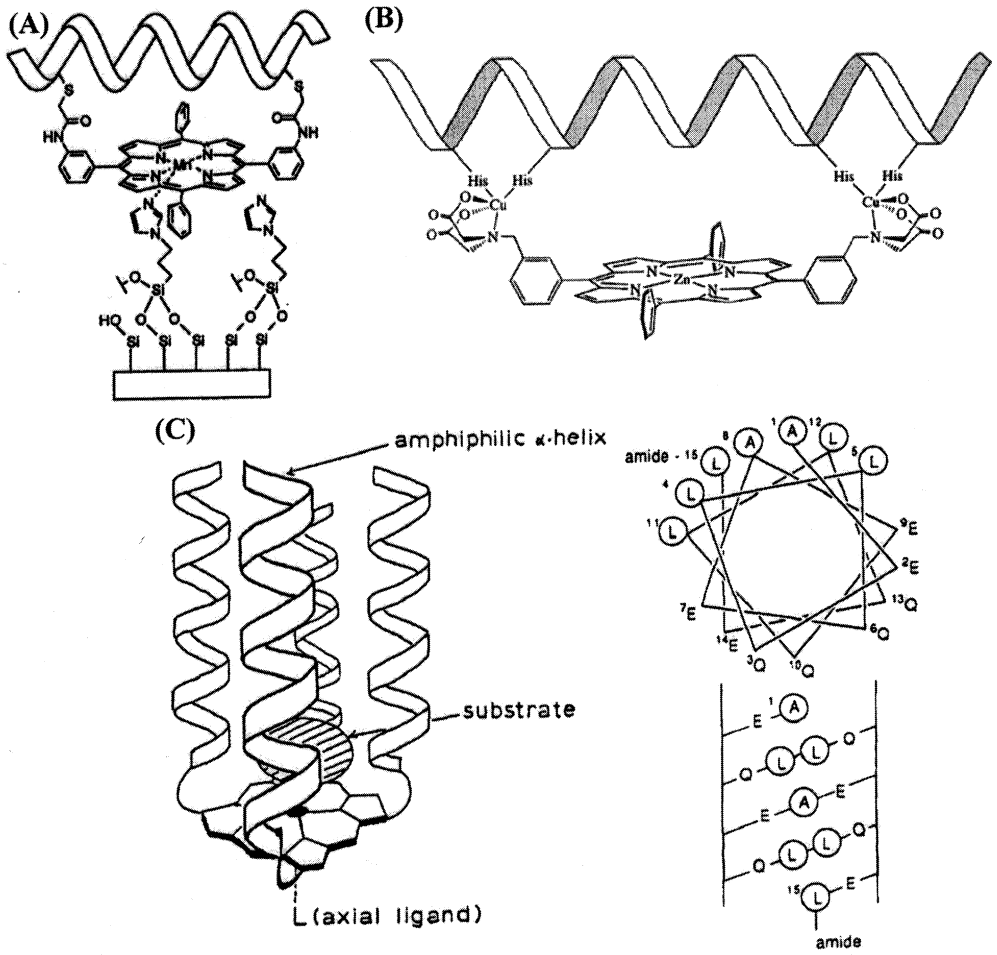

Figure 8. Templated designed heme proteins. (A) Chemical structure of a surface-bound Mn(III) porphyrin−peptide conjugate. (Reprinted with permission from ref 372. Copyright 1999 Elsevier.) (B) Diagram of helical−peptide-strapped zinc porphyrin highlighting the use of copper coordination to affix the peptide. (Reprinted with permission from ref 271. Copyright 1997 American Chemical Society.) (C) Schematic diagram of helichrome showing the proposed interaction with substrate (left) along with the helical wheel (top right) and net diagrams (bottom right) of the peptide sequence. (Reprinted with permission from ref 272. Copyright 1989 American Chemical Society.)

propionate, appear structurally similar to the microperoxidases.

Another class of covalent metalloporphyrinyl−peptides, the mimochromes,[265] are based on a natural sequence related to the β-chain F helix of hemoglobin. These mimochromes utilize a deuterioporphyrin macrocycle template attached to a hydrophobic nonapeptide rich in Leu and Ala. Like the PSMs, the peptide and heme are covalently linked by lysine side-chain−propionic acid amide bonds as well as through His coordination to the metal. Unlike the PSMs, the mimochromes require organic co-solvents or detergents for solubility because of the hydrophobicity of the designed peptide segments. The UV−vis and CD spectroscopy of the mimochromes showed the compounds to be bis-histidine-coordinated and α-helical (20%) in aqueous solutions containing 50% trifluoroethanol, a helix-stabilizing co-solvent.[265] NMR structural study[266] of the diamagnetic exchange-inert Co(III) analogue characterized the two mimochrome diastereomers in water−methanol, as described in previous reviews.[103,104] Notably, this NMR structure of Co(III) mimochrome I represents the only complete structural study of a de novo-designed heme protein.[266] Mimochrome II, a second generation design with longer peptides, was more helical due to a redesign of the flanking peptides into a leucine-rich core.[267] More recent mimochrome designs have focused on increasing the water solubility of the constructs.[104,268]

While the PSMs and mimochromes demonstrate metalloporphyrinyl−peptide construction using amide bonds to the heme propionates, other synthetic methods are available, as shown by the various models in Figure 8. The formation of thioether linkages between Cys residues and an iodoacetamide-modified free base tetraphenylporphyrin was utilized to synthesize a strapped metalloporphyrinyl−peptide complex. The 14-residue peptide was designed to fold as an amphipathic α-helix with the Leu core directed toward the porphyrin face. The pair of Cys residues were separated by three helical turns, ~16 Å, to span the porphyrin macrocycle. Consistent with the design, the free base porphyrin−peptide complex was 70% helical in 15% aqueous TFE.[269] The Mn(III) complex of this ligand, shown in Figure 8A, has been used to mediate alkene oxidation.[270] As shown in Figure 8B, a tetraphenylporphyrin moiety decorated with copper(II) ligands on two of the four *meso*-phenyl groups bound a peptide containing two appropriately spaced histidine residues and induced 47% α-helix formation.[271] Figure 8C shows that covalent attach-

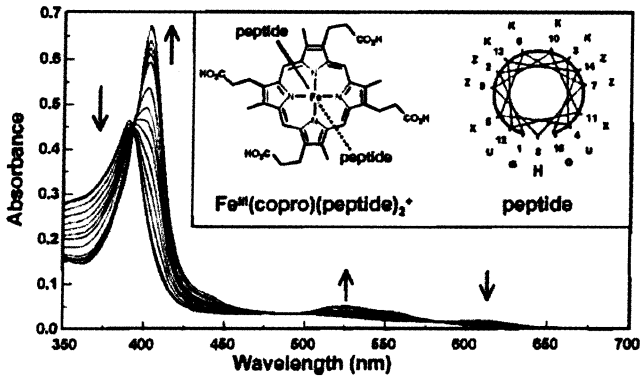

Figure 9. Spectrophotometric titration of coproporphyrin-I-ato iron(III) with peptide AA-A. Schematic representations of the peptide−porphyrin complex and helical wheel diagram are shown in the inset. (Reprinted with permission from ref 275. Copyright 1998 American Chemical Society.)

ment of four 15-residue amphiphilic peptides to the propionates of the C_4-symmetric coproporphyrin I was used to generate heliochrome, a catalytically active heme protein that mimics the function of cytochromes P-450 by oxidation of aniline to *p*-aminophenol. Attachment of the peptides to the porphyrin template induced the formation of the designed α-helices, as evidenced by CD spectroscopy. After iron insertion into the porphyrin and coordination by exogenous *N*-acetyl histidine, the oxidation catalysis was studied.[272,273] A similar approach was later used to synthesize an artificial proton channel. Four α-helical sequences were linked to free-base *meso*-tetrakis(3-carboxylphenyl)porphyrin to generate tetraphilin (well described in a previous review[104]), which forms proton-selective ion channels in lipid bilayers.[274] All of these systems utilize the attachment of the peptide to the porphyrin to template the protein secondary structure.

Spontaneous self-assembly reactions have also been used to construct metalloporphyrin−peptide complexes with a variety of peptide scaffold architectures. Palindromic 15-residue peptide sequences containing a single central histidine residue bind C_4-symmetric Fe(III)(coproporphyrin I) to form 2:1 complexes, as shown by the model in Figure 9.[275] The coordination of the iron(III) to the histidine residues can trigger up to ~40% α-helix formation in aqueous buffers. Increases in the relatively weak ferric heme association constants tracked well with the increased hydrophobicity of the peptide chain. Joining the linear peptides with a single disulfide bond increased the heme affinity by up to 6000-fold by reducing entropic penalties. Heme affinity was increased further, <2-fold, by incorporation of a second disulfide bond, which generates a cyclic peptide architecture. Preliminary paramagnetic NMR data on these constructs indicate structurally specific complexes suitable for full NMR structural study.[276] The observed increase in ferric heme affinity must also be mirrored by ferrous heme affinity since the reduction potentials remain invariant between the linear monomeric and cyclic dimeric forms of the peptide ligands. The increased affinity indicates the importance of a preorganized binding site for the heme macrocycle.[276] A helix−disulfide−helix scaffold related to the PSMs has also been utilized to investigate helix induction in a self-assembled metalloporphyrin−peptide complex. Incorporation of the exchange-inert Co(III)-octaethylporphyrin and Co(III)coproporphyrin I into a bis-His binding site results in 55% or 15% helix induction, respectively.[277] Such helix−disulfide−helix constructs can also be designed to oligomerize upon cysteine oxidation. Homodimer formation via disulfide formation between a pair of unfolded 14-residue peptides results in formation of a four-α-helix bundle scaffold. The scaffold is only 15% helical in the presence of trifluoroethanol. The non-covalent dimer binds ferric mesoporphyrin with a dissociation constant, or K_d value, of 1.7 μM, which increases the helix content of the construct to 70% α-helix in 20% TFE.[278]

Synthetic chemists have provided an interesting array of metalloporphyrin−peptide complexes. While the evaluation of many of these systems is complicated by their insolubility or instability in aqueous buffers, the minimalism of these systems has provided a clear demonstration of several concepts in metalloprotein folding. First, porphyrins are effective templates for the generation of template-assisted synthetic peptides (TASPs).[279] Second, the coordination of the metal by peptide and protein ligands can be used to nucleate and stabilize a protein fold. Third, heme binding may provide critical metal−ligand and protein−heme macrocycle contacts which may lead to uniquely structured constructs suitable for NMR and X-ray structural study. Fourth, the non-coordinating second-sphere amino acid side chains are critical to stabilizing the protein fold either by simple hydrophobic−porphyrin interactions or more specific aromatic−porphyrin contacts. Thus, hemes play a bifunctional role in protein folding. Hemes provide axial metal ion coordination sites for the interaction with polar ligands as well as the porphyrin macrocycle for interaction with hydrophobic amino acids. Interactions with either, or both, stabilize protein folds. While optimizing these interactions can be used to design desired protein folds, improper designs can lead to a competition between protein folding and metal ion ligation.

3.3. Heme Protein Design in Folded Scaffolds

As seen in Nature and mentioned earlier, heme incorporation is integral to the protein folding process. Thermodynamically, heme binding provides additional free energy for protein folding. In *apo*-proteins of low stability, heme incorporation is a major contributor to protein folding, and heme−protein interactions can trigger events such as the condensation of the unfolded state (cyt *c*) or nucleation of secondary structure elements (cyt b_{562}).[280,281] In *apo*-proteins of greater stability, the relative contribution of heme binding is lower, and heme binding may simply provide the final heme−protein contacts that define the structure to the final folded state of a natural protein (myoglobin). In either case, the accessibility of kinetic traps such as the observed misligated heme states in cyt *c* may interfere with the kinetic process of protein folding. Ultimately, the interactions of the protein at the iron via ligation as

well as at the porphyrin macrocycle by hydrophobic contacts are critical to the structural uniqueness of the hemoprotein native state, regardless of protein fold.

Using an existing stable heme protein as a structural scaffold minimizes the complexities of protein folding issues on the design of heme protein biomimetics and increases the likelihood of generating a conformationally specific design. As a type of mutational analysis of heme protein structure−function relationships, heme protein redesign attempts to alter the function of a heme protein within a natural protein scaffold. This approach involves altering key residues of a natural heme protein through site-directed mutagenesis or semi-synthesis in order to alter heme protein function. Typically, these amino acid substitutions are limited to those local to the heme binding site. Since this area has been expertly reviewed, only a cursory analysis of these research efforts will be discussed.[45,46]

The value of a priori structural knowledge of the heme protein in rational redesign cannot be overstated. The atomic-level detail of metal−ligand and protein−heme interactions provided by natural heme protein scaffolds of known structure provides a wealth of information for the redesigner. Myoglobin (Mb), the first structurally characterized heme protein, is a common scaffold for heme protein redesign. These redesigns are aided by the stability of the *apo* state of Mb and the tight affinity of Mb for heme.[120,121] We will use Mb here to exemplify the various types of redesign methodologies.

An obvious mechanism for altering the function of a heme protein such as Mb is to modify the primary coordination sphere. The axial His ligand in Mb has been replaced by either a Cys or a Tyr residue to replicate the metal ion coordination environments of cyt P-450s and catalases in the Mb scaffold, respectively.[282−285] The differences between these constructs and their natural counterparts (cyt P-450, catalase) illustrate the role of the heme microenvironment in modulating heme protein reactivity and function. While these studies alter the natural proximal His ligand, another method of varying the heme iron primary coordination sphere involves creating a cavity in the protein scaffold by replacing the axial His residue with a non-ligating Gly. This method has been successfully applied to Mb[286,287] and cytochrome *c* peroxidase.[47] These constructs have allowed for the detailed study of the effects of exogenous ligand introduction within an otherwise invariant scaffold.

The distal face of the heme binding site has also been modified to alter Mb function. Substitution of Val59 with a His residue generates a bis-His-ligated iron heme in Mb that is not capable of binding O_2 reversibly.[288−290] This construct replicates the primary coordination sphere of the electron-transfer protein cyt b_5 within the Mb scaffold. Not surprisingly, the spectroscopy and electrochemistry of this Mb mutant are similar to those of cyt b_5. The substitution of the distal His in Mb with a Phe residue removes the hydrogen bond that stabilizes the dioxygen adduct, Fe(III)($O_2^{\bullet-}$).[232] This mutation enhances the peroxidase activity 11-fold relative to that of wild-type Mb, illustrating the importance of this hydrogen bond interaction in designing against peroxidase activity.[291] These constructs demonstrate that the collection of amino acids arrayed around the heme in Mb can be modified to alter the oxygen transport function of Mb.

Redesign has also been employed to place another metal ion at the heme binding site. The introduction of two His residues on the distal face of the heme in Mb provides a distal trigonal copper binding site. The designed site shown in Figure 1D is similar to that observed at the heme a_3−Cu_B site in cytochrome *c* oxidase. The cyanide-bridged Cu−heme complex had spectroscopy similar to that of cytochrome *c* oxidase, consistent with the design.[292] Kinetic studies indicate the formation of peroxy−heme intermediates similar to those found in heme oxygenase due to the lack of protons to aid in ferryl−heme formation requisite for oxidase activity. Evidently, the globin scaffold of Mb is amenable enough to allow for the construction of complex heme protein active sites.

Aside from amino acid alterations, the porphyrin bound at the active site may be changed to modify Mb function. While the numerous studies of Mb with synthetic porphyrins cannot be detailed here in toto, two recent studies illustrate the breadth of the research in this area. First, iron mesoporphyrin IX with modifications at the propionic acids has been placed in Mb. The resulting positively or negatively charged Mbs bind other proteins or small molecules at the charged binding site.[293] The Mb scaffold has also been used to construct artificial photosynthetic reaction centers. Myoglobin was reconstituted with an iron or zinc protoporphyrin covalently bound to a photoactive ruthenium tris(2,2′-bipyridine) linked to a cyclobis(paraquat-*p*-phenylene). Laser flash photolysis of this complex resulted in long-lived charge separation.[127] Thus, the stability of the protein scaffold and the high affinity for heme make myoglobin amenable for heme protein redesign efforts based on cofactor substitution.

A more drastic example of heme protein redesign is observed in the re-engineering of non-heme natural protein scaffolds into heme proteins. The nucleic acid binding protein ROP,[294] the ColE1 repressor of primer from *E. coli*, is a coiled-coil protein composed of two antiparallel helix−turn−helix subunits. Protein redesign was first used to convert the natural dimeric construct into a monomeric protein architecture which retains the RNA binding ability of the natural scaffold.[295] The monomeric ROP was further modified first to remove potential heme-binding residues and then to incorporate a bis-histidine binding site for heme.[296] Upon heme incorporation, the protein had similar absorption spectra and electrochemical behavior compared to natural and synthetic heme proteins. While the conformational specificity of the *apo*- and *holo*-proteins is unreported, this example demonstrates that non-heme proteins may be used as scaffolds for heme protein design. Additionally, it demonstrates aspects of both negative (removal of other heme ligands) and positive (building the desired site) design.

Efforts to redesign heme proteins and insert heme binding sites into other natural proteins aided by structural data have shown notable success. This approach offers considerable flexibility in heme protein ligand design. The number and type of ligands, the type of heme, the presence of other cofactors, the polarity of the heme site, the solvent accessibility of the site, and the position of the heme relative to the backbone fold can all be altered using heme protein redesign. The only fundamental restraint is the use of an existing protein architecture as the scaffold.

The second approach to the construction of biomimetic heme protein assemblies, de novo heme protein design,[103,104] allows for complete tailoring of the protein ligand, including the global fold. As such, the complexities of protein folding become integral to the design process since each level of protein structure hierarchy must be specified. The primary structure, or sequence, is designed to fold into particular secondary structure elements, which combine to yield the tertiary and quaternary structure of the final design. In addition to solving the inverse protein folding problem, the selected sequence must also place the heme iron ligands and hydrophobic contacts in the appropriate three-dimensional arrangement for heme binding. This approach is considerably more challenging than protein redesign due to both the added complexities of protein folding/conformational specificity and the lack of a priori structural data. One consequence of this fact is the current lack of X-ray or NMR structures of any de novo-designed heme protein. Indeed, the NMR data on many designed heme proteins are consistent with dynamic hydrophobic cores and/or protein aggregation at NMR concentrations.[297] Such was the situation a decade ago with respect to *apo*-protein scaffolds, and rational, combinatorial, and computational methods have evolved to provide X-ray and NMR structures consistent with the intended designs.[298−306] The studies indicate the importance of properly packing the hydrophobic core with low-strain rotamers to achieve singularity of structure. In fact, the alteration of a few residues can transform a sequence with poor chemical shift dispersion and large linewiths in the NMR spectrum, due to folding−unfolding equilibria, hydrophobic core mobility, poor packing, and/or nonspecific oligomerization, into a protein with NMR characteristics similar to those of natural proteins.[307−309] A recent report that utilizes a rational design strategy based on the *apo*-maquette structure indicates that a structure of a diheme maquette is on the horizon.[310] Despite the current lack of a structurally characterized heme protein, de novo heme protein design has shown remarkable progress in the past 10 years, aided by advances in protein design.

In a report that predates the incorporation of a heme into ROP by nearly a decade, one member of a family[311] of minimalist amphiphilic α-helical peptides that self-assemble into four-helix bundles was redesigned to incorporate a heme group. The construct, α_2(S−S), was composed of two helix−loop−helix monomers, α_2, linked by an N-terminal cysteine disulfide bond, (S−S), which provides a monomeric construct from two identical subunits. While there is no detailed structure of α_2(S−S), rational redesign of a related sequence yielded a conformationally specific *apo*-protein, α_2-D, whose structure was determined by NMR methods.[301] The centrally located Leu at position 25 of each α_2 monomer in α_2(S−S) was replaced by a His to bind a single heme in a bis-His fashion across the bundle interior. Computer modeling suggested further changes to the core residues in order to accommodate the heme macrocycle: positions 22 and 29 were changed to Val and position 11 was changed to Ala. Thus, the design attempted to account for the requirements of the metal center as well as the heme macrocycle. The resulting design, $VAVH_{25}$(S−S), and its sequence-reversed analogue, called retro(S−S) and shown as a molecular model in Figure 10A, both formed four-helix bundles in solution and bound heme with differing consequences.[56] The peptide $VAVH_{25}$(S−S) was highly helical in the absence of heme, the *apo* state, and bound heme with minimal change in helical content or hydrodynamic radius. However, UV−vis, EPR, and cyanide binding experiments suggested a mixture of six- and five-coordinate ferric iron, indicating some deviation from the intended design. The retro(S−S) protein, however, had spectroscopic signatures of pure six-coordinate ferric heme by the same methods and also showed a decrease in hydrodynamic size and a 20% increase in helicity upon heme binding. Additionally, the UV−vis spectra of ferric and ferrous heme in retro(S−S) was comparable to that of cyt b_{559}, a natural bis-His-ligated heme protein. Compared to $VAVH_{25}$(S−S), retro(S−S) bound ferric heme more tightly (>70-fold) and had a 50 mV more negative reduction potential at −220 mV vs SHE. The authors suggested that the retro(S−S) protein had a less structured hydrophobic core in the *apo* state that allowed it to better accommodate the heme than $VAVH_{25}$(S−S), which is more structured in the *apo* state.

Four-α-helix bundle heme proteins have also been fabricated using an alternative strategy of affixing the helices to a template to generate a TASP. The early heme protein TASPs, heliochrome[272] and tetraphilin,[274] utilized modified porphyrins as templates to generate C_4-symmetric four-α-helix bundles. Using organic templates allows for the design of self-assembled heme binding sites within the attached peptides themselves. The modular proteins (MOPs)[312] utilize a cyclic decapeptide with four covalent attachment points as the template and rely on self-assembly reactions for heme incorporation. Figure 10B illustrates a molecular model of one of the di-heme MOPs, MOP1, whose pairs of different helices were covalently linked to the template in a C_2-symmetric array. One of the two pairs of peptides contains a central histidine to affect heme binding, and the other pair is devoid of histidine residues. The mono-heme MOPs, mMOP1 and mMOP2, are constructed from 21-amino acid peptide modules that contain a single bis-His heme binding site.[313] UV−vis and EPR spectroscopy demonstrate ferric heme binding to mMOP1 and mMOP2, which differ in sequence on the peptides that do not contain His ligands. Detailed EPR

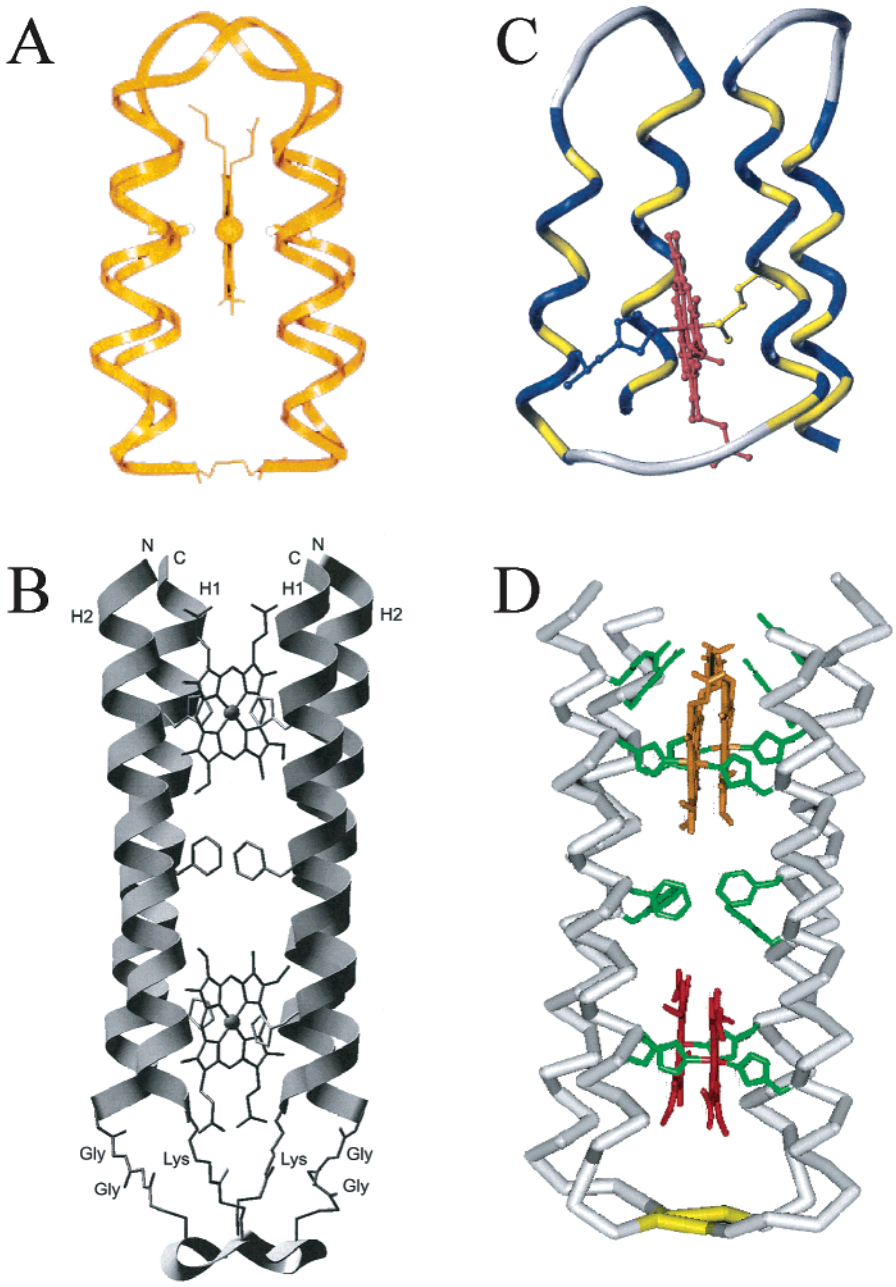

Figure 10. Molecular models of several four-α-helix bundle heme protein designs. The designs of (A) retro(S−S) (Reprinted with permission from ref 56. Copyright 1994 American Chemical Society.), (B) MOP1 (Reprinted with permission from ref 312. Copyright 1998 American Chemical Society.), (C) Protein 86 (Reprinted with permission from ref 324. Copyright 1997 The Protein Society.), and (D) $[H10H24]_2$ (Reprinted with permission from ref 73. Copyright 1994 Nature Publishing Group.) are discussed in the text.

of both heme proteins shows evidence of heterogeneous structure at the heme with histidine planes parallel (major) or twisted (minor) relative to each other. The electrochemistry of the constructs was within experimental error of each other, -164 ± 10 mV for both and -153 ± 5 mV for mMOP2, despite the expected electrostatic changes due to the replacement of two cationic arginine residues in mMOP1 for two neutral tryptophans in mMOP2. As illustrated here, TASPs provide another viable approach toward to the fabrication of synthetic heme proteins.

Heme protein designs are not restricted to four-helix bundle scaffolds. A two-α-helix bundle, H2α(17), was designed to bind Fe(III) mesoheme between a pair of amphiphilic peptides.[314] The pair of 17-amino acid peptides of H2α(17) contained a centrally located histidine residue and a C-terminal cysteine that was oxidized to form the homodimer. Ferric mesoheme binding was tight and resulted in minor changes in peptide helicity and stability. The peptides were then used to quantify the effects of leucine hydrophobes in the hydrophobic core and the presence of a salt bridge on the ability of the protein to bind mesoheme. Three-helix bundles have also been utilized as heme protein scaffolds. Using a series of disulfide bonds, a three-α-helix bundle scaffold was constructed in a helix−disulfide−helix−disulfide−helix architecture.[315] One of the helical peptides in the scaffold contains an iron mesoporphryin covalently attached to a lysine residue in an analogous

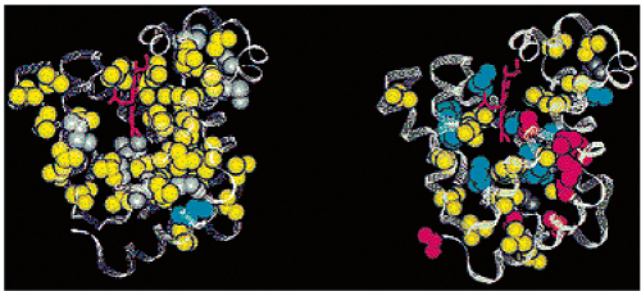

Figure 11. Comparison of Designed Globin-1 to sperm whale myoglobin. The distribution of Leu (yellow), Met (white), Val (red), and Ile (blue) residues in each is shown. (Reprinted with permission from ref 390. Copyright 2000 American Chemical Society.)

fashion to the PSMs. Heme ligation in this scaffold has been designed to be either bis-His or mono-His as a model for peroxidases. In the bis-His design, the complex is six-coordinate in the ferric state but may lose a ligand upon reduction. The ferric heme iron designed at the mono-His site recruited a distal histidine, one helix turn away, to generate a six-coordinate bis-His coordination sphere. Thus, this system provides an unmistakable example of the competition between the preferences of the metal ion ligation and protein folding.

The use of a larger, more stable protein fold might appear to allow the protein designer to use protein folding to dominate the inherent coordination preferences of the heme iron. One design aimed at generating a five-coordinate mono-His-ligated heme has utilized the globin fold.[316] Designed Globin-1 (DG1) was computationally designed to obtain a sequence that could match the backbone trace of sperm whale myoglobin, the prototype five-coordinate mono-His-ligated heme in a globin fold. As shown in Figure 11 as a model, DG1 represents a whole-scale redesign of myoglobin as the pair have only a 26% sequence identity, including the proximal and distal heme-binding histidines, which were fixed in order to retain function. DG1 is a highly α-helical monomeric protein of molecular dimensions comparable to Mb, consistent with the intended design. However, UV−vis and resonance Raman spectroscopies show evidence of a low-spin, six-coordinate ferric state and a mixed low-spin, six-coordinate/high-spin, five-coordinate ferrous state, indicating that the heme iron has recruited the distal histidine as an axial ligand. DG1 was not able to bind dioxygen reversibly but did show similar CO binding spectroscopy. DG1 was redesigned by replacing Leu with more conformationally restricted Ile and Val residues to increase structural specificity.[317] Thus, even in larger, more stable folds, evidence is seen for the competition between the requirements of protein folding and metal ion ligation.

Aside from all α-helical protein folds, forays into the design of heme proteins containing β-sheets have been made. A unique design of a $\beta\alpha\beta\alpha$-like heme protein has been made by covalently linking two identical peptides to an iron tetratolylporphyrin via an ornithine residue on the hydrophobic side of the first β sequence.[318] Each α sequence contains a His to bind the heme iron in a bis-His fashion. The helical content was 33%, only slightly lower than the 45% predicted by design. CD and UV−vis spectroscopy of the ferric heme were consistent with low-spin intramolecular bis-His coordination in pH 7.2 buffer. There is also an example of a designed protein which converts from β-sheet to α-helix upon heme binding.[319,320] A variant of the H2α(17) peptide discussed above was found to be β-sheet and highly aggregated in 1% trifluoroethanol. However, addition of ferric mesoheme resulted in the formation of a tetrameric α-helix-containing heme. Thus, in this case the protein aggregation state as well as the global fold are in competition with heme iron ligation.

While the systems described above have relied on rational design approaches implemented with iterative cycles of design−synthesis−analysis, combinatorial methods have also proven successful in heme protein design. Two different combinatorial libraries of four-α-helix bundle heme proteins have been de novo designed. The initial library was designed to demonstrate that the simple binary pattern of hydrophobic and hydrophilic amino acids was sufficient to generate a folded four-α-helical bundle structure.[321] Out of a possible 10^6 sequences in the library, 108 clones were chosen, of which 48 possessed sequences consistent with the binary pattern design. Of these 48, 29 were resistant to proteolytic degradation and expressed well. All were four-α-helix bundles, and one contained a conformationally specific hydrophobic core.[322] Indeed, recent NMR studies from a related combinatorial library of larger four-α-helix bundles show several candidates for structural characterization.[323,305] Since the potential heme ligands His and Met were included in the original library as hydrophilic and hydrophobic residues, respectively, the library was screened for heme binding. Of the 29 four-helix bundle proteins, all contain His and Met and 15 contain bound Fe(III) heme.[324] UV−vis and resonance Raman spectroscopy indicated low-spin, six-coordinate hemes in proteins F, G, and 86, the three library members selected for detailed study. The ferric hemes in proteins F and G are bis-His-ligated; however, the precise positions of the ligands are not known since proteins F and G contain four and seven histidines, respectively. Despite the lack of a sulfur-to-iron charge-transfer band in the absorbance spectrum, the authors suggest that Protein 86 (5 His, 3 Met) is His-Met-ligated, as modeled in Figure 10C, on the basis of the resonance Raman spectroscopy results. The binding of CO to the ferrous Protein 86−heme complex suggests that an endogenous ligand can be replaced.[325] Furthermore, a resonance Raman spectrum of the CO complex shows the macrocycle to be more solvent exposed than in Mb and not in contact with a Lewis acid or base. Additionally, the library of heme-binding proteins has been screened for peroxidase activity, with Protein 86 displaying significant reactivity.[92] Recently, the midpoint reduction potentials of several of these proteins along with three others from a subsequent library were determined. The potentials ranged from −112 to −176 mV vs SHE.[326] The success of this combinatorial library illustrates that heme binding and catalytic function need not be designed a priori.

A second combinatorial library utilized the modular synthesis developed for MOP1, the rationally designed heme-binding four-α-helix bundle, to generate a library of 462 proteins by varying residues within the protein interior.[327] A shorter, C_2-symmetric MOP scaffold was designed with two A helices and two B helices diagonally disposed across the template. The B helices (the binding helix) contained a central His, at position 9, and the amino acids within a helical turn were varied at positions 4, 5, 8, and 12. Similarly, the hydrophobic core amino acids on helix A (the shielding helix) thought to contact the heme were altered, to positions 4, 5, 8, 11, and 12. The heme-binding His residues were not altered, and all of the library members bound heme, as evinced by UV−vis spectroscopy. A cursory evaluation of the midpoint reduction potentials of the heme proteins on a cellulose membrane indicated a range of −90 to −150 mV vs SHE. While a clear relationship between the midpoint reduction potentials and the amino acid sequences is not readily apparent, it is interesting to note that the peptides with QVLL as the binding helix have more positive potentials and the peptides with GLGGL as the shielding helix show lower potentials. These data show a ∼1.5 kcal/mol modulation of heme electrochemical function in this library.

The progress of rational and combinatorial methods of heme protein design is shown by the success of these de novo metalloproteins. Heme incorporation into a variety of α-helical and mixed α/*β* protein scaffolds has been accomplished using histidine ligands. While four-α-helix bundles remain a common scaffold choice, examples of globin designs and more elaborate α/*β* scaffolds exist. The emerging structures of related *apo*-proteins suggests that structures of *holo* de novo-designed heme proteins may be forthcoming. In terms of heme ligands, the vast majority of designs utilize histidine to ligate the ferric heme iron, typically as six-coordinate low-spin bis-His Fe(III) heme. While these systems mimic the most prevalent secondary structure and ligand choice found in the CATH wheel analysis of natural heme proteins, all of the designs represent novel heme proteins whose spectroscopic and electrochemical properties mimic those of natural heme proteins. Thus, these systems clearly demonstrate that peptide and protein ligands can be used to generate a variety of biomimetic heme protein assemblies.

3.4. Complex Metalloprotein Construction

The documented success of heme protein design efforts has led to ever more ambitious metalloprotein designs. One of the unique properties of natural protein ligands[98] is their ability to organize sites in multi-center enzymes such as those found in photosynthesis and respiration. The elegance of natural coordination chemistry is illustrated by the cytochrome bc_1 complex, which is composed of two *b*-hemes, one *c*-heme, a [2Fe-2S] cluster, and two quinones within multiple protein subunits.[328] Inspired by the complexities of natural protein enzymes, bioinorganic chemists have begun to employ protein design to assemble multi-cofactor proteins as synthetic analogues. These designs provide the ability to model the electron-transfer chains and active sites of enzymes involved in multi-electron catalysis. Complex metalloprotein systems have been engineered either to contain more than one heme moiety or to combine a heme with another biological cofactor. Thus, protein design has progressed to allow synthetic routes to the construction of models of complex metalloproteins.

The first report of a de novo-designed multi-heme protein was $[H10H24]_2$, the prototype heme protein maquette whose molecular model is shown in Figure 10D.[73] In analogy to the architectural definition of the term "maquette" as a scaled-down model of a building, protein maquettes are simplified models of natural proteins, or peptide-based synthetic analogues, as shown in Figure 12A. The design of $[H10H24]_2$ was the conceptual amalgamation of the de novo-designed α_2 protein, a dimeric four-α-helix bundle,[311] and the di-heme cytochrome *b* subunit of the cytochrome bc_1 complex.[329] The design was based on a minimalist designed 27-amino acid α-helix sequence with an N-terminal CGGG segment that upon disulfide bond formation provided the loop for (α-SS-α) construct. The (α-SS-α) monomers self-assemble in aqueous solution to form the four-α-helix bundle, or $(\alpha\text{-SS-}\alpha)_2$. Thus, the maquette architecture is a homotetrameric four-α-helix bundle arranged as a non-covalent dimer of disulfide-bridged di-α-helical subunits, an architecture not observed in biology. While many of the *apo*- and *holo*-maquettes are not uniquely structured in solution, iterative redesign has provided several *apo*-maquette scaffolds[67] and an initial *holo*-maquette[310] with high levels of conformational specificity suitable for NMR structural study. The solution[302] structure of one of these *apo*-maquette scaffolds demonstrates excellent conformational specificity within the di-α-helical mononer but disorder between the disulfide-bridged monomers which is not observed in the solid-state structure.[303] The X-ray structure shown in Figure 12B demonstrates that significant reorganization of the maquette occurs upon heme binding, i.e., rotation, separation, and realignment of the helices, which leads to a loss of conformational specifity.

$[H10H24]_2$ contains several deviations from a minimalist protein design,[330] all of which are in functional analogy to the cyt bc_1 complex. Histidines were placed at positions 10 and 24 of each helix, hence the name $[H10H24]_2$, to provide for axial ligands for heme. A phenylalanine was placed between the histidine positions to separate the heme binding sites, and an arginine was placed local to the His24 heme binding site to modulate the heme affinity and electrochemistry. $[H10H24]_2$ is a stable, folded four-α-helix bundle in the *apo* and *holo* states. As designed, $[H10H24]_2$ binds four equivalents of ferric heme with sub-nanomolar to micromolar dissociation constants, as evinced by spectrophometric titrations.[73] UV−vis, resonance Raman, and EPR spectroscopies confirm low-spin, six-coordinate bis-histidyl ligation within a low-dielectric hydrophobic core.[331] Electrochemical measurements, E_m values of −80 to −230 mV, show a heme−heme electrostatic interaction across the hydrophobic core due to a low-dielectric protein

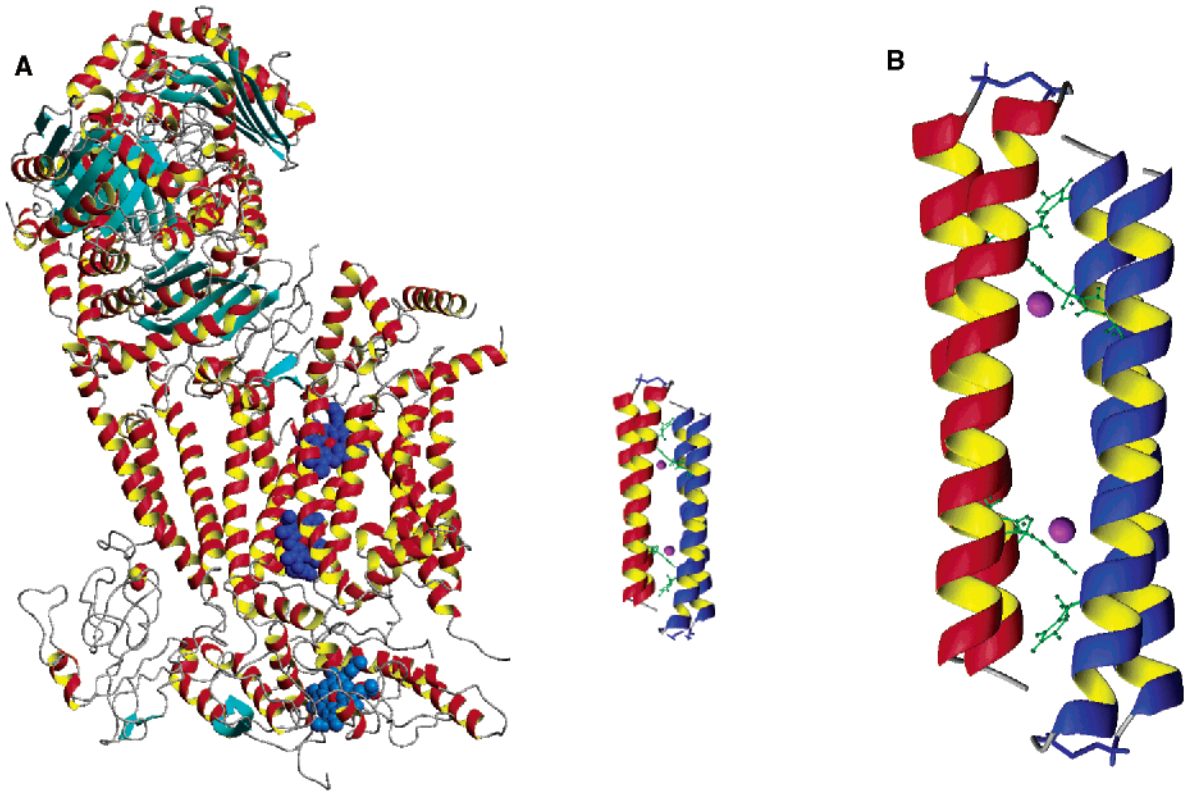

Figure 12. (A) Comparison of the X-ray structures of the cytochrome bc_1 complex[328] and the *apo*-maquette scaffold, $[H10H24\text{-}L6I,L13F,L31M]_2$,[303] demonstrating the relative size and complexity of each. (B) For clarity, the X-ray structure of the maquette scaffold is shown on a larger scale with the heme-binding His residues.[303]

interior. The replacement of the histidine residues in $[H10H24]_2$ with non-ligating alanine residues, generating the di-heme $[H10A24]_2$ and $[A10H24]_2$ heme protein maquettes, reduced the heme:protein stoichiometry and allowed delineation of the electrochemical behavior of the parent $[H10H24]_2$. Ultimately, these studies demonstrate the individuality of each of the heme binding sites within this ligand, a property common to natural multi-cofactor proteins.

While the prototype heme maquettes are 28 amino acids in length, in analogy to the membrane-spanning helices of the cyt bc_1 complex, smaller heme protein maquettes closer in size to retro(S−S) have been prepared. Truncation of the maquette sequence by seven amino acids (a heptad) provides a mechanism to shorten the $(\alpha\text{-SS-}\alpha)_2$ scaffold length and evaluate the transferability of metal binding function.[332] The initial truncated maquette, $[\Delta 7\text{-}H_{10}I_{14}I_{21}]_2$, demonstrates ferric heme affinity (140 pM), spectroscopy ($\lambda_{max}^{Fe(III)} = 412$ nm), and electrochemistry (−222 mV vs SHE) similar to the parent maquette, suggesting that, in the absence of protein folding issues, function can be transferred between maquette scaffolds reliably.

The full-size $[H10H24]_2$ maquette scaffold has also been used to incorporate other porphyrin cofactors. A series of natural and synthetic hemes were incorporated into the $[H10A24]_2$ to evaluate the steric aspects of hemes binding at adjacent sites. A pair of free-base coproporphyrins was appended to $[H10H24]_2$ to mimic the special pair of bacteriochlorophylls in an initial photosynthetic reaction center maquette.[83] The stepwise addition of heme *b* and then heme *a* to $[H10H24]_2$ and $[H10A24]_2$ has been used to study the effect of porphyrin architecture on heme reduction potentials and to construct an initial cytochrome ba_3 oxidase maquette.[333] To study the influence of heme−heme electrostatics on heme reduction potentials, the di-heme $[H10H24]_2$ was compared to the mixed Zn(II)(protoporphyrin IX)−Fe(III)(protoporphyrin IX) complex. Last, Zn(II)(protoporphyrin IX) was incorporated into a designed helix−loop−helix protein based on $[H10H24]_2$ with one histidine per monomer. This construct demonstrated tighter affinity for $[Zn(II)(protoporphyrin\ IX)]^0$ than $[Fe(III)(protoporphyrin\ IX)]^+$.[334]

An all-parallel four-helix bundle similar to the maquette scaffold was designed to incorporate four hemes perpendicular to each other, similar to the orientation of hemes *a* and a_3 in cytochrome *c* oxidase.[335] This design, 6H7H, utilized a side-chain packing algorithm, CORE, to computationally design the hydrophobic core. Two 27-amino acid peptides were linked by C-terminal disulfide bonds and formed a non-covalent four-helix bundle in solution. The four heme binding sites were located at the N-termini with histidine residues at positions 6 and 7 on each helix. The protein bound four hemes *b*, although the third and fourth hemes bound weakly with millimolar dissociation constants. Electrochemical measurements demonstrated two reduction potentials of −150 and −250 mV due to heme−heme electrostatic interactions.

Multi-porphyrin complexes have also been assembled in the TASP architectures. The original four-α-helix bundle TASP, MOP1, was designed on the

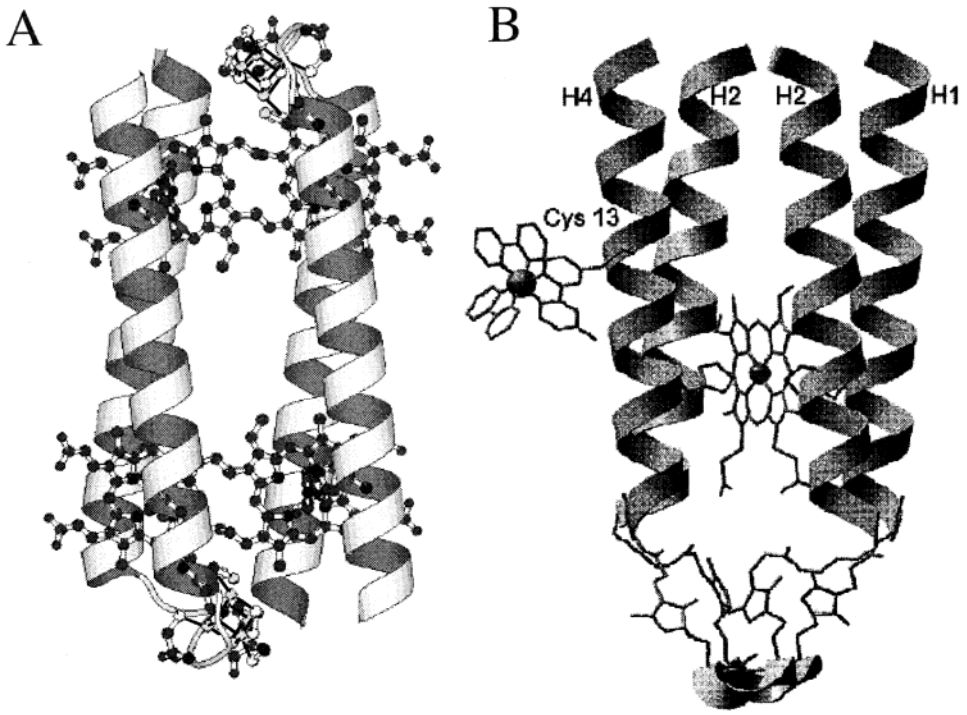

Figure 13. Molecular models of (A) the ferredoxin-heme maquette (Reprinted with permission from ref 70. Copyright 1996 National Academy of Sciences.) and (B) Ru-MOP3 (Reprinted with permission from ref 347. Copyright 1998 National Academy of Sciences.), two examples of multi-component complex metalloprotein designs.

basis of the cytochrome *b* subunit of the cytochrome bc_1 complex.[312] The heme-binding residues and those in contact with the heme were conserved from the natural bc_1 complex, while exterior residues on the helices were changed to charged amino acids to impart aqueous solubility to MOP1. The protein was highly helical in both the *apo* and *holo* states, with a moderate increase in helicity upon heme binding. The binding to two bis-His-ligated hemes stabilized the protein scaffold by 4.0 kcal/mol. EPR spectroscopy demonstrated the presence of a low-spin ($S = {}^1/_2$) ferric heme, consistent with the bis-His design. Furthermore, the rhombic splitting of the EPR signal demonstrated that one ferric heme had a parallel orientation of the histidine imidazole ligands while the other ferric heme was bound by perpendicularly orientated histidines.[336] ENDOR spectroscopy confirmed that the imidazole histidines were binding through the N^{ϵ}.[337] More recently, these modular proteins have been used to study the binding of Zn-chlorophyll derivatives[338] and Cu(II) to four-α-helix bundle scaffolds.[76]

Another multi-porphyrin TASP was developed to construct a synthetic heme protein with multiple hemes in contact with each other. The template, α_4-*meso*-tetra(*o*-aminophenyl)porphyrin, was designed to condense four 18-amino acid peptides into a monomeric four-α-helix bundle.[339] Each peptide contains two histidine residues as potential heme ligands, for a designed heme:TASP stoichiometry of 4:1. The TASP displays only 7% α-helix secondary structure content in aqueous solution, indicating that proximity of the peptides was not sufficient to impart helix structure. Heme binding increases the helical content of the peptide and shifts the aggregation state equilibrium of the construct from dimer to trimer. Ultimately, three exogenous hemes bind to a trimer of TASPs.[340]

Last, in multi-heme protein design, a single polypeptide four-helix bundle protein was designed for the incorporation of a di-porphyrin cofactor.[341] Histidines are placed on the first and third helices of the design to provide ligands to a metalloporphyrin. The bis-His binding site was offered a lysine with a Zn(II) mesoporphyrin and a Ni(II) mesoporphyrin covalently linked to the α- and ϵ-amine groups, respectively. CD and UV−visible spectroscopy were consistent with ligation of the Zn(II) mesoporphyrin into the bundle in the presence of a micelle. The resulting construct shows efficient energy transfer, as studied by fluorescence.

The engineering of mixed-cofactor constructs introduces the complexities of binding site selectivity and specificity into design process. The heme protein maquette $[H10H24]_2$ has been converted from the $(\alpha\text{-SS-}\alpha)_2$ architecture into an $(\alpha\text{-loop-}\alpha)_2$ protein to provide a construct amenable for mixed-cofactor metalloprotein design.[342] Figure 13A shows a model of the ferredoxin−heme maquette that was designed from $[H10H24]_2$ by using the inherent coordination chemistry preferences of hemes and [4Fe-4S] clusters to provide the necessary binding site selectivity.[70] Combining the linear bis-His heme binding sites from the helices of $[H10H24]_2$ with a loop region containing a tetrahedral $(Cys)_4$ site for [4Fe-4S] incorporation yielded a successful multi-cofactor metalloprotein. The order of cofactor incorporation was critical to the assembly of the multi-cofactor protein. Attempts to incorporate the ferric hemes prior to insertion of the [4Fe-4S] clusters led to Cys ligation as a kinetic product that converted into the bis-His thermodynamic product over time. The ferredoxin−heme

maquette design has since been modified to generate a bridged Ni(II)−[4Fe-4S] center as a model for the spectroscopic A-cluster of carbon monoxide dehydrogenase, further demonstrating the versatility of the maquette as a scaffold for mixed-cofactor designs.[87,88]

While the mixed [4Fe-4S]−heme and [4Fe-4S]−Ni(II) designs utilized cysteine residues for [4Fe-4S] binding, mixed-cofactor designs need not utilize different ligand types to provide specificity. A four-α-helix bundle containing two different metal cofactors bound by bis-His ligation and capable of photoinduced electron transfer has been designed using the aforementioned CORE algorithm.[343] The designed artificial reaction center (aRC) consists of two 54-amino acid helix−loop−helix proteins linked by a C-terminal disulfide bond. A photoactive ruthenium bis(bipyridine) (cis bis-His ligation) electron donor and a ferric heme electron acceptor (axial bis-His) were introduced at two interior bis-histidine binding sites and used to facilitate electron transfer from cytochrome *c* to naphthoquinone-2-sulfonate. More commonly, designers utilize cysteine residues to covalently attach cofactors, which provides binding site specificity. The flavocytochrome maquette was constructed by attaching a flavin analogue, 1-acetyl-10-methylisoalloxazine, to a unique cysteine residue two helix turns removed from the heme-binding His residue.[84] Incorporation of either Fe(III)(protoporphyrin IX) or Fe(III)(1-methyl-2-oxomesoporphyrin XIII) resulted in a functional photoactive electron-transfer protein. Similar chemistry has been utilized to attach flavins to a variety of designed protein scaffolds. A membrane-bound flavohemoprotein design utilized a Mn(III)(porphyrin) as a template for four-α-helical peptides whose sequences were based on the membrane-embedded segment of bacteriorhodopsin.[344] The flavin was covalently attached to a Cys on one of the helices 13 amino acids away from the Mn(III)(porphyrin). The presence of both cofactors was confirmed by UV−vis and fluorescence spectroscopy. Another designed flavohemoprotein was constructed by incorporation of a flavin, 7-acetyl-10-methylisoalloxazine, in the $\beta\alpha\beta\alpha$-like heme protein.[345] The flavin was attached to the hydrophilic surface of the second β sequence using a unique Cys residue. The flavin did not disrupt helicity (34% found, 37% expected) or iron coordination (low-spin, monomeric ferric porphyrin by CD and UV−vis) and increased the rate of electron transfer from an exogenous reductant to the heme by a factor of 6.

Cysteine residues have also been used to provide attachment points for other cofactors. A nitroxide spin-label was linked to a Cys residue in a dimeric helix−loop−helix maquette with free-base coproporphyrin attached to the N-terminus via an amide bond.[346] The constructs containing either or both cofactors were used to study the influence of the two cofactors on the four-helix bundle topology. A cysteine was used to append a ruthenium tris(bipyridine) complex to the diheme MOP four-α-helix bundle as a photoactive electron donor, as modeled in Figure 13B.[347] The cysteine residue was placed in either position 13 or 16 on one helix in order to study the distance dependence of photoinduced electron transfer. A tetratolylporphyrin was covalently linked to a cysteine in a 29-residue helix−loop−helix amphiphilic peptide designed to dimerize into a four-α-helix bundle.[348] The position of the porphyrin on the Cys residue was at the interface of the hydrophilic and hydrophobic faces of the helices and was designed to assist protein dimerization by way of porphyrin−porphyrin cofacial stacking. Both the free base and ferric porphyrin peptides formed di-heme four-helix bundles despite the lack of axial ligands for the latter.

Protein design in de novo or natural scaffolds facilitates the construction of multi-component complex metalloproteins. These initial forays catalogued above illustrate the feasibility of using designed scaffolds for the construction of multi-component proteins. The incorporation of multiple copies of the same cofactor involves creating several sites at the design stage. Often, these complex metalloprotein designs utilize symmetry as a conceptual tool to generate multiple copies of the binding site within a scaffold. The asymmetry required for the design of complex metalloproteins with different cofactors requires the introduction of some level of selectivity or specificity. In the case of systems that rely on spontaneous self-assembly, this selectivity can be achieved by the simple order of addition as observed in the case of the heme *a*−heme *b* maquette, or by the design of cofactor binding sites with different ligand types/numbers/geometries, as evinced by the design of the ferredoxin−heme maquette. In covalently bound constructs, the attachment of cofactors to the protein scaffold provides site specificity driven by the synthesis, as illustrated by the spin label/coproporphyrin construct used to evaluate the topology of the maquette scaffold. The design of Ru-MOP3 and the flavocytochrome maquette demonstrate that covalent attachment of cofactors can be readily combined with self-assembly to generate complex metalloproteins. The combination of hemes with other metalloporphyrins, iron−sulfur clusters, flavins, and Ru(bipyridyl) complexes has provided simple design concepts for the construction of multicenter complex metalloproteins. The current challenge is to continue to develop the coordination chemistry of proteins to generate novel design concepts for the fabrication of complex metalloproteins.

4. Designed Heme Protein Engineering

4.1. Structural Engineering

The collection of heme protein designs enumerated above contains a diverse and ever-expanding range of proposed structures that are not specifically found in nature. Analysis of this collection begins to provide insight into the fundamental engineering of heme proteins absent the constraints imposed by biology. Here, we explore the range of designed heme proteins in order to set down the engineering specifications and tolerances for heme protein design, cognizant of the fact that new designs continue to expand these limits. A future comparison of natural and designed heme protein structure and engineering may begin to reveal the constraints imposed by biology and provide further insight into heme proteins.

As observed in natural heme protein structures, histidine is the most common ligand in de novo heme protein design. Most frequently, designed proteins utilize six-coordinate bis-His ligation to effect heme incorporation. Typically, designed heme proteins are presumed to utilize N^{ϵ} to coordinate the heme iron, as demonstrated for MOP by ENDOR spectroscopy,[336] but a single example of designed N^{δ} coordination is extant.[56] These bis-His designs normally yield low-spin ($S = {}^1/_2$) ferric hemes with characteristic optical ($\lambda_{max} = 412-414$ nm; $\epsilon \approx 110-140$ mM^{-1} cm^{-1}) and EPR spectra (rhombic, *g*-values of 2.92, 2.27, and 1.51) consistent with the proposed coordination sphere. One-electron reduction yields low-spin ferrous hemes with shifted and more intense optical spectra ($\lambda_{max} = 424-426$ nm, $\epsilon \approx 150-200$ mM^{-1} cm^{-1}), including α/β bands indicative of coordination number and spin state. The observation of less intense reduced state spectra than the corresponding ferric heme spectra in several designs indicates loss of ligands/heme/protein during reduction.[296]

As expected, the relative location of the histidine residues in proteins impacts the ability to bind heme. In the case of the peptide-sandwiched mesohemes, an $i,i+4$ or $i,i-4$ spacing of the ligating histidine and the lysine tether is optimal, with other spacing resulting in springboard strain, as evidenced by minor high-spin species.[264] In the case of helical bundle proteins, the only systematic study of histidine position demonstrates that bis-His ligation in a maquette scaffold is best accomplished using interior heptad *a* positions followed by the exterior heptad *b* positions (600-fold weaker).[349] Consistent with these findings, many successful designs utilize *a*-*a* histidine ligation ($[H10H24]_2$, MOP1), while some employ the interfacial positions, *e*-*e* (retro(S−S)[56]) and *d*-*d* (ROP[296]). Interestingly, the combinatorial heme proteins 86, F, and G use histidines in exterior positions (*b*, *c*, *f*, or *g*) exclusively for heme ligation due to their sequence design. The Met ligand in Protein 86 is derived from an interfacial helix *e* position. The other members of the library demonstrate that the mere presence of multiple His and Met residues does not ensure heme binding; e.g., Protein 49 does not bind heme and contains 10 His and 7 Met residues.[324] The ferric heme affinity constants, or K_a values, for folded designed proteins are highly variable (10^5 to $>10^{12}$ M^{-1}) and are generally tighter than those for the corresponding metalloporphyrin−peptide systems, which are not fully folded prior to heme incorporation.

Synthetic heme proteins designed with coordination motifs other than bis-histidine remain relatively rare. The earliest heme protein complexes utilized lysine ϵ-amine ligands to bind hemes at pH 11.[251] Two metalloporphyrinyl−peptide systems provide examples of mono-histidyl-ligated hemes: the microperoxidases and the monopeptide-PSMs.[37] In addition to the endogenous histidine ligand, microperoxidases contain aquo or hydroxo ligands in the sixth coordination site, depending on solution pH. The identity of the sixth axial ligand can be altered by addition of exogenous ligands to provide mixed ligand coordination spheres such as His-Met and His-Tyr. The His-H_2O ligation motif of microperoxidases is mimicked by the ferric monopeptide-PSMs, which are mono-histidine-ligated mesohemes with an exogenous water ligand. In larger folded protein scaffolds, two other coordination motifs are observed, His-Met and bis-(4-β-(pyridyl)-L-alanine). His-Met ligation to ferric heme is proposed for Protein 86, shown in Figure 10C, which should result in significant alteration of the heme reduction potential relative to other bis-His members of the library.[311] More recently, the non-natural amino acid 4-β-(pyridyl)-L-alanine (Pal) has been introduced to bind heme in a truncated maquette scaffold, monoheme-$[\Delta 7\text{-}Pal_{10}I_{14}I_{21}]_2$.[350] The use of a bis-pyridine coordination results in a shifting of the oxidized and reduced optical spectra peak positions and a highly anisotropic low-spin (HALS) EPR spectrum. The bis-pyridine axial coordination shifts the midpoint reduction potential by +280 mV (6.6 kcal/mol) relative to bis-His by binding Fe(II) heme tightly ($K_a > 10^{10}$ M^{-1}) and Fe(III) heme weakly ($K_a = 1.6 \times 10^4$ M^{-1}). Thus, while designed systems have not accessed all the observed natural ligation motifs, they have demonstrated that novel non-natural coordination environments are feasible.

Aside from the location and type, the context of the ligating amino acid is also critical in heme binding. De novo heme proteins have proven useful in delineating the contextual factors that influence the ability of His to ligate heme. The factors impacting histidine ligation to hemes include iron oxidation state, peptide length, protein architecture, sequence hydrophobicity, and aromatic amino acid content. All of these studies belie the fundamental goal of designing a pre-organized heme binding site within a protein scaffold which is suitable for structural study and comparison to the compendium of natural heme protein structures.

In terms of peptide length, the simple fact that microperoxidases function with minimal modification indicates that the peptide ligand needed to fabricate biomimetic heme protein complexes is minimal. The designed mimochromes (9 amino acids[265]), PSMs (13 amino acids[37]), and related self-assembled systems (15 amino acids[275]) are all only slightly larger than the microperoxidases. Even larger are the four-α-helix bundle designs Protein 86 (74 amino acids[324]), retro(S−S) (76 amino acids[56]), and the truncated maquette $[\Delta 7\text{-}H_{10}I_{14}I_{21}]_2$ (96 amino acids[332]). The largest systems include $[H10H24]_2$ (124 amino acids[73]), MOP1 (122 amino acids[312]), and Designed Globin-1 (153 amino acids[316]).

In one self-assembled metalloporphyrin−peptide system, the effects of peptide length on heme affinity have been quantified. The binding of histidine to Fe(III)(coproporphyrin I) in aqueous solution is weak and increases dramatically (up to 16 000-fold) when the histidine is placed in a peptide.[351] Lowering the entropic penalty for heme binding by joining the linear sequences in a hairpin or cyclic structure further increases heme affinity, as expected. These data implicate ligand pre-organization, i.e., protein folding, as a significant factor in His-heme ligation, just as observed for natural heme proteins. Interestingly, the cyclic peptide heme affinity, 369 mM^{-1},

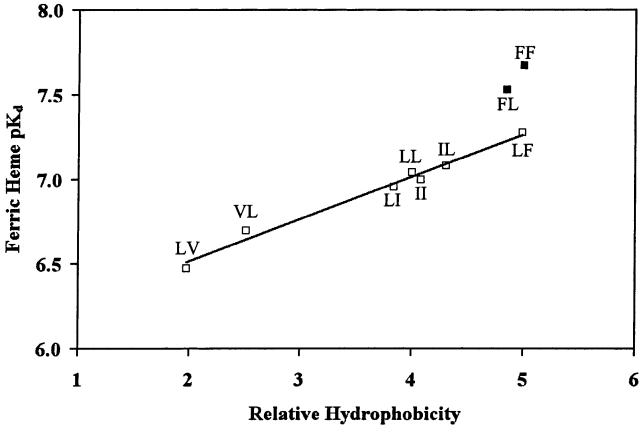

Figure 14. Influence of peptide hydrophobicity on heme affinity in metalloporphyrinyl−peptide systems. A plot of ferric heme affinity vs the relative hydrophobicity of the histidine containing peptide ligand. Data from ref 320.

approaches the weaker limit observed in the full four-α-helix bundle designs that are folded prior to heme incorporation.[276]

Several studies have shown the impact of varying the hydrophobicity of the peptides on heme binding in metalloporphyrin−peptide systems. As shown in Figure 14, ferric binding constants in self-associated metalloporphyrin−peptide systems get tighter with increasing hydrophobicity of the peptides.[275,320,352] In the specific case of aromatic amino acids, the peptide-sandwiched mesohemes have provided valuable insight into the role of edge-to-face aromatic interactions. The introduction of a tryptophan into the PSM at a position $i - 4$ from the iron-binding His increases the peptide helicity from 50% to 83%, while a phenylalanine at this position has no effect. The dramatic increase observed for Trp is ascribed to a favorable edge-to-face interaction between the residue and porphyrin, as observed by NMR spectroscopy.[171,261] These aromatic effects cause deviations in the observed trend of ferric binding constants with hydrophobicity. A similar observation was made in a self-assembled two-α-helix heme protein scaffold that forms a tetramer upon heme binding. In this designed system, a phenylalanine placed in the $i + 4$ position with respect to the ligating His improved heme affinity.[320] These data illustrate the importance of second-coordination-sphere amino acids in heme protein design.

In folded protein scaffolds, synthetic heme proteins have demonstrated the importance of establishing a hydrophobic core in order to bind the heme. A designed four-α-helix bundle of minimal stability showed increased heme affinity as the helical content was increased by addition of the co-solvent TFE. However, high TFE concentrations weakened heme binding by solvating and dissociating the hydrophobic core.[278] Thus, using metal ion ligation to fold or assemble proteins reduces the inherent Fe(III) heme affinity. At the other extreme, folded proteins with rigidly packed cores can inhibit ferric heme binding either kinetically or thermodynamically.[301] For example, $VAVH_{25}$(S−S) was more structurally rigid compared to the retro(S−S) protein that resulted in weaker Fe(III) heme binding.[56] Between these two extremes where the scaffold is fully folded and not very rigid, there is no obvious relationship between protein size or stability and heme affinity. In the case of the maquettes, truncation of a maquette scaffold by two helical turns, which lowers the *apo*-protein global stability substantially,[332] exerts less of an effect on heme affinity than that observed in the maquettes when the histidine positions are altered.[349]

In terms of secondary structure, biomimetic heme protein assemblies are dominated by α-helices, just as observed for the natural heme proteins in the CATH wheel of Figure 3. De novo-designed heme proteins are often built upon parallel or up−down−up−down bundles of amphiphilic α-helices grouped as two-, three-, or four-helix bundles. There are single examples of both a globin fold design[316] and a mixed α/β structure[318] that represent the initial forays into more diverse scaffold design. Obviously, recent advances in the protein design of β-sheet[66] and mixed α/β architectures[68] will impact the design of future heme protein assemblies and allow for comparison of heme protein structural engineering between protein folds.

4.2. Functional Engineering

The engineering of protein structure provides an avenue to design precise chemical properties into de novo heme proteins. This progress will, in turn, provide for the design of efficient chemical catalysts. While the robust biochemical literature on heme protein function coupled with the compendium of known heme protein structures serves as a guide, controlling the reactivity of a heme at a designed protein active site represents a daunting challenge. De novo-designed heme proteins have demonstrated remarkable progress in delineating the factors that modulate heme protein redox activity, which provides a basis from which to design the driving force component of electron-transfer chains. Additionally, the development of designed heme proteins as incipient chemical catalysts has begun to yield functional mimics of peroxidases. Thus, despite the scale of the challenge and the lack of detailed structural information on de novo-designed heme proteins, significant progress is being made.

As discussed in section 2.2, the equilibrium midpoint reduction potential of heme proteins belies their biochemical functions. Natural heme proteins are able to modulate the Fe(III)/Fe(II) electrochemical couple by nearly a full volt using a combination of environmental variables. Figure 15 shows that the reduction potentials of synthetic heme protein complexes span a range of 395 mV (9.4 kcal/mol) at pH 7−8 that covers the more negative half of the range observed for natural heme proteins. The Trp-containing PSM (−337 mV[352]) and the 4-β-(pyridyl)-L-alanine-ligated maquette (+58 mV[350]) represent the extrema of the currently observed designed heme protein redox activities. Restriction to the same porphyrin architecture, hemes *b*, results in a slightly smaller range, from −230 (tetraheme-$[H10H24]_2$[73]) to +58 mV (monoheme-$[\Delta 7\text{-}Pal_{10}I_{14}I_{21}]_2$[350]). Within bis-His-ligated heme protein design, the most com-

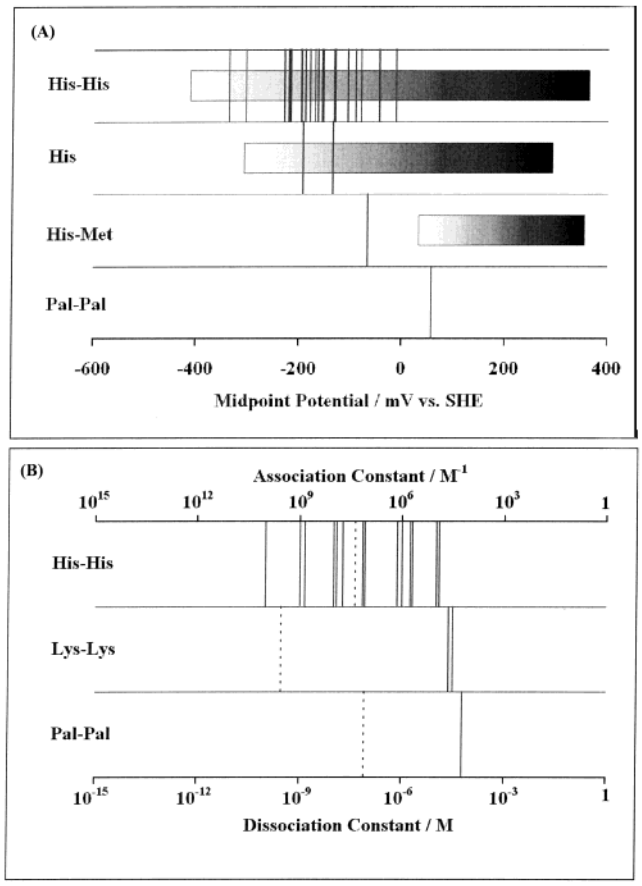

Figure 15. (A) Synthetic heme protein midpoint reduction potentials vs SHE as a function of coordination motif. The gray boxes represent the range of natural heme proteins of the same coordination type. (B) Ferric (solid) and ferrous (dashed) equilibrium constants of synthetic heme proteins as a function of coordination motif.

mon coordination type, midpoint values span from −337[352] to −12 mV[353] vs SHE, while natural bis-His-ligated *b*-hemes range from −150 (*Synechocystis* hemoglobin[354]) to +360 mV (cyt b_{559}[207]). Thus, the shaded areas in Figure 15, representing the natural heme protein midpoint potential range in Figure 4, demonstrate the coincidence of natural and synthetic heme protein electrochemical properties, which exemplifies the effectiveness of these biomimetics in modeling heme electrochemical activity.

The relative simplicity and the high degree of tailorability of designed heme protein ligands compared with their natural counterparts has aided in deciphering the range of environmental variables that modulate heme redox activity. In a series of studies using the mono-heme maquette, several of these factors were defined and used in combination to control the heme electrochemistry from −285 to +170 mV vs SHE, a 435 mV (10.3 kcal/mol) range.[353] These environmental modulators of heme redox activity included the type of heme macrocycle, the axial ligands to the heme, the extent of heme burial, and the presence of charges local to the heme. These results compare favorably with the findings from natural protein scaffolds, which demonstrate the utility of using designed proteins as synthetic analogues. Furthermore, the results of these stepwise studies provide the fundamental understanding with which to interpret the results from combinatorial libraries of heme proteins.

In terms of setting the basic reduction potential, the heme type and coordination motif are fundamental. Since the majority of designed proteins utilize bis-His coordination, it is instructive to compare the electrochemistry of the bis-imidazole complexes of hemes used in protein design: Fe(III)1-methyl-2-oxomesoheme XIII (−45 mV vs SHE), heme *a* (−120 mV),[194,195] Fe(III)coproporphyrin I (−214 mV, bis-His),[275] heme *b* (−235 mV),[353] and Fe(III)mesoheme (−285 mV).[353] Within the designed protein maquette monoheme-$[H10A24]_2$, a similar trend is observed with values spanning 214 mV: +18 (heme *a*), −12 (1-methyl-2-oxo mesoheme XIII), −156 (heme *b*), and −196 mV (mesoheme IX).[353] The electron-donating/withdrawing nature of the peripheral substituents alone can alter the reduction potential by 245 mV (5.8 kcal/mol) in bis-His-ligated designed heme proteins.[353] Notably, the incorporation of Fe(III)(porphycene) into myoglobin generates the blue myoglobin and lowers the midpoint reduction potential by 245 mV (5.8 kcal/mol), from 52 (ferric protoporphyrin IX) to −193 mV.[293] Clearly, these effects are due to the identity of the primary coordination sphere ligands. As will be discussed later, the differences between the bis-imidazole and maquette complexes of these hemes have been used to describe various second coordination sphere effects on heme redox activity.

As seen with natural heme proteins, alteration in the axial ligands has significant effects on the resulting heme electrochemistry. The ability to bind exogenous ligands to the microperoxidases has been exploited to determine the intrinsic differences between the various naturally observed coordination motifs. The reduction potential of the His-H_2O-ligated acetylated microperoxidase-11 (AcMP-11) is −134 mV vs SHE at pH 7.[203] The formation of the bis-His-coordinated AcMP-11 lowers the midpoint potential by 55 mV, while His-Met coordination raises the E_m value by 67 mV. The observed ΔE_m between bis-His to His-Met coordination in AcMP-11 (122 mV) is not as dramatic as the corresponding change in cytochrome *c* (219 mV[355]), most likely due to the higher solvent exposure of AcMP-11. The only de novo-designed protein which has been used to compare axial ligand contributions to E_m is the truncated maquette scaffold, $[\Delta 7\text{-}X_{10}I_{14}I_{21}]_2$. When X was His, the ferric heme was bound in a bis-His manner and the reduction potential was −222 mV.[332] When X was the non-natural amino acid 4-*β*-(pyridyl)-L-alanine (Pal), the heme was bound by two pyridylalanines and the midpoint potential rose to 58 mV, a difference of 280 mV (6.6 kcal/mol[350]). Thus, non-natural amino acids ligands can impact the heme electrochemistry as much as their natural counterparts.

Comparison of the electrochemistry of the aqueous bis-imidazole complexes with the bis-His heme maquette indicates that burial of the heme within this scaffold results in a more positive heme midpoint reduction potential. For the four heme types studied in the maquette, macrocycle burial raised the E_m value by 36 to 138 mV (0.8−3.3 kcal/mol), presumably

by destabilization of the formally cationic ferric heme, [Fe(III)(porphyrin)]$^+$, within the low-dielectric hydrophobic core—one of the unique properties of protein ligands.[98] The variability of this E_m modulation, 36−138 mV, is ascribed to differences in the solvent accessibility of the bound heme: the farnesyl chain on heme *a* aids in heme burial (ΔE_m = 138 mV),[333] and the ketone on 1-methyl-2-oxomesoheme XIII resists heme burial (ΔE_m = 36 mV).[353] In concert with this analysis, (1) the metalloporphyrinyl−peptide complexes that expose their hemes to solvent have more negative heme midpoint potentials, e.g. PSM (−317 vs −285 mV for Fe(mesoporphyrin IX)-$(Im)_2$);[37] (2) designed heme proteins that ligate the heme diagonally across the hydrophobic core may have slightly more positive heme *b* reduction potentials, e.g. MOP1 (−107 mV[312]), than those that ligate the heme on adjacent helices, e.g. $[H10A24]_2$ (−156 mV), due to greater heme burial; and (3) a comparison of *apo*-maquette scaffolds that are poorly packed or well packed indicates that the poorly packed *apo*-state maquettes bury the heme better, resulting in more positive midpoint potentials.[297] Thus, as observed for natural heme proteins, the extent to which the heme is buried with a low-dielectric hydrophobic core influences the reduction potential.

Since many of the designed heme proteins utilize the bis-His coordination motif, any observable deviation from the intrinsic midpoint reduction potential value of −235 mV for Fe(protoporphyrin IX)$(Im)_2$ is due to second coordination sphere interactions within the protein matrix. The extent of metalloporphyrin burial, above, is one of several scaffold effects on Fe(III)/Fe(II) heme midpoint reduction potentials. The introduction of charged species in the vicinity of the heme can have a ±50 mV effect on heme redox activities in designed proteins, whereas in natural proteins that fully sequester the heme charged amino acids can modulate the E_m value by 100−200 mV.[44] As observed in the prototype maquette, $[H10H24]_2$, the presence of a formally cationic second ferric heme in close proximity results in a 42−126 mV (1−3 kcal/mol) splitting in the pair of heme reduction potentials. Similar heme−heme electrostatic effects are observed in multi-heme proteins such as the tetraheme subunit of the *Rhodospeudomonas viridis* photosynthetic reaction center protein.[356] Placement of a Glu residue at a Leu position one helical turn away from the heme-binding histidine of the heme protein maquette lowers the heme reduction potential by 42 mV (1 kcal/mol) to −198 mV, presumably by stabilization of the cationic ferric heme. However, attempts to destabilize the ferric state by substitution of the Leu with an Arg residue resulted in no shift in the reduction potential presumably due to the ability of the Arg side chain to move the charged guanidinium group out of the protein core and into solvent. Last, the substitution of a Gln for the Glu residue following the heme-binding His residue, E11Q, resulted in a +52 mV shift in the reduction potential to −104 mV. Thus, charged amino acids can have a 40−50 mV effect on heme reduction potentials if they are local to the heme binding site and within a low dielectric core.[353]

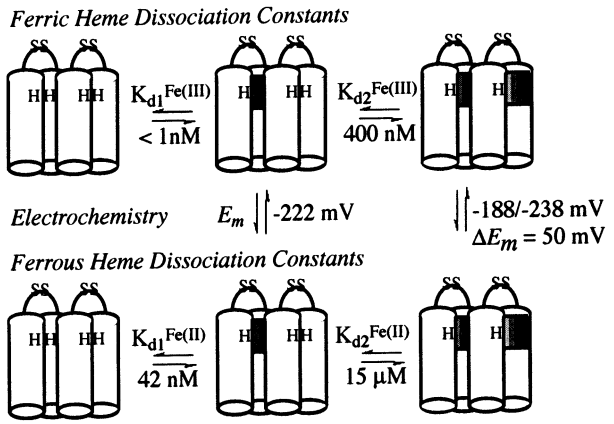

Figure 16. Thermodynamic analysis of the coordination chemistry of the di-heme maquette $[\Delta 7\text{-}H_{10}I_{14}I_{21}]_2$. (Reprinted with permission from ref 332. Copyright 2003 Royal Society of Chemistry.)

Interestingly, a similar 44 mV modulation in the heme reduction potential was observed for conservative hydrophobic amino acid changes in a heme protein maquette, suggesting that hydrophobic interactions were as important as charged interactions in modulating heme reduction potentials.[297] While the origin of this 44 mV effect was ascribed to differences in heme burial in the maquette, a similar change observed in the PSMs allowed for full delineation of the changes to ferric and ferrous heme stability.[352] Replacement of an Ala with a Trp residue resulted in a lowering of the PSM E_m value from −281 to −337 mV vs SHE. Detailed analysis of the ferric and ferrous heme affinities showed that the observed 56 mV difference was due to stabilization of the ferric state by 90 mV, with a 34 mV stabilization of the ferrous state due to shielding of the porphyrin. Thus, second coordination sphere effects alter both the stability of the ferric and ferrous states.

Figure 16 shows the results of an analogous analysis carried out with a two-heme-binding four-α-helix bundle, $[\Delta 7\text{-}H_{10}I_{14}I_{21}]_2$.[332] The results delineate several important features of this maquette design. First, the designed bis-His sites bind ferric heme more tightly than ferrous heme by a factor of 300-fold (3.4 kcal/mol), a property ascribed to the inherent coordination preference of imidazoles for ferric over ferrous heme. Second, the binding of the second heme is sterically hindered by 357-fold (3.5 kcal/mol) by the presence of the first bound heme, which results in relatively weak affinity for the second ferrous heme, $K_a = 6.6 \times 10^4$ M^{-1}. Third, the observed 50 mV (1.2 kcal/mol) [Fe(III)protoporphyrin IX]$^+$−[Fe(III)protoporphyrin IX]$^+$ electrostatic interaction weakens the binding of the second ferric heme. Thus, the affinity for the first ferric heme can be calculated at 7.1×10^9 M^{-1}, K_d = 140 pM (4.7 kcal/mol tighter than the affinity for the second Fe(III) heme). This analysis of heme binding and electrochemistry within the truncated maquette provides lucid insight into the engineering of $[\Delta 7\text{-}H_{10}I_{14}I_{21}]_2$ and demonstrates that it fundamentally behaves as a simple coordination compound.

Another second coordination sphere effect that is a property of the protein ligands is a redox Bohr

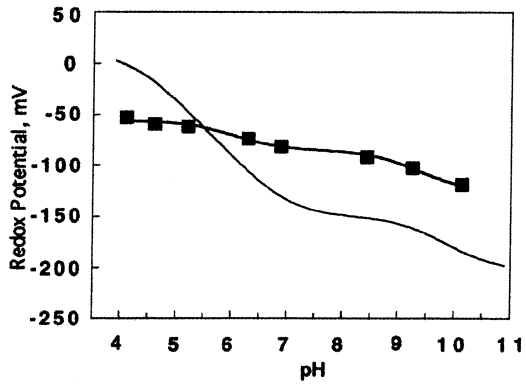

Figure 17. pH dependency of the reduction potential of heme-$[H10A24]_2$ (solid line) and its variant with all Glu replaced with Gln (line with square data points). The data were fit to a pH-dependent Nernst equation, eq 2 in the text. (Reprinted with permission from ref 91. Copyright 1998 American Chemical Society.)

effect. The ability of the protein structure to bind/release protons in response to oxidation/reduction at the heme, and thus maintain charge neutrality, provides a mechanism to modulate the reduction potential in designed heme proteins by 210 mV (5.0 kcal/mol). Furthermore, such charge compensation reactions are a unique property of protein ligands[98] that are elemental to the proton pumping capabilities of the metal centers in respiratory enzyme complexes such as NADPH-ubiquinone oxidoreductase.[357] In monoheme-$[H10A24]_2$, the stability of the ferric and ferrous heme protein maquette allowed its electrochemical behavior to be studied over the range of pH 3−11. The observed 210 mV shift in E_m over this pH range was due to two separate proton-coupled electron-transfer events, as shown in Figure 17. The data were adequately fit using the pH-dependent Nernst equation, below:

$$E_m = E_0 + (RT/nF) \ln [([H^+] + K_{a1}^{red})([H^+] + K_{a2}^{red})/([H^+] + K_{a1}^{ox})([H^+] + K_{a2}^{ox})] \quad (2)$$

The larger event showed a reduced-state pK_{a1}^{red} of 7.0 and an oxidized pK_{a1}^{ox} of 4.2, with a 60 mV/pH unit slope indicative of a $1H^+/1e^-$ stoichiometry. Substitution of the Glu residues with Gln diminished this redox Bohr effect, as shown in Figure 17, and indicated that the Glu residues are the site of proton coupling. A smaller proton-coupling event ascribed to the Lys residues was observed at higher pH, with an oxidized pK_{a2}^{ox} of 9.4 and a reduced pK_{a2}^{red} of 10.3. Delineation of the molecular basis for this biochemical phenomenon demonstrates the utility of these designed proteins in probing natural heme protein structure−function relationships. Furthermore, since many of the designed four-α-helix bundle scaffolds utilize similar patterns of amino acids, these data suggest that many of these systems might display proton-coupled electron-transfer events as well.[91]

The description, and relative impact, of the factors which modulate the midpoint potentials in designed heme proteins provides a fundamental basis from which to design redox activity. Ranked by the magnitude of their effect on E_m, the choice of the axial ligands (280 mV), metalloporphyrin type (245 mV), and the response of the protein to oxidation/reduction via a redox Bohr effect (210 mV), heme burial (36−138 mV, perhaps up to 500 mV[196]), and local charges (40−135 mV, perhaps up to 200 mV[43]) all provide the rational designer with mechanisms to shift the electrochemical activity. Scaffold effects and porphyrin effects have been combined to yield predictable results over a 435 mV (10.3 kcal/mol) range from −285 mV, a low-potential heme at high pH (Fe(mesoheme)-$[H10A24]_2$ +170 mV vs SHE at pH 11), to +170 mV, a high-potential heme at low pH (heme *a* − $[H10A24]_2$ at pH 4), without changing the axial ligand set. However, the influence of these factors on the individual ferric and ferrous heme stabilities is not yet described.

While much progress has been made in describing the various factors that set and modulate heme reduction potentials, there are several key areas left to explore. First, the influence of heme protein burial within a membrane is unknown. The similarity of the electrochemistry of the $[H10H24]_2$ and MOP1 to that of cyt b_L and cyt b_H,[358] on which these designs were based, suggests that the presence of the membrane may not be a critical determinant of heme reduction potential. However, the highly positive E_m values of cyt *a* and cyt a_3 in cyt *c* oxidase and cyt b_{559} in Photosystem II suggests that the low dielectric of a membrane may raise reduction potentials. Second, the influence of these environmental factors on ferric and ferrous heme affinity is poorly understood. Since the observed potential shifts are directly related to the relative stabilization/destabilization of the two oxidation states as shown in eq 1 (section 2.2), precise determination of the factors influencing ferric and ferrous stability will provide for more accurate control of heme midpoint potentials for electron-transfer chain design.

Considerable progress has been made in elucidating the fundamental governors of heme protein redox activity, due in part to the availability of numerous six-coordinate heme protein designs. While these coordinatively saturated heme proteins prove excellent models for electron-transfer proteins, the lack of an open coordination site may appear to restrict the development of catalytic heme proteins. Despite this apparent limitation, several six-coordinate designs have proven to contain a ligand that is readily displaced, which provides an opportunity for the design of heme proteins for catalytic and sensor applications. In time, these nascent functional heme protein systems may discern the basic engineering principles of catalytic heme protein design.

As mentioned above, several of the designed heme protein systems discussed in section 3.2 undergo ligand substitution reactions with exogenous ligands. The bis-His-ligated PSMs react with protons to dissociate protonated histidine ligands, His-H^+, which provides a method a compare the stability of His-Fe coordination. Additionally, the bis-His-ligated ferrous heme PSMs react with carbon monoxide to yield the His-CO-ligated heme adduct.[359] Perhaps the increase in entropy upon protein unfolding coupled to His ligand dissociation might serve to favor ligand dis-

placement. In larger folded protein systems, the stability of the protein scaffold may serve to stabilize the iron−ligand interaction and prevent ligand substitution. However, several designed heme proteins bind CO in the ferrous heme state, including [α-loop-α]$_2$ (a maquette)[333] and DG-1.[316] The only detailed kinetic study of the binding of CO to a designed protein, Protein 86, demonstrated a CO association constant of 1.8×10^8 M^{-1}, a value slightly tighter than that for Mb ($(2.7-4.5) \times 10^7$ M^{-1}).[55] In the ferric state, the binding of cyanide has been observed for [α-loop-α]$_2$ and VAVH$_{25}$(S−S), but not for retro(S−S), suggesting that the tighter heme affinity of retro-(S−S) prevents CN^- binding.[56]

In designed heme protein systems, ligand substitution has been utilized to develop biomimetics of two types of heme chemical function, oxygen binding and peroxidase activity. Figure 6B shows the oxygen binding curve for the poly-L-lysine−ferroheme complex, the only system for which dioxygen binding has been detailed. Interestingly, the data show an allosteric interaction with dioxygen with a Hill coefficient of 2.0, which mimics the 2.7−2.9 value of hemoglobin.[360,361] Thus, designed heme proteins mimic the dioxygen binding activity of the globins and access one of the unique properties of protein ligands, i.e. allostery.[98]

In heme peroxidases such as HRP, the binding of exogenous hydrogen peroxide provides for the catalytic $2e^-$ oxidation of substrate.[7] The first step of the general heme peroxidase mechanism is a rapid $2e^-$ oxidation of ferric heme to form Compound I, $k = 10^6-10^7$ M^{-1} s^{-1} for HRP.[7,362] Compound I has been identified as an oxo-ferryl porphyrin π-cation radical.[363] The subsequent second and third steps involve substrate oxidation that generates Compound II, an oxo-ferryl iron porphyrin, and the resting ferric state of the enzyme, respectively. Colorimetric assays of peroxidase function based on organic substrates such as 2,2′,5,5′-tetramethylbenzidine (TMB) or 2,2′-azinodi(3-ethylbenzthiazoline-6-sulfonic acid) (ABTS) have been developed for natural peroxidases. Several designed heme protein systems utilized these colorimetric assays to demonstrate peroxidase-like activity.

The microperoxidases have been extensively characterized as mimics of peroxidases and P-450 monooxygenase enzymes, with a sample product distribution shown in Figure 5B for a P-450 peroxide shunt reaction. As a family of peroxidases, MPs oxidize a variety of organic substrates, including ABTS. The broad spectrum of reactivity is due in part to the open distal face.[364,365] Intriguingly, MP-11 has been shown to oxidize sulfides enantioselectively with modest ee values (16−25%).[366] Furthermore, MP-8 has also been shown to oxidize *N*-hydroxyguanidines with hydrogen peroxide, releasing NO in a reaction which mimics part of the NO synthase reaction scheme.[367] As a mimic of cyt P-450 enzymes, MPs have been shown to activate O_2 in the presence of sodium dithionite as a reductant and perform hydroxylations,[368] *N*- and *O*-dealkylations, dehalogenations,[369] and epoxidations. The ability of His coordinated MPs to mimic the functional activity of cyt P-450s indicates that the identity of the axial ligand is not the sole determinant of enzymatic activity in the natural protein. The addition of a general acid−base group to MP has been used to increase the peroxidase activity. The proline-modified MP-8 showed a faster rate of oxidation of *p*-cresol with hydrogen peroxide relative to MP-8, 1100 vs 680 M^{-1} s^{-1}.[237] Last, enhanced rates were seen when mimics of the distal arginine, involved in the push−pull mechanism, such as guanidinium chloride, were added.[370]

Aside from microperoxidases, several designed heme proteins have demonstrated the ability to oxidize peroxidase substrates. The development of these catalysts as enzymes is in the early stages, but several themes have emerged on the role of the peptide in controlling heme reactivity in designed protein scaffolds. First, mimochrome I, a bis-histidine porphyrinyl peptide, was able to epoxidize and oxidize styrene using H_2O_2 under both aerobic and anaerobic environments. While the presence of rapidly interconverting diastereomers resulted in no observable asymmetric induction, protecting the deuterioheme within the mimochrome construct reduced the oxidative degradation of the porphyrin.[371] Thus, encapsulating the heme active site within a conformationally restricted protein structure serves to prevent porphyrin degradation and may enhance regio- or stereoselectivity. Second, the helichrome complex,[272] which hydroxylates aniline to yield *p*-aminophenol, contains a designed hydrophobic pocket for substrate.[272,273] Thus, the design of substrate-selective active sites may provide for the design of highly specific catalysts. Third, a metalloporphryinyl peptide complex containing Mn(III) was deposited on an imidazole propyl silica gel substrate, as shown in Figure 8A. The catalyst oxidized a variety of alkenes in the presence of iodosylbenzene, however not asymmetrically.[270,372] Thus, designed protein catalysts may be amenable to incorporation into bed catalysts for industrial applications. Fourth, the His-2α complex, a bis-histidine de novo-designed two-α-helix bundle that oligomerizes to a tetramer upon heme addition, catalyzes the demethylation of *N*,*N*-dimethylaniline using H_2O_2. The H_2O_2 dependence and substrate independence of the reaction rate indicate that the rate-determining step is the initial reaction between the ferric heme peptide and the peroxide.[278] Furthermore, a correlation between stronger bis-histidyl binding and lower peroxidase-like activity was observed by using a series of peptides of varying lengths, number of Leu residues in the core, and topologies. Thus, weakly bound ligands facilitate heme reactivity due to a higher concentrations of a catalytically active five-coordinate iron.[314] Fifth, a four-α-helix bundle with hydrophobic core devoid of potential ligands has been shown to oxidize guaiacol with H_2O_2 in the presence of exogenous imidazole. Interestingly, the rate of substrate oxidation increased as a function of methanol concentration, which may stabilize the protein fold or solvate the hydrophobic core.[348] Additionally, Figure 18 shows that Protein 86 is the most active combinatorial heme protein. Protein 86 catalyzes the oxidation of ABTS by H_2O_2 at a rate of at least 5000 min^{-1}.[92] Conse-

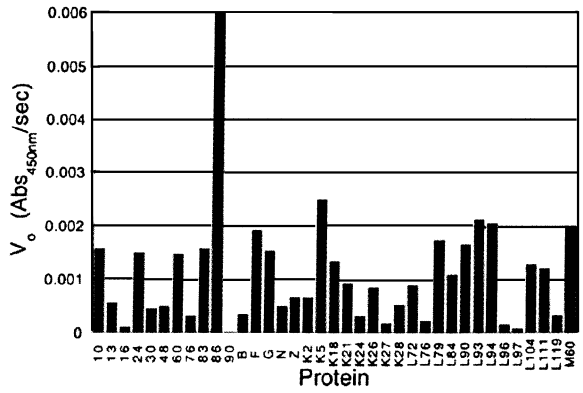

Figure 18. Screen for peroxidase activity of a combinatorial library of heme proteins. (Reprinted with permission from ref 92. Copyright 2000 American Chemical Society.)

quently, precise design of the heme ligands or microenvironment may not be critical to observe peroxidase reactivity in designed heme proteins.

The mechanistic details of a couple of the observed reactions in designed heme proteins have been investigated for comparison to the corresponding natural enzymes. In the case of the MPs, the rate-determining step in peroxidase chemistry is the reaction of the aquo complex with hydroperoxide to form the reactive intermediate, whereas in HRP the formation of Compound I is not rate limiting.[370] Despite this kinetic difference, MPs have been proposed to go through a similar reaction mechanism as the natural peroxidases, including the Compound I and II intermediates.[373−376] Spectroscopic evidence is available for a Compound I-type intermediate which suggests a reactive pathway similar to that of HRP,[377] but a flash photolysis study suggests that a ferric porphyrin radical may be the kinetically competent species.[378] In the case of P-450-like aromatic hydroxylations, there is evidence that MPs utilize the P-450-like oxygen rebound mechanism.[379] In the case of designed heme proteins which catalyze peroxidase-type reactions, the kinetic details demonstrate a rate-determining first step of hydrogen peroxide reaction to form the reactive intermediate with rapid successive steps. Hence, as observed for the microperoxidases, the designed systems have different mechanistic details than the natural peroxidases and more closely mimic the microperoxidases. The further development of these nascent catalysts promises to provide systems which faithfully mimic the functional and mechanistic details of natural peroxidases and provide great insight into controlling heme reactivity in protein scaffolds. These insights, once developed, will provide for the rational design of faithful mimics of the full range of functional heme proteins involved in ligand transport, ligand sensing, and substrate oxidation.

5. Perspective

As described above, remarkable progress in the incorporation of heme and other metal centers into de novo-designed protein ligand scaffolds has been made over the past decade.[95] These studies have demonstrated a number of fundamental concepts in the engineering and construction of metalloproteins from first principles. As demonstrated herein, the design and synthesis of proteins containing one or more copies of a single type of metal cofactor is well established, and successful designs of complex multi-cofactor proteins composed of different metal cofactors continue to emerge. As the field progresses, novel coordination chemistry will continue to be developed to provide for the high-fidelity incorporation and stabilization of an ever-increasing array of biological and abiological metal centers into designed protein scaffolds to test the fundamental tenets of bioinorganic chemistry.

These designed metalloproteins provide a conceptual bridge between the time-honored small-molecule synthetic analogue approach to bioinorganic chemistry and the traditional biochemical approach of metalloprotein structure−function studies. Metalloproteins, designed or natural, are complex coordination compounds that obey the fundamental chemical principles of coordination chemistry. These designed metalloprotein systems continue to provide insight into both coordination chemistry under physiologically relevant conditions and natural protein structure−function relationships. As a natural progression from small-molecule synthetic analogues, designed metalloproteins begin to allow for the delineation of cofactor−protein interactions beyond the primary coordination sphere. The designed heme proteins catalogued herein have demonstrated their utility in elucidating the molecular basis of biological phenomena, such as the engineering specification and tolerances of heme protein construction,[349] the induction of protein folding by metals,[90] the modulation of heme reduction potentials by environmental factors,[353] and the governors of electron transfer between redox cofactors.[84,347] As metalloproteins, these systems are simplified relative to their highly complex natural counterparts. Despite this simplification, the underlying principles of natural and synthetic heme proteins remain invariant. Thus, the insight gained from designed heme proteins appears applicable to natural heme proteins and vice versa. The ability to tailor all aspects of the protein ligand affords the designer with incredible flexibility with which to control the metal ion chemistry. Arranging the entire constellation of amino acids interacting with the metal center offers the opportunity to access the unique spectroscopic and functional properties observed at natural metalloprotein active sites.

The utility of peptide-based coordination compounds is not only in delineating the fundamental concepts of genomic metallobiochemistry but also in using that insight constructively to expand biochemical catalysis beyond its current limitations.[380] From the perspective of a de novo protein designer, every level of the hierarchy of protein structure provides an opportunity to expand the scope of biochemical catalysis. Sequence space,[51] the compendium of all possible amino acid sequences, is being augmented by the addition of non-natural amino acids to protein structures.[381−383] Considering the vast range of biochemical functionality derived from a paltry 21 amino acid monomers, the promise of expanded protein alphabets is apparent. Aside from non-natural amino

acids, abiological metal centers and cofactors also provide a significant opportunity to broaden the scope of biochemical catalysis. At the level of protein secondary structure, current efforts to decipher the engineering principles of α-helices and β-sheets and their combinations provide the fundamental basis from which to begin to design novel protein secondary structures. New secondary structures may be fabricated from α-amino acid monomers or the growing collection of foldamers including β-amino acids.[384,385] Additionally, imaginative combinations of α-helices, β-sheets, and perhaps new structures will yield additional entries into shape space, the collection of known protein folds. Progress in design at every level of protein structure provides the fundamental basis to reach the eventual goal of expanding functional space, the collection of all biochemical functions. Therefore, future challenges reside at all levels of protein structure−function design on the path to fulfilling the promise of molecular design and synthetic biology[380] to decipher, and then expand, biochemical function.

6. Acknowledgments

B.R.G. thanks the National Science Foundation (CHE-02-12884) and the American Chemical Society Petroleum Research Fund (37347-G3) for financial support of his research. C.J.R. acknowledges the National Institutes of Health for a biophysics traineeship (T32 GM08281).

7. Note Added in Proof

Detailed NMR structures of two Co(III) metalloporphyrinyl-peptides have recently appeared. Rosenblatt, M. M.; Wang, J.; Suslick, K. S. *Proc. Natl. Acad. Sci. U.S.A.* **2003**, *100*, 13140. Lombardi, A.; Nastri, F.; Marasco, D.; Maglio, O.; De Sanctis, G.; Sinibaldi, F.; Santucci, R.; Coletta, M.; Pavone, V. *Chem. Eur. J.* **2003**, *9*, 5643.

8. Abbreviations

CD	circular dichroism
cyt	cytochrome
ϵ	molar absorbtivity
ee	enantiomeric excess
E_m	equilibrium midpoint reduction potential
E_0	solution potential
EPR	electron paramagnetic resonance
ENDOR	electron nuclear double resonance
HAO	hydroxylamine oxidoreductase
HRP	horseradish peroxidase
Mb	myoglobin
MP	microperoxidase
PDB	Protein Data Bank
PSM	peptide-sandwiched mesoheme
ROP	ColE1 repressor of primer from *E. coli*
SHE	standard hydrogen electrode
SHP	sphaeroides heme protein
TASP	template-assembled synthetic peptide
TFE	2,2,2-trifluoroethanol
X	amino acid residue (generalized)

9. Supporting Information Available

Tables listing the non-redundant heme proteins used to construct the CATH wheel in Figure 3, the midpoint reduction potentials of the natural heme proteins used in Figure 4, and the synthetic heme protein reduction potentials and dissociation constants in Figure 15. This material is available free of charge via the Internet at http://pubs.acs.org

10. References

(1) Chapman, S. K.; Daff, S.; Munro, A. W. *Struct. Bond.* **1997**, *88*, 39.
(2) Dawson, J. H. *Science* **1988**, *240*, 433.
(3) Paoli, M.; Marles-Wright, J.; Smith, A. *DNA Cell Biol.* **2002**, *21*, 271.
(4) Martin, A. C.; Orengo, C. A.; Hutchinson, E. G.; Jones, S.; Karmirantzou, M.; Laskowski, R. A.; Mitchell, J. B.; Taroni, C.; Thornton, J. M. *Struct. Fold. Des.* **1998**, *6*, 875.
(5) Scott, R. A.; Mauk, A. G. *Cytochrome c−A multidisciplinary approach*; University Science Books: Sausalito, CA, 1996.
(6) Gray, H. B.; Winkler, J. R. *Annu. Rev. Biochem.* **1996**, *65*, 537.
(7) Dunford, H. B. *Heme peroxidases*; John Wiley: New York, 1999.
(8) Ortiz de Montellano, P. R. *Cytochrome P450: structure, mechanism, and biochemistry*; Plenum Press: New York, 1995.
(9) Harrison, P.; Huehns, E. R. *Nature* **1979**, *279*, 476.
(10) Chan, M. K. *J. Porphyrins Phthalocyanines* **2000**, *4*, 358.
(11) Rodgers, K. R. *Curr. Opin. Chem. Biol.* **1999**, *3*, 158.
(12) Chan, M. K. *Curr. Opin. Chem. Biol.* **2001**, *5*, 216.
(13) Antonini, E.; Brunori, M. *Hemoglobin and Myoglobin in their Reactions with Ligands*; North-Holland: Amsterdam, 1971.
(14) Privalle, C. T.; Crivello, J. F.; Jefcoate, C. R. *Proc. Natl. Acad. Sci. U.S.A.* **1983**, *80*, 702.
(15) Pikuleva, I.; Waterman, M. *Mol. Asp. Med.* **1999**, *20*, 43.
(16) Yoshikawa, S. *Adv. Protein Chem.* **2002**, *60*, 341.
(17) Narula, J.; Pandey, P.; Arbustini, E.; Haider, N.; Narula, N.; Kolodgie, F. D.; Dal Bello, B.; Semigran, M. J.; Bielsa-Masdeu, A.; Dec, G. W.; Israels, S.; Ballester, M.; Virmani, R.; Saxena, S.; Kharbanda, S. *Proc. Natl. Acad. Sci. U.S.A.* **1999**, *96*, 8144.
(18) Kendrew, J. C.; Bodo, G.; Dintzis, H. M.; Parrish, R. G.; Wyckoff, H. W.; Phillips, D. C. *Nature* **1958**, *181*, 662.
(19) Takano, T. *Refinement of Myoglobin and Cytochrome c*; Clarendon Press: New York, 1984.
(20) Mitchell, P. *Nature* **1961**, *191*, 144.
(21) Bai, Y. W.; Sosnick, T. R.; Mayne, L.; Englander, S. W. *Science* **1995**, *269*, 192.
(22) Telford, J. R.; Wittung-Stafshede, P.; Gray, H. B.; Winkler, J. R. *Acc. Chem. Res.* **1998**, *31*, 755.
(23) Pauling, L.; Itano, H. A.; Singer, S. J.; Wells, I. C. *Science* **1949**, *110*, 543.
(24) Ibers, J. A.; Holm, R. H. *Science* **1980**, *209*, 223.
(25) Karlin, K. D. *Science* **1993**, *261*, 701.
(26) Kadish, K. M.; Bottomley, L. A. *Inorg. Chem.* **1980**, *19*, 832.
(27) Kadish, K. M.; Dsouza, F.; Villard, A.; Autret, M.; Vancaemelbecke, E.; Bianco, P.; Antonini, A.; Tagliatesta, P. *Inorg. Chem.* **1994**, *33*, 5169.
(28) Kadish, K. M.; Autret, M.; Ou, Z. P.; Tagliatesta, P.; Boschi, T.; Fares, V. *Inorg. Chem.* **1997**, *36*, 204.
(29) Cheesman, M. R.; Walker, F. A. *J. Am. Chem. Soc.* **1996**, *118*, 7373.
(30) Nesset, M. J. M.; Shokhirev, N. V.; Enemark, P. D.; Jacobson, S. E.; Walker, F. A. *Inorg. Chem.* **1996**, *35*, 5188.
(31) Raitsimring, A. M.; Borbat, P.; Shokhireva, T. K.; Walker, F. A. *J. Phys. Chem.* **1996**, *100*, 5235.
(32) Bertini, I.; Luchinat, C.; Parigi, G.; Walker, F. A. *J. Biol. Inorg. Chem.* **1999**, *4*, 515.
(33) Scheidt, W. R.; Cheng, B.; Safo, M. K.; Cukiernik, F.; Marchon, J. C.; Debrunner, P. G. *J. Am. Chem. Soc.* **1992**, *114*, 4420.
(34) Scheidt, W. R.; Ellison, M. K. *Acc. Chem. Res.* **1999**, *32*, 350.
(35) Collman, J. P.; Reed, C. A. *J. Am. Chem. Soc.* **1973**, *95*, 2048.
(36) Collman, J. P.; Gagne, R. R.; Halbert, T. R.; Marchon, J. C.; Reed, C. A. *J. Am. Chem. Soc.* **1973**, *95*, 7868.
(37) Benson, D. R.; Hart, B. R.; Zhu, X.; Doughty, M. B. *J. Am. Chem. Soc.* **1995**, *117*, 8502.
(38) Collman, J. P.; Rapta, M.; Broring, M.; Raptova, L.; Schwenninger, R.; Boitrel, B.; Fu, L.; L'Her, M. *J. Am. Chem. Soc.* **1999**, *121*, 1387.
(39) Collman, J. P.; Fudickar, W.; Shiryaeva, I. M. *Inorg. Chem.* **2003**, *42*, 3384.
(40) Jackson, D. A.; Berg, P.; Symons, R. H. *Proc. Natl. Acad. Sci. U.S.A.* **1972**, *69*, 2904.
(41) Saiki, R. K.; Gelfand, D. H.; Stoffel, S.; Scharf, S. J.; Higuchi, R.; Horn, G. T.; Mullis, K. B.; Erlich, H. A. *Science* **1988**, *239*, 487.
(42) Mullis, K. B. *Angew. Chem., Int. Ed. Engl.* **1994**, *33*, 1209.
(43) Stellwagen, E. *Nature* **1978**, *275*, 73.
(44) Varadarajan, R.; Zewert, T. E.; Gray, H. B.; Boxer, S. G. *Science* **1989**, *243*, 69.
(45) Lu, Y.; Berry, S. M.; Pfister, T. D. *Chem. Rev.* **2001**, *101*, 3047.

(46) Watanabe, Y. *Curr. Opin. Chem. Biol.* **2002**, *6*, 208.
(47) McRee, D. E.; Jensen, G. M.; Fitzgerald, M. M.; Siegel, H. A.; Goodin, D. B. *Proc. Natl. Acad. Sci. U.S.A.* **1994**, *91*, 12847.
(48) Sigman, J. A.; Kim, H. K.; Zhao, X. A.; Carey, J. R.; Lu, Y. *Proc. Natl. Acad. Sci. U.S.A.* **2003**, *100*, 3629.
(49) Farinas, E. T.; Schwaneberg, U.; Glieder, A.; Arnold, F. H. *Adv. Synth. Catal.* **2001**, *343*, 601.
(50) Cirino, P. C.; Arnold, F. H. *Curr. Opin. Chem. Biol.* **2002**, *6*, 130.
(51) Smith, J. M. *Nature* **1970**, *225*, 563.
(52) Richardson, J. S.; Richardson, D. C.; Erickson, B. W. *Biophys. J.* **1984**, *45*, A25.
(53) DeGrado, W. F.; Summa, C. M.; Pavone, V.; Nastri, F.; Lombardi, A. *Annu. Rev. Biochem.* **1999**, *68*, 779.
(54) Baltzer, L.; Nilsson, H.; Nilsson, J. *Chem. Rev.* **2001**, *101*, 3153.
(55) Moffet, D. A.; Hecht, M. H. *Chem. Rev.* **2001**, *101*, 3191.
(56) Choma, C. T.; Lear, J. D.; Nelson, M. J.; Dutton, P. L.; Robertson, D. E.; DeGrado, W. F. *J. Am. Chem. Soc.* **1994**, *116*, 856.
(57) Hodges, R. S.; Saund, A. K.; Chong, P. C. S.; St. Pierre, S. A.; Reid, R. E. *J. Biol. Chem.* **1981**, *256*, 1214.
(58) Marqusee, S.; Robbins, V. H.; Baldwin, R. L. *Proc. Natl. Acad. Sci. U.S.A.* **1989**, *86*, 5286.
(59) Hecht, M. H.; Richardson, J. S.; Richardson, D. C.; Ogden, R. C. *Science* **1990**, *249*, 884.
(60) Harbury, P. B.; Zhang, T.; Kim, P. S.; Alber, T. *Science* **1993**, *262*, 1401.
(61) Munson, M.; O'Brien, R.; Sturtevant, J. M.; Regan, L. *Protein Sci.* **1994**, *3*, 2015.
(62) Bryson, J. W.; Betz, S. F.; Lu, H. S.; Suich, D. J.; Zhou, H. X. X.; O'Neil, K. T.; DeGrado, W. F. *Science* **1995**, *270*, 935.
(63) Desjarlais, J. R.; Handel, T. M. *Protein Sci.* **1995**, *4*, 2006.
(64) Dolphin, G. T.; Brive, L.; Johansson, G.; Baltzer, L. *J. Am. Chem. Soc.* **1996**, *118*, 11297.
(65) Dahiyat, B. I.; Mayo, S. L. *Science* **1997**, *278*, 82.
(66) Kortemme, T.; Ramirez-Alvarado, M.; Serrano, L. *Science* **1998**, *281*, 253.
(67) Gibney, B. R.; Rabanal, F.; Skalicky, J. J.; Wand, A. J.; Dutton, P. L. *J. Am. Chem. Soc.* **1999**, *121*, 4952.
(68) Silverman, J. A.; Balakrishnan, R.; Harbury, P. B. *Proc. Natl. Acad. Sci. U.S.A.* **2001**, *98*, 3092.
(69) Hill, R. B.; Raleigh, D. P.; Lombardi, A.; DeGrado, W. F. *Acc. Chem. Res.* **2000**, *33*, 745.
(70) Gibney, B. R.; Mulholland, S. E.; Rabanal, F.; Dutton, P. L. *Proc. Natl. Acad. Sci. U.S.A.* **1996**, *93*, 15041.
(71) Scott, M. P.; Biggins, J. *Protein Sci.* **1997**, *6*, 340.
(72) Coldren, C. D.; Hellinga, H. W.; Caradonna, J. P. *Proc. Natl. Acad. Sci. U.S.A.* **1997**, *94*, 6635.
(73) Robertson, D. E.; Farid, R. S.; Moser, C. C.; Urbauer, J. L.; Mulholland, S. E.; Pidikiti, R.; Lear, J. D.; Wand, A. J.; DeGrado, W. F.; Dutton, P. L. *Nature* **1994**, *368*, 425.
(74) Regan, L.; Clarke, N. D. *Biochemistry* **1990**, *29*, 10878.
(75) Hellinga, H. W. *J. Am. Chem. Soc.* **1998**, *120*, 10055.
(76) Schnepf, R.; Horth, P.; Bill, E.; Wieghardt, K.; Hildebrandt, P.; Haehnel, W. *J. Am. Chem. Soc.* **2001**, *123*, 2186.
(77) Daugherty, R. G.; Wasowicz, T.; Gibney, B. R.; DeRose, V. J. *Inorg. Chem.* **2002**, *41*, 2623.
(78) Suzuki, K.; Hiroaki, H.; Kohda, D.; Nakamura, H.; Tanaka, T. *J. Am. Chem. Soc.* **1998**, *120*, 13008.
(79) Dieckmann, G. R.; McRorie, D. K.; Tierney, D. L.; Utschig, L. M.; Singer, C. P.; O'Halloran, T. V.; Penner-Hahn, J. E.; DeGrado, W. F.; Pecoraro, V. L. *J. Am. Chem. Soc.* **1997**, *119*, 6195.
(80) Farrer, B. T.; McClure, C. P.; Penner-Hahn, J. E.; Pecoraro, V. L. *Inorg. Chem.* **2000**, *39*, 5422.
(81) Kovacic, R. T.; Welch, J. T.; Franklin, S. J. *J. Am. Chem. Soc.* **2003**, *125*, 6656.
(82) Ghadiri, M. R.; Case, M. A. *Angew. Chem., Int. Ed. Engl.* **1993**, *32*, 1594.
(83) Rabanal, F.; DeGrado, W. F.; Dutton, P. L. *J. Am. Chem. Soc.* **1996**, *118*, 473.
(84) Sharp, R. E.; Moser, C. C.; Rabanal, F.; Dutton, P. L. *Proc. Natl. Acad. Sci. U.S.A.* **1998**, *95*, 10465.
(85) Mutz, M. W.; Case, M. A.; Wishart, J. F.; Ghadiri, M. R.; McLendon, G. L. *J. Am. Chem. Soc.* **1999**, *121*, 858.
(86) Kornilova, A. Y.; Wishart, J. F.; Xiao, W. Z.; Lasey, R. C.; Fedorova, A.; Shin, Y. K.; Ogawa, M. Y. *J. Am. Chem. Soc.* **2000**, *122*, 7999.
(87) Laplaza, C. E.; Holm, R. H. *J. Am. Chem. Soc.* **2001**, *123*, 10255.
(88) Musgrave, K. B.; Laplaza, C. E.; Holm, R. H.; Hedman, B.; Hodgson, K. O. *J. Am. Chem. Soc.* **2002**, *124*, 3083.
(89) Fedorova, A.; Chaudhari, A.; Ogawa, M. Y. *J. Am. Chem. Soc.* **2003**, *125*, 357.
(90) Farrer, B. T.; Pecoraro, V. L. *Proc. Natl. Acad. Sci. U.S.A.* **2003**, *100*, 3760.
(91) Shifman, J. M.; Moser, C. C.; Kalsbeck, W. A.; Bocian, D. F.; Dutton, P. L. *Biochemistry* **1998**, *37*, 16815.
(92) Moffet, D. A.; Certain, L. K.; Smith, A. J.; Kessel, A. J.; Beckwith, K. A.; Hecht, M. H. *J. Am. Chem. Soc.* **2000**, *122*, 7612.
(93) Bolon, D. N.; Mayo, S. L. *Proc. Natl. Acad. Sci. U.S.A.* **2001**, *98*, 14274.
(94) Anderson, L. K.; Caspersson, M.; Baltzer, L. *Chem. Eur. J.* **2002**, *8*, 3687.
(95) Kennedy, M. L.; Gibney, B. R. *Curr. Opin. Struct. Biol.* **2001**, *11*, 485.
(96) Xing, G.; DeRose, V. J. *Curr. Opin. Chem. Biol.* **2001**, *5*, 196.
(97) Lu, Y.; Valentine, J. S. *Curr. Opin. Struct. Biol.* **1997**, *7*, 495.
(98) Holm, R. H.; Kennepohl, P.; Solomon, E. I. *Chem. Rev.* **1996**, *96*, 2239.
(99) Braisted, A. C.; Wells, J. A. *Proc. Natl. Acad. Sci. U.S.A.* **1996**, *93*, 5688.
(100) Mulholland, S. E.; Gibney, B. R.; Rabanal, F.; Dutton, P. L. *Biochemistry* **1999**, *38*, 10442.
(101) Cochran, A. G.; Skelton, N. J.; Starovasnik, M. A. *Proc. Natl. Acad. Sci. U.S.A.* **2001**, *98*, 5578.
(102) Chin, J. W.; Schepartz, A. *J. Am. Chem. Soc.* **2001**, *123*, 2929.
(103) Gibney, B. R.; Dutton, P. L. *Adv. Inorg. Chem.* **2001**, *51*, 409.
(104) Lombardi, A.; Nastri, F.; Pavone, V. *Chem. Rev.* **2001**, *101*, 3165.
(105) Teichmann, L. Z. *Ration. Med.* **1853**, *3*, 375.
(106) McMunn, C. A. *J. Physiol.* **1886**, *5*, xxiv.
(107) Keilin, D. *Proc. R. Soc. London, B* **1925**, *98*, 312.
(108) Berry, E. A.; Trumpower, B. L. *Anal. Biochem.* **1987**, *161*, 1.
(109) Sono, M.; Roach, M. P.; Coulter, E. D.; Dawson, J. H. *Chem. Rev.* **1996**, *96*, 2841.
(110) Ferguson-Miller, S.; Babcock, G. T. *Chem. Rev.* **1996**, *96*, 2889.
(111) Fischer, H.; Zeile, K. *Justus Liebigs Ann. Chem.* **1929**, *468*, 98.
(112) Sellers, V. M.; Wu, C. K.; Dailey, T. A.; Dailey, H. A. *Biochemistry* **2001**, *40*, 9821.
(113) Wu, C. K.; Dailey, H. A.; Rose, J. P.; Burden, A.; Sellers, V. M.; Wang, B. C. *Nat. Struct. Biol.* **2001**, *8*, 156.
(114) O'Brian, M. R.; Thony-Meyer, L. *Adv. Microb. Physiol.* **2002**, *46*, 257.
(115) Mogi, T.; Saiki, K.; Anraku, Y. *Mol. Microbiol.* **1994**, *14*, 391.
(116) Brown, K. R.; Allan, B. A.; Do, P.; Hegg, E. L. *Biochemistry* **2002**, *41*, 10906.
(117) Hargrove, M. S.; Barrick, D.; Olson, J. S. *Biochemistry* **1996**, *35*, 11293.
(118) Hargrove, M. S.; Olson, J. S. *Biochemistry* **1996**, *35*, 11310.
(119) Hargrove, M. S.; Wilkinson, A. J.; Olson, J. S. *Biochemistry* **1996**, *35*, 11300.
(120) Breslow, E.; Koehler, R. *J. Biol. Chem.* **1965**, *240*, 2266.
(121) Breslow, E.; Koehler, R.; Girotti, A. W. *J. Biol. Chem.* **1967**, *242*, 4149.
(122) Moore, G. R.; Pettigrew, G. W. *Cytochromes c: Evolutionary, Structural and Physiochemical Aspects*; Springer-Verlag: New York, 1990.
(123) Drygas, M. E.; Lambowitz, A. M.; Nargang, F. E. *J. Biol. Chem.* **1989**, *264*, 17897.
(124) Sano, S.; Tanaka, K. *J. Biol. Chem.* **1964**, *1964*, 3109.
(125) Barker, P. D.; Nerou, E. P.; Cheesman, M. R.; Thomson, A. J.; deOliveira, P.; Hill, H. A. O. *Biochemistry* **1996**, *35*, 13618.
(126) Tomlinson, E. J.; Ferguson, S. J. *Proc. Natl. Acad. Sci. U.S.A.* **2000**, *97*, 5156.
(127) Arnesano, F.; Banci, L.; Bertini, I.; Ciofi-Baffoni, S.; Woodyear, T. D.; Johnson, C. M.; Barker, P. D. *Biochemistry* **2000**, *39*, 1499.
(128) Martinez, S. E.; Huang, D.; Ponomarev, M.; Cramer, W. A.; Smith, J. L. *Protein Sci.* **1996**, *5*, 1081.
(129) Vainshtein, B. K.; Melikadamyan, W. R.; Barynin, V. V.; Vagin, A. A.; Grebenko, A. I.; Borisov, V. V.; Bartels, K. S.; Fita, I.; Rossmann, M. G. *J. Mol. Biol.* **1986**, *188*, 49.
(130) Williams, P. A.; Fulop, V.; Garman, E. F.; Saunders: N. F. W.; Ferguson, S. J.; Hajdu, J. *Nature* **1997**, *389*, 406.
(131) Igarashi, N.; Moriyama, H.; Fujiwara, T.; Fukumori, Y.; Tanaka, N. *Nat. Struct. Biol.* **1997**, *4*, 276.
(132) Crane, B. R.; Siegel, L. M.; Getzoff, E. D. *Science* **1995**, *270*, 59.
(133) Lemberg, R.; Falk, J. E. *Biochem. J.* **1951**, *49*, 674.
(134) Page, C. C.; Moser, C. C.; Chen, X. X.; Dutton, P. L. *Nature* **1999**, *402*, 47.
(135) Devreese, B.; Costa, C.; Demol, H.; Papaefthymiou, V.; Moura, I.; Moura, J. J. R.; VanBeeumen, J. *Eur. J. Biochem.* **1997**, *248*, 445.
(136) Matias, P. M.; Morais, J.; Coelho, A. V.; Meijers, R.; Gonzalez, A.; Thompson, A. W.; Sieker, L.; LeGall, J.; Carrondo, M. A. *J. Biol. Inorg. Chem.* **1997**, *2*, 507.
(137) Abreu, I. A.; Lourenco, A. I.; Xavier, A. V.; LeGall, J.; Coelho, A. V.; Matias, P. M.; Pinto, D. M.; Carrondo, M. A.; Teixeira, M.; Saraiva, L. M. *J. Biol. Inorg. Chem.* **2003**, *8*, 360.
(138) Perutz, M. F.; Rossmann, M. G.; Cullis, A. F.; Muirhead, H.; Will, G.; North, A. C. T. *Nature* **1960**, *185*, 416.
(139) Fulop, V.; Moir, J. W. B.; Ferguson, S. J.; Hajdu, J. *Cell* **1995**, *81*, 369.
(140) Houseman, A. L. P.; Doan, P. E.; Goodin, D. B.; Hoffman, B. M. *Biochemistry* **1993**, *32*, 4430.
(141) Deisenhofer, J.; Epp, O.; Sinning, I.; Michel, H. *J. Mol. Biol.* **1995**, *246*, 429.
(142) Munro, A. W.; Leys, D. G.; McLean, K. J.; Marshall, K. R.; Ost, T. W. B.; Daff, S.; Miles, C. S.; Chapman, S. K.; Lysek, D. A.; Moser, C. C.; Page, C. C.; Dutton, P. L. *Trends Biochem. Sci.* **2002**, *27*, 250.

(143) Crane, B. R.; Siegel, L. M.; Getzoff, E. D. *Biochemistry* **1997**, *36*, 12120.
(144) Han, S. W.; Madden, J. F.; Siegel, L. M.; Spiro, T. G. *Biochemistry* **1989**, *28*, 5477.
(145) Enemark, J. H.; Cosper, M. M. *Met. Ions Biol. Syst.* **2002**, *39*, 621.
(146) Kniemeyer, O.; Heider, J. *J. Biol. Chem.* **2001**, *276*, 21381.
(147) Iwata, S.; Ostermeier, C.; Ludwig, B.; Michel, H. *Nature* **1995**, *376*, 660.
(148) Tsukihara, T.; Aoyama, H.; Yamashita, E.; Tomizaki, T.; Yamaguchi, H.; Shinzawaitoh, K.; Nakashima, R.; Yaono, R.; Yoshikawa, S. *Science* **1995**, *269*, 1069.
(149) Babcock, G. T.; Wikström, M. *Nature* **1992**, *356*, 301.
(150) Adelroth, P.; Gennis, R. B.; Brzezinski, P. *Biochemistry* **1998**, *37*, 2470.
(151) Michel, H. *Proc. Natl. Acad. Sci. U.S.A.* **1998**, *95*, 12819.
(152) Paula, S.; Sucheta, A.; Szundi, I.; Einarsdöttir, O. *Biochemistry* **1999**, *38*, 3025.
(153) Namslauer, A.; Branden, M.; Brzezinski, P. *Biochemistry* **2002**, *41*, 10369.
(154) Tomson, F. L.; Morgan, J. E.; Gu, G. P.; Barquera, B.; Vygodina, T. V.; Gennis, R. B. *Biochemistry* **2003**, *42*, 1711.
(155) Berman, H. M.; Westbrook, J.; Feng, Z.; Gilliland, G.; Bhat, T. N.; Weissig, H.; Shindyalov, I. N.; Bourne, P. E. *Nucleic Acids Res.* **2000**, *28*, 235.
(156) Iverson, T. M.; Arciero, D. M.; Hsu, B. T.; Logan, M. S. P.; Hooper, A. B.; Rees, D. C. *Nat. Struct. Biol.* **1998**, *5*, 1005.
(157) Karlin, S.; Zhu, Z. Y.; Karlin, K. D. *Proc. Natl. Acad. Sci. U.S.A.* **1997**, *94*, 14225.
(158) Karlin, S.; Zhu, Z. Y.; Karlin, K. D. *Biochemistry* **1998**, *37*, 17726.
(159) Durley, R. C. E.; Mathews, F. S. *Acta Crystallogr., Sect. D: Biol. Crystallogr.* **1996**, *52*, 65.
(160) Aragao, D.; Frazao, C.; Sieker, L.; Sheldrick, G. M.; LeGall, J.; Carrondo, M. A. *Acta Crystallogr., Sect. D: Biol. Crystallogr.* **2003**, *59*, 644.
(161) Dickerson, R. E.; Takano, T.; Eisenberg, D.; Kallai, O. B.; Samson, L.; Cooper, A.; Margoliash, E. *J. Biol. Chem.* **1971**, *246*, 1511.
(162) Lanzilotta, W. N.; Schuller, D. J.; Thorsteinsson, M. V.; Kerby, R. L.; Roberts, G. P.; Poulos, T. L. *Nat. Struct. Biol.* **2000**, *7*, 876.
(163) Einsle, O.; Messerschmidt, A.; Stach, P.; Bourenkov, G. P.; Bartunik, H. D.; Huber, R.; Kroneck, P. M. H. *Nature* **1999**, *400*, 476.
(164) Leys, D.; Backers, K.; Meyer, T. E.; Hagen, W. R.; Cusanovich, M. A.; Van Beeumen, J. J. *J. Biol. Chem.* **2000**, *275*, 16050.
(165) Arnoux, P.; Haser, R.; Izadi, N.; Lecroisey, A.; Delepierre, M.; Wandersman, C.; Czjzek, M. *Nat. Struct. Biol.* **1999**, *6*, 516.
(166) Perutz, M. F.; Pulsinelli, P.; Ranney, H. M. *Nature New Biol.* **1972**, *237*, 259.
(167) Andrews, S. C.; Arosio, P.; Bottke, W.; Briat, J. F.; Vondarl, M.; Harrison, P. M.; Laulhere, J. P.; Levi, S.; Lobreaux, S.; Yewdall, S. J. *J. Inorg. Biochem.* **1992**, *47*, 161.
(168) Poulos, T. L.; Finzel, B. C.; Howard, A. J. *J. Mol. Biol.* **1987**, *195*, 687.
(169) Kotsonis, P.; Frohlich, L. G.; Raman, C. S.; Li, H. Y.; Berg, M.; Gerwig, R.; Groehn, V.; Kang, Y. H.; Al-Masoudi, N.; Taghavi-Moghadam, S.; Mohr, D.; Munch, U.; Schnabel, J.; Martasek, P.; Masters, B. S. S.; Strobel, H.; Poulos, T.; Matter, H.; Pfleiderer, W.; Schmidt, H. H. H. W. *J. Biol. Chem.* **2001**, *276*, 49133.
(170) Karmirantzou, M.; Thornton, J. M. *Computational approaches to protein ligand interactions: protein−heme complexes*; Munksgaard: Copenhagen, 1998.
(171) Liu, D. H.; Williamson, D. A.; Kennedy, M. L.; Williams, T. D.; Morton, M. M.; Benson, D. R. *J. Am. Chem. Soc.* **1999**, *121*, 11798.
(172) Mathews, F. S.; Bethge, P. H.; Czerwinski, E. W. *J. Biol. Chem.* **1979**, *254*, 1699.
(173) Weber, P. C.; Bartsch, R. G.; Cusanovich, M. A.; Hamlin, R. C.; Howard, A.; Jordan, S. R.; Kamen, M. D.; Meyer, T. E.; Weatherford, D. W.; Xuong, N. H.; Salemme, F. R. *Nature* **1980**, *286*, 302.
(174) Weber, P. C.; Salemme, F. R.; Mathews, F. S.; Bethge, P. H. *J. Biol. Chem.* **1981**, *256*, 7702.
(175) Hayashi, T.; Hitomi, Y.; Suzuki, A.; Takimura, T.; Ogoshi, H. *Chem. Lett.* **1995**, 911.
(176) Gajhede, M.; Schuller, D. J.; Henriksen, A.; Smith, A. T.; Poulos, T. L. *Nat. Struct. Biol.* **1997**, *4*, 1032.
(177) Poulos, T. L. *Adv. Inorg. Biochem.* **1988**, *7*, 1.
(178) Orengo, C. A.; Michie, A. D.; Jones, S.; Jones, D. T.; Swindells, M. B.; Thornton, J. M. *Structure* **1997**, *5*, 1093.
(179) Gardner, P. R.; Gardner, A. M.; Martin, L. A.; Salzman, A. L. *Proc. Natl. Acad. Sci. U.S.A.* **1998**, *95*, 10378.
(180) Louie, G. V.; Brayer, G. D. *J. Mol. Biol.* **1990**, *214*, 527.
(181) Breslow, R. *Chem. Soc. Rev.* **1972**, *1*, 553.
(182) Breslow, R. *Acc. Chem. Res.* **1980**, *13*, 170.
(183) Dumont, M. E.; Corin, A. F.; Campbell, G. A. *Biochemistry* **1994**, *33*, 7368.
(184) Frolow, F.; Kalb, A. J.; Yariv, J. *Nat. Struct. Biol.* **1994**, *1*, 453.
(185) Cobessi, D.; Huang, L. S.; Ban, M.; Pon, N. G.; Daldal, F.; Berry, E. A. *Acta Crystallogr., Sect. D: Biol. Crystallogr.* **2002**, *58*, 29.
(186) Yankovskaya, V.; Horsefield, R.; Tornroth, S.; Luna-Chavez, C.; Miyoshi, H.; Leger, C.; Byrne, B.; Cecchini, G.; Iwata, S. *Science* **2003**, *299*, 700.
(187) Beinert, H.; Holm, R. H.; Münck, E. *Science* **1997**, *277*, 653.
(188) Izadi, N.; Henry, Y.; Haladjian, J.; Goldberg, M. E.; Wandersman, C.; Delepierre, M.; Lecroisey, A. *Biochemistry* **1997**, *36*, 7050.
(189) Metzger, S. U.; Cramer, W. A.; Whitmarsh, J. *Biochim. Biophys. Acta* **1997**, *1319*, 233.
(190) Winkler, J. R.; Wittung-Stafshede, P.; Leckner, J.; Malmström, B. G.; Gray, H. B. *Proc. Natl. Acad. Sci. U.S.A.* **1997**, *94*, 4246.
(191) Moore, G. R.; Williams, R. J. P. *FEBS Lett.* **1977**, *79*, 229.
(192) Gunner, M. R.; Alexov, E.; Torres, E.; Lipovaca, S. *J. Biol. Inorg. Chem.* **1997**, *2*, 126.
(193) Zhou, H. X. *J. Biol. Inorg. Chem.* **1997**, *2*, 109.
(194) Vanderkooi, G.; Stotz, E. *J. Biol. Chem.* **1966**, *241*, 3316.
(195) Vanderkooi, G.; Stotz, E. *J. Biol. Chem.* **1966**, *241*, 2260.
(196) Walker, F. A.; Lo, M. W.; Ree, M. T. *J. Am. Chem. Soc.* **1976**, *98*, 5552.
(197) Caughey, W. S.; Fujimoto, W. Y.; Johnson, B. P. *Biochemistry* **1966**, *5*, 3830.
(198) Pearson, R. G. *J. Am. Chem. Soc.* **1963**, *85*, 3533.
(199) Tezcan, F. A.; Winkler, J. R.; Gray, H. B. *J. Am. Chem. Soc.* **1998**, *120*, 13383.
(200) Harbury, H. A.; Loach, P. A. *J. Biol. Chem.* **1960**, *235*, 3640.
(201) Harbury, H. A.; Cronin, J. R.; Fanger, M. W.; Hettinge, T. P.; Murphy, A. J.; Myer, Y. P.; Vinograd, S. N. *Proc. Natl. Acad. Sci. U.S.A.* **1965**, *54*, 1658.
(202) Santucci, R.; Reinhard, H.; Brunori, M. *J. Am. Chem. Soc.* **1988**, *110*, 8536.
(203) Battistuzzi, G.; Borsari, M.; Cowan, J. A.; Ranieri, A.; Sola, M. *J. Am. Chem. Soc.* **2002**, *124*, 5315.
(204) Blair, D. F.; Ellis, W. R.; Wang, H.; Gray, H. B.; Chan, S. I. *J. Biol. Chem.* **1986**, *261*, 1524.
(205) Antonini, E.; Wyman, J.; Brunori, M.; Taylor, J. F.; Rossi-Fanelli, A.; Caputo, A. *J. Biol. Chem.* **1964**, *239*, 907.
(206) Collins, M. J.; Arciero, D. M.; Hooper, A. B. *J. Biol. Chem.* **1993**, *268*, 14655.
(207) Roncel, M.; Ortega, J. M.; Losada, M. *Eur. J. Biochem.* **2001**, *268*, 4961.
(208) Schichman, S. A.; Gray, H. B. *J. Am. Chem. Soc.* **1981**, *103*, 7794.
(209) Bertrand, P.; Mbarki, O.; Asso, M.; Blanchard, L.; Guerlesquin, F.; Tegoni, M. *Biochemistry* **1995**, *34*, 11071.
(210) Dikiy, A.; Carpentier, W.; Vandenberghe, I.; Borsari, M.; Safarov, N.; Dikaya, E.; Van Beeumen, J.; Ciurli, S. *Biochemistry* **2002**, *41*, 14689.
(211) Watt, G. D.; Frankel, R. B.; Papaefthymiou, G. C.; Spartalian, K.; Stiefel, E. I. *Biochemistry* **1986**, *25*, 4330.
(212) Andersen, J. F.; Ding, X. D.; Balfour, C.; Shokhireva, T. K.; Champagne, D. E.; Walker, F. A.; Montfort, W. R. *Biochemistry* **2000**, *39*, 10118.
(213) Presta, A.; Weber-Main, A. M.; Stankovich, M. T.; Stuehr, D. J. *J. Am. Chem. Soc.* **1998**, *120*, 9460.
(214) Reid, L. S.; Taniguchi, V. T.; Gray, H. B.; Mauk, A. G. *J. Am. Chem. Soc.* **1982**, *104*, 7516.
(215) Meyer, T. E.; Cheddar, G.; Bartsch, R. G.; Getzoff, E. D.; Cusanovich, M. A.; Tollin, G. *Biochemistry* **1986**, *25*, 1383.
(216) Barker, P. D.; Butler, J. L.; de Oliveira, P.; Hill, H. A. O.; Hunt, N. I. *Inorg. Chim. Acta* **1996**, *252*, 71.
(217) Springs, S. L.; Bass, S. E.; McLendon, G. L. *Biochemistry* **2000**, *39*, 6075.
(218) Kassner, R. J. *Proc. Natl. Acad. Sci. U.S.A.* **1972**, *69*, 2263.
(219) Kassner, R. J. *J. Am. Chem. Soc.* **1973**, *95*, 2674.
(220) Edholm, O.; Nordlander, P.; Chen, W.; Ohlsson, P. I.; Smith, M. L.; Paul, J. *Biochem. Biophys. Res. Commun.* **2000**, *268*, 683.
(221) Mao, J. J.; Hauser, K.; Gunner, M. R. *Biochemistry* **2003**, *42*, 9829.
(222) Kannt, A.; Lancaster, C. R. D.; Michel, H. *Biophys. J.* **1998**, *74*, 708.
(223) Pereira, M. M.; Gomes, C. M.; Teixeira, M. *FEBS Lett.* **2002**, *522*, 14.
(224) Churg, A. K.; Warshel, A. *Biochemistry* **1986**, *25*, 1675.
(225) Warshel, A.; Papazyan, A.; Muegge, I. *J. Biol. Inorg. Chem.* **1997**, *2*, 143.
(226) Gunner, M. R.; Alexov, E. *Biochim. Biophys. Acta* **2000**, *1458*, 63.
(227) Yang, Y.; Beck, B. W.; Shenoy, V. S.; Ichiye, T. *J. Am. Chem. Soc.* **1993**, *115*, 7439.
(228) Stephens, P. J.; Jollie, D. R.; Warshel, A. *Chem. Rev.* **1996**, *96*, 2491.
(229) Beratan, D. N.; Onuchic, J. N.; Winkler, J. R.; Gray, H. B. *Science* **1992**, *258*, 1740.
(230) Millett, F.; Miller, M. A.; Geren, L.; Durham, B. *J. Bioenerg. Biomembr.* **1995**, *27*, 341.
(231) Moser, C. C.; Keske, J. M.; Warncke, K.; Farid, R. S.; Dutton, P. L. *Nature* **1992**, *355*, 796.

(232) Weiss, J. J. *Nature* **1964**, *202*, 83.
(233) Aron, J.; Baldwin, D. A.; Marques, H. M.; Pratt, J. M.; Adams, P. A. *J. Inorg. Biochem.* **1986**, *27*, 227.
(234) Othman, S.; Lelirzin, A.; Desbois, A. *Biochemistry* **1993**, *32*, 9781.
(235) Munro, O. Q.; Marques, H. M. *Inorg. Chem.* **1996**, *35*, 3752.
(236) Carraway, A. D.; McCollum, M. G.; Peterson, J. *Inorg. Chem.* **1996**, *35*, 6885.
(237) Casella, L.; De Gioia, L.; Silvestri, G. F.; Monzani, E.; Redaelli, C.; Roncone, R.; Santagostini, L. *J. Inorg. Biochem.* **2000**, *79*, 31.
(238) Ippoliti, R.; Picciau, A.; Santucci, R.; Antonini, G.; Brunori, M.; Ranghino, G. *Biochem. J.* **1997**, *328*, 833.
(239) Low, D. W.; Yang, G.; Winkler, J. R.; Gray, H. B. *J. Am. Chem. Soc.* **1997**, *119*, 4094.
(240) Low, D. W.; Gray, H. B.; Duus, J. O. *J. Am. Chem. Soc.* **1997**, *119*, 1.
(241) Mondelli, R.; Scaglioni, L.; Mazzini, S.; Bolis, G.; Ranghino, G. *Magn. Reson. Chem.* **2000**, *38*, 229.
(242) Elöve, G. A.; Bhuyan, A. K.; Roder, H. *Biochemistry* **1994**, *33*, 6925.
(243) Warme, P. K.; Hager, L. P. *Biochemistry* **1970**, *9*, 1599.
(244) Heijden, A. V. D.; Peer, H. G.; Vandenoo, A. H. *Chem. Commun.* **1971**, 369.
(245) Casella, L.; Gullotti, M.; Degioia, L.; Monzani, E.; Chillemi, F. *J. Chem. Soc., Dalton Trans.* **1991**, 2945.
(246) Casella, L.; Gullotti, M.; Degioia, L.; Bartesaghi, R.; Chillemi, F. *J. Chem. Soc., Dalton Trans.* **1993**, 2233.
(247) Casella, L.; Monzani, E.; Fantucci, P.; Gullotti, M.; DeGioia, L.; Strini, A.; Chillemi, F. *Inorg. Chem.* **1996**, *35*, 439.
(248) Franceschi, F.; Gullotti, M.; Monzani, E.; Casella, L.; Papaefthymiou, V. *Chem. Commun.* **1996**, 1645.
(249) Monzani, E.; Casella, L.; Gullotti, M.; Panigada, N.; Franceschi, F.; Papaefthymiou, V. *J. Mol. Catal.* **1997**, *117*, 199.
(250) Monzani, E.; Linati, L.; Casella, L.; De Gioia, L.; Favretto, M.; Gullotti, M.; Chillemi, F. *Inorg. Chim. Acta* **1998**, *273*, 339.
(251) Blauer, G. *Nature* **1961**, *189*, 396.
(252) Blauer, G.; Ehrenberg, A. *Acta Chem. Scand.* **1963**, *17*, 8.
(253) Blauer, G. *Biochim. Biophys. Acta* **1964**, *79*, 547.
(254) Blauer, G.; Yonath, A. *Arch. Biochem. Biophys.* **1967**, *121*, 587.
(255) Tohjo, M.; Shibata, K. *Arch. Biochem. Biophys.* **1963**, *103*, 401.
(256) Englander, S. W.; Sosnick, T. R.; Mayne, L. C.; Shtilerman, M.; Qi, P. X.; Bai, Y. W. *Acc. Chem. Res.* **1998**, *31*, 737.
(257) Telford, J. R.; Tezcan, F. A.; Gray, H. B.; Winkler, J. R. *Biochemistry* **1999**, *38*, 1944.
(258) Leutzinger, Y.; Beychok, S. *Proc. Natl. Acad. Sci. U.S.A.* **1981**, *78*, 780.
(259) Ghadiri, M. R.; Soares, C.; Choi, C. *J. Am. Chem. Soc.* **1992**, *114*, 825.
(260) Gochin, M.; Khorosheva, V.; Case, M. A. *J. Am. Chem. Soc.* **2002**, *124*, 11018.
(261) Williamson, D. A.; Benson, D. R. *Chem. Commun.* **1998**, 961.
(262) Nakanishi, K.; Berova, N.; Woody, R. W. *Circular dichroism: Principles and applications*; VCH: New York, 1994.
(263) Liu, D. H.; Lee, K. H.; Benson, D. R. *Chem. Commun.* **1999**, 1205.
(264) Arnold, P. A.; Benson, D. R.; Brink, D. J.; Hendrich, M. P.; Jas, G. S.; Kennedy, M. L.; Petasis, D. T.; Wang, M. X. *Inorg. Chem.* **1997**, *36*, 5306.
(265) Nastri, F.; Lombardi, A.; Morelli, G.; Maglio, O.; D'Auria, G.; Pedone, C.; Pavone, V. *Chem. Eur. J.* **1997**, *3*, 340.
(266) D'Auria, G.; Maglio, O.; Nastri, F.; Lombardi, A.; Mazzeo, M.; Morelli, G.; Paolillo, L.; Pedone, C.; Pavone, V. *Chem. Eur. J.* **1997**, *3*, 350.
(267) Lombardi, A.; Nastri, F.; Sanseverino, M.; Maglio, O.; Pedone, C.; Pavone, V. *Inorg. Chim. Acta* **1998**, *276*, 301.
(268) Lombardi, A.; Nastri, F.; Maglio, O.; Marasco, D.; Coletta, M.; Pavone, V. *J. Inorg. Biochem.* **2001**, *86*, 318.
(269) Geier, G. R.; Sasaki, T. *Tetrahedron Lett.* **1997**, *38*, 3821.
(270) Geier, G. R.; Lybrand, T. P.; Sasaki, T. *Tetrahedron* **1999**, *55*, 1871.
(271) Karpishin, T. B.; Vannelli, T. A.; Glover, K. J. *J. Am. Chem. Soc.* **1997**, *119*, 9063.
(272) Sasaki, T.; Kaiser, E. T. *J. Am. Chem. Soc.* **1989**, *111*, 380.
(273) Sasaki, T.; Kaiser, E. T. *Biopolymers* **1990**, *29*, 79.
(274) Åkerfeldt, K. S.; Kim, R. M.; Camac, D.; Groves, J. T.; Lear, J. D.; DeGrado, W. F. *J. Am. Chem. Soc.* **1992**, *114*, 9656.
(275) Huffman, D. L.; Rosenblatt, M. M.; Suslick, K. S. *J. Am. Chem. Soc.* **1998**, *120*, 6183.
(276) Rosenblatt, M. M.; Huffman, D. L.; Wang, X. T.; Remmer, H. A.; Suslick, K. S. *J. Am. Chem. Soc.* **2002**, *124*, 12394.
(277) Arnold, P. A.; Shelton, W. R.; Benson, D. R. *J. Am. Chem. Soc.* **1997**, *119*, 3181.
(278) Sakamoto, S.; Sakurai, S.; Ueno, A.; Mihara, H. *Chem. Commun.* **1997**, 1221.
(279) Mutter, M.; Altmann, E.; Altmann, K. H.; Hersperger, R.; Koziej, P.; Nebel, K.; Tuchscherer, G.; Vuilleumier, S.; Gremlich, H. U.; Muller, K. *Helv. Chim. Acta* **1988**, *71*, 835.
(280) Feng, Y. Q.; Sligar, S. G.; Wand, A. J. *Nat. Struct. Biol.* **1994**, *1*, 30.
(281) Fuentes, E. J.; Wand, A. J. *Biochemistry* **1998**, *37*, 3687.
(282) Adachi, S.; Nagano, S.; Watanabe, Y.; Ishimori, K.; Morishima, I. *Biochem. Biophys. Res. Commun.* **1991**, *180*, 138.
(283) Adachi, S.; Nagano, S.; Ishimori, K.; Watanabe, Y.; Morishima, I.; Egawa, T.; Kitagawa, T.; Makino, R. *Biochemistry* **1993**, *32*, 241.
(284) Egeberg, K. D.; Springer, B. A.; Martinis, S. A.; Sligar, S. G.; Morikis, D.; Champion, P. M. *Biochemistry* **1990**, *29*, 9783.
(285) Hildebrand, D. P.; Burk, D. L.; Maurus, R.; Ferrer, J. C.; Brayer, G. D.; Mauk, A. G. *Biochemistry* **1995**, *34*, 1997.
(286) Barrick, D. *Biochemistry* **1994**, *33*, 6546.
(287) Pond, A. E.; Roach, M. P.; Thomas, M. R.; Boxer, S. G.; Dawson, J. H. *Inorg. Chem.* **2000**, *39*, 6061.
(288) Dou, Y.; Admiraal, S. J.; Ikedasaito, M.; Krzywda, S.; Wilkinson, A. J.; Li, T. S.; Olson, J. S.; Prince, R. C.; Pickering, I. J.; George, G. N. *J. Biol. Chem.* **1995**, *270*, 15993.
(289) Lloyd, E.; Hildebrand, D. P.; Tu, K. M.; Mauk, A. G. *J. Am. Chem. Soc.* **1995**, *117*, 6434.
(290) Qin, J.; Lamar, G. N.; Dou, Y.; Admiraal, S. J.; Ikedasaito, M. *J. Biol. Chem.* **1994**, *269*, 1083.
(291) Matsui, T.; Ozaki, S.; Liong, E.; Phillips, G. N.; Watanabe, Y. *J. Biol. Chem.* **1999**, *274*, 2838.
(292) Sigman, J. A.; Kwok, B. C.; Lu, Y. *J. Am. Chem. Soc.* **2000**, *122*, 8192.
(293) Hayashi, T.; Dejima, H.; Matsuo, T.; Sato, H.; Murata, D.; Hisaeda, Y. *J. Am. Chem. Soc.* **2002**, *124*, 11226.
(294) Banner, D. W.; Kokkinidis, M.; Tsernoglou, D. *J. Mol. Biol.* **1987**, *196*, 657.
(295) Predki, P. F.; Regan, L. *Biochemistry* **1995**, *34*, 9834.
(296) Wilson, J. R.; Caruana, D. J.; Gilardi, G. *Chem. Commun.* **2003**, 356.
(297) Gibney, B. R.; Huang, S. S.; Skalicky, J. J.; Fuentes, E. J.; Wand, A. J.; Dutton, P. L. *Biochemistry*, **2001**, *40*, 10550.
(298) Struthers, M. D.; Cheng, R. P.; Imperiali, B. *Science* **1996**, *271*, 342.
(299) Dahiyat, B. I.; Mayo, S. L. *Science* **1997**, *278*, 82.
(300) Walsh, S. T. R.; Cheng, H.; Bryson, J. W.; Roder, H.; DeGrado, W. F. *Proc. Natl. Acad. Sci. U.S.A.* **1999**, *96*, 5486.
(301) Hill, R. B.; DeGrado, W. F. *J. Am. Chem. Soc.* **1998**, *120*, 1138.
(302) Skalicky, J. J.; Gibney, B. R.; Rabanal, F.; Urbauer, R. J. B.; Dutton, P. L.; Wand, A. J. *J. Am. Chem. Soc.* **1999**, *121*, 4941.
(303) Willis, M. A.; Bishop, B.; Regan, L.; Brunger, A. T. *Structure* **2002**, *8*, 1319.
(304) Huang, S. S.; Gibney, B. R.; Stayrook, S. E.; Dutton, P. L.; Lewis, M. *J. Mol. Biol.* **2003**, *326*, 1219.
(305) Wei, Y.; Kim, S.; Fela, D.; Baum, J.; Hecht, M. H. *Proc. Natl. Acad. Sci. U.S.A.*, **2003**, *100*, 13270.
(306) Dai, Q.-H.; Tommos, C.; Fuentes, E. J.; Blomberg, M. R. A.; Dutton, P. L.; Wand. A. J. *J. Am. Chem. Soc.*, **2002**, *124*, 10952.
(307) Gibney, B. R.; Rabanal, F.; Skalicky, J. J.; Wand, A. J.; Dutton, P. L. *J. Am. Chem. Soc.* **1997**, *119*, 2323−2324.
(308) Munson, M.; Balasubramanian, S.; Fleming, K. G.; Nagi, A. D.; O'Brien, R. O.; Sturtevant, J. M.; Regan, L. *Protein Science* **1996**, *5*, 1584.
(309) Bryson, J. W.; Desjarlais, J. M.; Handel, T. M.; DeGrado, W. F. *Protein Sci.*, **1998**, *7*, 1404.
(310) Huang, S. S.; Koder, R. L.; Lewis, M.; Wand, A. J.; Dutton, P. L. *Proc. Natl. Acad. Sci. U.S.A.*, submitted.
(311) Ho, S. P.; DeGrado, W. F. *J. Am. Chem. Soc.* **1987**, *109*, 6751.
(312) Rau, H. K.; Haehnel, W. *J. Am. Chem. Soc.* **1998**, *120*, 468.
(313) Fahnenschmidt, M.; Bittl, R.; Schlodder, E.; Haehnel, W.; Lubitz, W. *Phys. Chem. Chem. Phys.* **2001**, *3*, 4082.
(314) Sakamoto, S.; Ueno, A.; Mihara, H. *J. Chem. Soc., Perkin Trans. 2* **1998**, 2395.
(315) Obataya, I.; Kotaki, T.; Sakamoto, S.; Ueno, A.; Mihara, H. *Bioorg. Med. Chem. Lett.* **2000**, *10*, 2719.
(316) Isogai, Y.; Ota, M.; Fujisawa, T.; Izuno, H.; Mukai, M.; Nakamura, H.; Iizuka, T.; Nishikawa, K. *Biochemistry* **1999**, *38*, 7431.
(317) Isogai, Y.; Ishii, A.; Ishida, M.; Mukai, M.; Ota, M.; Nishikawa, K.; Iizuka, T. *Proc. Indian Acad. Sci. Chem. Sci.* **2000**, *112*, 215.
(318) Tomizaki, K.; Nishino, H.; Kato, T.; Miike, A.; Nishino, N. *Chem. Lett.* **2000**, 648.
(319) Sakamoto, S.; Obataya, I.; Ueno, A.; Mihara, H. *Chem. Commun.* **1999**, 1111.
(320) Sakamoto, S.; Obataya, I.; Ueno, A.; Mihara, H. *J. Chem. Soc., Perkin Trans. 2* **1999**, 2059.
(321) Kamtekar, S.; Schiffer, J. M.; Xiong, H. Y.; Babik, J. M.; Hecht, M. H. *Science* **1993**, *262*, 1680.
(322) Rosenbaum, D. M.; Roy, S.; Hecht, M. H. *J. Am. Chem. Soc.* **1999**, *121*, 9509.
(323) Wei, Y. N.; Liu, T.; Sazinsky, S. L.; Moffet, D. A.; Pelczer, I.; Hecht, M. H. *Protein Sci.* **2003**, *12*, 92.
(324) Rojas, N. R. L.; Kamtekar, S.; Simons, C. T.; Mclean, J. E.; Vogel, K. M.; Spiro, T. G.; Farid, R. S.; Hecht, M. H. *Protein Sci.* **1997**, *6*, 2512.
(325) Moffet, D. A.; Case, M. A.; House, J. C.; Vogel, K.; Williams, R. D.; Spiro, T. G.; McLendon, G. L.; Hecht, M. H. *J. Am. Chem. Soc.* **2001**, *123*, 2109.
(326) Moffet, D. A.; Foley, J.; Hecht, M. H. *Biophys. Chem.* **2003**, *105*, 231.

(327) Rau, H. K.; DeJonge, N.; Haehnel, W. *Angew. Chem., Int. Ed.* **2000**, *39*, 250.
(328) Berry, E. A.; Guergova-Kuras, M.; Huang, L. S.; Crofts, A. R. *Annu. Rev. Biochem.* **2000**, *69*, 1005.
(329) Gao, X. G.; Wen, X. L.; Yu, C. A.; Esser, L.; Tsao, S.; Quinn, B.; Zhang, L.; Yu, L.; Xia, D. *Biochemistry* **2002**, *41*, 11692.
(330) DeGrado, W. F.; Wasserman, Z. R.; Lear, J. D. *Science* **1989**, *243*, 622.
(331) Kalsbeck, W. A.; Robertson, D. E.; Pandey, R. K.; Smith, K. M.; Dutton, P. L.; Bocian, D. F. *Biochemistry* **1996**, *35*, 3429.
(332) Reedy, C. J.; Kennedy, M. L.; Gibney, B. R. *Chem. Commun.* **2003**, 570.
(333) Gibney, B. R.; Isogai, Y.; Rabanal, F.; Reddy, K. S.; Grosset, A. M.; Moser, C. C.; Dutton, P. L. *Biochemistry* **2000**, *39*, 11041.
(334) Sharp, R. E.; Diers, J. R.; Bocian, D. F.; Dutton, P. L. *J. Am. Chem. Soc.* **1998**, *120*, 7103.
(335) Xu, Z. J.; Farid, R. S. *Protein Sci.* **2001**, *10*, 236.
(336) Iakovleva, O.; Reiner, M.; Rau, H.; Haehnel, W.; Parak, F. *Phys. Chem. Chem. Phys.* **2002**, *4*, 655.
(337) Fahnenschmidt, M.; Rau, H. K.; Bittl, R.; Haehnel, W.; Lubitz, W. *Chem. Eur. J.* **1999**, *5*, 2327.
(338) Rau, H. K.; Snigula, H.; Struck, A.; Robert, B.; Scheer, H.; Haehnel, W. *Eur. J. Biochem.* **2001**, *268*, 3284.
(339) Ushiyama, M.; Arisaka, F.; Yamamura, T. *Chem. Lett.* **1999**, 127.
(340) Ushiyama, M.; Yoshino, A.; Yamamura, T.; Shida, Y.; Arisaka, F. *Bull. Chem. Soc. Jpn.* **1999**, *72*, 1351.
(341) Takeuchi, Y.; Watanabe, H.; Kashiwada, A.; Nagata, M.; Ohtsuka, T.; Nishino, N.; Kawai, H.; Nagamura, T.; Kurono, Y.; Oku, N.; Nango, M. *Chem. Lett.* **2002**, 848.
(342) Gibney, B. R.; Rabanal, F.; Reddy, K. S.; Dutton, P. L. *Biochemistry* **1998**, *37*, 4635.
(343) Cristian, L.; Piotrowiak, P.; Farid, R. S. *J. Am. Chem. Soc.* **2003**, *125*, 11814.
(344) Mihara, H.; Tomizaki, K.; Fujimoto, T.; Sakamoto, S.; Aoyagi, H.; Nishino, N. *Chem. Lett.* **1996**, 187.
(345) Tomizaki, K. Y.; Nishino, H.; Arai, T.; Kato, T.; Nishino, N. *Chem. Lett.* **2003**, *32*, 6.
(346) Gibney, B. R.; Johansson, J. S.; Rabanal, F.; Skalicky, J. J.; Wand, A. J.; Dutton, P. L. *Biochemistry* **1997**, *36*, 2798.
(347) Rau, H. K.; DeJonge, N.; Haehnel, W. *Proc. Natl. Acad. Sci. U.S.A.* **1998**, *95*, 11526.
(348) Tomizaki, K. Y.; Murata, T.; Kaneko, K.; Miike, A.; Nishino, N. *J. Chem. Soc., Perkin Trans. 2* **2000**, *5*, 1067.
(349) Gibney, B. R.; Dutton, P. L. *Protein Sci.* **1999**, *8*, 1888.
(350) Privett, H. K.; Reedy, C. J.; Kennedy, M. L.; Gibney, B. R. *J. Am. Chem. Soc.* **2002**, *124*, 6828.
(351) Huffman, D. L.; Suslick, K. S. *Inorg. Chem.* **2000**, *39*, 5418.
(352) Kennedy, M. L.; Silchenko, S.; Houndonougbo, N.; Gibney, B. R.; Dutton, P. L.; Rodgers, K. R.; Benson, D. R. *J. Am. Chem. Soc.* **2001**, *123*, 4635.
(353) Shifman, J. M.; Gibney, B. R.; Sharp, R. E.; Dutton, P. L. *Biochemistry* **2000**, *39*, 14813.
(354) Lecomte, J. T. J.; Scott, N. L.; Vu, B. C.; Falzone, C. J. *Biochemistry* **2001**, *40*, 6541.
(355) Raphael, A. L.; Gray, H. B. *Proteins: Struct., Funct. Genet.* **1989**, *6*, 338.
(356) Gunner, M. R.; Honig, B. *Proc. Natl. Acad. Sci. U.S.A.* **1991**, *88*, 9151.
(357) Ohnishi, T. *Biochim. Biophys. Acta* **1998**, *1364*, 186.
(358) Dutton, P. L.; Jackson, J. B. *Eur. J. Biochem.* **1972**, *30*, 495.
(359) Lee, K. H.; Kennedy, M. L.; Buchalova, M.; Benson, D. R. *Tetrahedron* **2000**, *56*, 9725.
(360) Tsuchida, E.; Honda, K.; Hasegawa, E. *Biochim. Biophys. Acta* **1975**, *393*, 483.
(361) Tsuchida, E.; Hasegawa, E.; Honda, K. *Biochim. Biophys. Acta* **1976**, *427*, 520.
(362) Keilin, D.; Mann, T. *Proc. R. Soc. London, B* **1937**, *122B*, 119.
(363) Orf, H. W.; Dolphin, D. *Proc. Natl. Acad. Sci. U.S.A.* **1971**, *74*, 2646.
(364) Cunningham, I. D.; Bachelor, J. L.; Pratt, J. M. *J. Chem. Soc., Perkin Trans. 2* **1991**, 1839.
(365) Ricoux, R.; Boucher, J. L.; Mansuy, D.; Mahy, J. P. *Eur. J. Biochem.* **2001**, *268*, 3783.
(366) Colonna, S.; Gaggero, N.; Carrea, G.; Pasta, P. *Tetrahedron Lett.* **1994**, *35*, 9103.
(367) Ricoux, R.; Boucher, J. L.; Mandon, D.; Frapart, Y. M.; Henry, Y.; Mansuy, D.; Mahy, J. P. *Eur. J. Biochem.* **2003**, *270*, 47.
(368) Adams, P. A.; Adams, C. *J. Inorg. Biochem.* **1988**, *34*, 177.
(369) Veeger, C. *J. Inorg. Biochem.* **2002**, *91*, 35.
(370) Baldwin, D. A.; Marques, H. M.; Pratt, J. M. *FEBS Lett.* **1985**, *183*, 309.
(371) Nastri, F.; Lombardi, A.; Morelli, G.; Pedone, C.; Pavone, V.; Chottard, G.; Battioni, P.; Mansuy, D. *J. Biol. Inorg. Chem.* **1998**, *3*, 671.
(372) Geier, G. R.; Sasaki, T. *Tetrahedron* **1999**, *55*, 1859.
(373) Adams, P. A. *J. Chem. Soc., Perkin Trans. 2* **1990**, 1407.
(374) Cunningham, I. D.; Snare, G. R. *J. Chem. Soc., Perkin Trans. 2* **1992**, 2019.
(375) Primus, J. L.; Grunenwald, S.; Hagedoorn, P. L.; Albrecht-Gary, A. M.; Mandon, D.; Veeger, C. *J. Am. Chem. Soc.* **2002**, *124*, 1214.
(376) Cunningham, I. D.; Bachelor, J. L.; Pratt, J. M. *J. Chem. Soc., Perkin Trans. 2* **1994**, 1347.
(377) Adams, P. A.; Goold, R. D. *Chem. Commun.* **1990**, 97.
(378) Low, D. W.; Winkler, J. R.; Gray, H. B. *J. Am. Chem. Soc.* **1996**, *118*, 117.
(379) Osman, A. M.; Koerts, J.; Boersma, M. G.; Boeren, S.; Veeger, C.; Rietjens, I. M. C. M. *Eur. J. Biochem.* **1996**, *240*, 232.
(380) Benner, S. A. *Nature* **2003**, *421*, 118.
(381) Mehl, R. A.; Anderson, J. C.; Santoro, S. W.; Wang, L.; Martin, A. B.; King, D. S.; Horn, D. M.; Schultz, P. G. *J. Am. Chem. Soc.* **2003**, *125*, 935.
(382) Hofmann, R. M.; Muir, T. W. *Curr. Opin. Biotechnol.* **2002**, *13*, 297.
(383) Dawson, P. E.; Kent, S. B. H. *Annu. Rev. Biochem.* **2000**, *69*, 923.
(384) Gademann, K.; Hane, A.; Rueping, M.; Jaun, B.; Seebach, D. *Angew. Chem., Int. Ed.* **2003**, *42*, 1534.
(385) Raguse, T. L.; Lai, J. R.; Gellman, S. H. *J. Am. Chem. Soc.* **2003**, *125*, 5592.
(386) Koradi, R.; Billeter, M.; Wüthrich, K. *J. Mol. Graphics* **1996**, *14*, 51.
(387) Roberts, S. A.; Weichsel, A.; Qiu, Y.; Shelnutt, J. A.; Walker, F. A.; Montfort, W. R. *Biochemistry* **2001**, *40*, 11327.
(388) Gong, W. M.; Hao, B.; Mansy, S. S.; Gonzalez, G.; Gilles-Gonzalez, M. A.; Chan, M. K. *Proc. Natl. Acad. Sci. U.S.A.* **1998**, *95*, 15177.
(389) Mashino, T.; Nakamura, S.; Hirobe, M. *Tetrahedron Lett.* **1990**, *31*, 3163.
(390) Isogai, Y.; Ishii, A.; Fujisawa, T.; Ota, M.; Nishikawa, K. *Biochemistry* **2000**, *39*, 5683.

CR0206115